AIAA 2020-2021 Undergraduate Light Attack Aircraft

Final Design Report

Amanda R. Moores, Austin P. Piper, Evan R. McElmurray, Jackson R. Elpers, Michael C. Burgess Jr., William A. Kelly, and Zachariah L. Phillips

Department of Aerospace Engineering and Engineering Mechanics

University of Cincinnati College of Engineering and Applied Science, Cincinnati, Ohio, 45219

LAB-7 ZA-21 "SHRIKE"

AEEM 5022 Aircraft Design

Faculty Advisor: Professor Mark Fellows | AIAA Member #1204566

Department of Aerospace Engineering and Engineering Mechanics

University of Cincinnati College of Engineering and Applied Science, Cincinnati, Ohio, 45219

Date of Submission: May 8th, 2021

Meet the Team

Michael Burgess
Chief Engineer
AIAA-1207195

Jackson Elpers
Mechanical Systems
AIAA-738242

William Kelly
Team Lead
AIAA-1217465

Evan McElmurray
Propulsion
AIAA-1181291

Amanda Moores
Systems
AIAA-1218467

Zach Phillips
Payload / CAD
AIAA-1217466

Austin Piper
Structures / Weights
AIAA-1207192

Mark Fellows
Advisor
AIAA-1204566

Table of Contents

List of Figures

List of Tables

Acronyms

AIAA	=	American Institute of Aeronautics and Astronautics
AR	=	Aspect Ratio
BPR	=	Bypass Ratio
CAD	=	Computer-Aided Design
CBR	=	California Bearing Ratio
CG	=	Center of Gravity
EW	=	Empty Weight
FTA	=	Flight Test Aircraft
KEAS	=	Knots Equivalent Airspeed
KTAS	=	Knots True Airspeed
LE	=	Leading Edge
LF	=	Load Factor Measured in g's
MAC	=	Mean Aerodynamic Chord
MTOGW	=	Maximum Takeoff Gross Weight
QFD	=	Quality Function Deployment
RFP	=	Request for Proposal
SFC	=	Specific Fuel Consumption
SL	=	Altitude at Sea Level: 0 ft
TE	=	Trailing Edge
T/W	=	Thrust to Weight Ratio
TFD	=	Time, Fuel, Distance
W/S	=	Wing Loading

Nomenclature

α	=	Angle of Attack
b	=	Span
λ	=	Taper Ratio
$\Lambda_{c/4}$	=	Quarter-Chord Sweep Angle
C_a	=	Aircraft Cost Without Engine
C_{avi}	=	Avionics Cost

C_e	=	Cost per Engine
C_D	=	Lift Drag Coefficient
C_{D0}	=	Zero-Lift Drag Coefficient
C_{HT}	=	Horizontal Tail Volume Coefficient
C_{VT}	=	Vertical Tail Volume Coefficient
C_L	=	Coefficient of Lift
C_{Lmax}	=	Maximum Lift Coefficient
$C_{L\beta}$	=	Derivative of Rolling-Moment Coefficient with Respect to Sideslip Angle
C_{Lp}	=	Vehicle Rolling Derivative
C_{Lr}	=	Vehicle Rolling Derivative
$C_{n\beta}$	=	Derivative of Yawing-Moment Coefficient with Respect to Sideslip Angle
C_{np}	=	Vehicle Rolling Derivative
C_{nr}	=	Vehicle Yawing Derivative
C_{yp}	=	Vehicle Rolling Derivative
I_{HT}	=	Distance Between CG and Horizontal Tail Aerodynamic Center
I_{VT}	=	Distance Between CG and Vertical Tail Aerodynamic Center
M_{max}	=	Engine Maximum Mach Number
N_{eng}	=	Number of Engines
q	=	Dynamic Pressure
R/C	=	Rate of Climb
S_{ref}	=	Reference Area
S_{wet}	=	Wetted Area
s_L	=	Landing Distance
T_{max}	=	Maximum Thrust
T_{turb}	=	Turbine Inlet Temperature
V	=	Velocity
V_c	=	Cruise Velocity
W_e	=	Empty Weight
W_o	=	Design Takeoff Gross Weight

I. Executive Summary

Modern combat environments are ever-changing with new challenges, weapons, and technologies always arising. As foreign threats continue to improve, so must the technology of allied forces. At the same time, this constant improvement of technology and capability in a military environment comes with added cost. The ultimate goal of new combat aircraft is not only to ensure superiority over opponents, but also to maintain low operational costs. One class of aircraft slated for this improvement is light attack and ground support aircraft. This report summarizes the preliminary design of a new light attack aircraft as outlined by the AIAA Request for Proposal (RFP), destined to take on the roles of attack helicopters, close air support vehicles, and even light bombers, all while maintaining a far lower operational cost.

The formal requirements of the RFP call for a light attack aircraft that can take off and land from austere fields in 4000 ft over a 50 ft obstacle, carry 3,000 lbs of armament, have a service life of 15,000 hours over 25 years, and hold two crew members. The RFP calls for a consideration of survivability, employing measures such as armor for the cockpit and engine, reduced infrared and visual signatures, and countermeasures. Provisions for carrying and deploying a variety of weapons, including rail-launched missiles, rockets, and bombs must also be met. Lastly the aircraft must include an integrated gun for ground targets.

The following report outlines the preliminary design of the LAB-7 ZA-21 "Shrike" Light Attack Aircraft, which meets or exceeds all requirements set forth by the RFP. The Shrike is capable of a maximum Mach of 0.80 with a maximum armament payload of 6,600 lbs and a maximum onboard fuel storage of 4,200 lbs. The MTOGW and empty weight are 24,850 lbs and 13,650 lbs respectively. The combat range is an impressive 900 NM, and the total cost of the project is expected to be $1.6 billion with an estimated flyaway cost of $32 million per aircraft and an operating cost of $6,333 per hour.

Figure 1: LAB-7 ZA-21 "Shrike" Rendering

II.   Introduction

Modern combat requirements call for a new type of light attack aircraft to be developed in order to ensure superiority over opponents and maintain low operational costs. The overall objective of the project, as outlined in the AIAA Request for Proposal [26], is to design an affordable light attack aircraft that can operate from short, austere fields near the front lines to provide close air support to ground forces at short notice and complete some missions currently only feasible with attack helicopters. As a result, common missions require long loiter times and forward airfield operability.

This report outlines the design of the ZA-21 "Shrike", developed by LAB-7. The Shrike is a subsonic light attack/ground attack aircraft capable of employing most typical ground support weaponry. With a MTOGW of 24,850 lbs, the ZA-21 is amongst the same class of aircraft as modern day ground support aircraft, such as those submitted for the US Air Force's Light Attack/Armed Reconnaissance Program in 2010. With a maximum Mach of 0.8, a maximum payload weight of 6,600 lbs, and an on-station loiter time of 4 hours, the Shrike performs outstandingly, well in line with the requirements set by the RFP. Detailed design information, as well as considerations of the design process are detailed in the remainder of this report.

III.   Concept of Operations

The requirements for the Light Attack Aircraft set by Request for Proposal (RFP) were set by AIAA. These requirements outline the basic capabilities of the aircraft and can be split into three sections: general requirements, design mission requirements, and ferry mission requirements. The general RFP requirements can be found in Table 1, the design mission requirements can be found in Table 2, and the ferry mission requirements can be found in Table 3. The aircraft must be capable of performing the design mission with the full payload requirement. The design should also be able to perform a long-range ferry mission with a full crew and 60% of the payload requirement.

Requirement	Comments
Austere Field Performance: Takeoff and landing over a 50' obstacle in ≤ 4,000 ft when operating from austere fields at density altitude up to 6,000 ft with semi-prepared runways such as grass or dirt surfaces with CBR of 5	Mandatory Requirement
Survivability: Consideration for survivability, such as armor for the cockpit and engine, reduced infrared and visual signatures, and countermeasures (chaff, flares, etc.)	Objective or Goal
Payload: 3,000 lbs of armament	Mandatory Requirement
Provisions for carrying/deploying a variety of weapons, including rail-launches missiles, rockets, and 500 lb (maximum) bombs	Objective or Goal
Integrated gun for ground targets	Mandatory Requirement
Service Life: 15,000 hours over 25 years	Mandatory Requirement
Service Ceiling: ≥ 30,000 ft	Mandatory Requirement
Crew: Two, both with zero-zero ejection seats	Mandatory Requirement

Table 1: RFP General Requirements

Type	Requirement
Warm Up/Taxi	5 minutes
Climb	To cruise altitude, ≥ 10,000 ft with range credit
Cruise	100 n mi
Descent	To 3,000 ft, no range credit; completed within 20 minutes of initial climb
Loiter	On station, four hours, no stores drops
Climb	To cruise altitude, ≥ 10,000 ft with range credit
Cruise	100 n mi
Descent/Landing	To austere field over 50 ft obstacle in ≤ 4,000 ft
Taxi/Shutdown	5 minutes
Reserves	Sufficient for climb to 3,000 ft and loiter for 45 mins

Table 2: Design Mission Requirements

Type	Requirement
Warm Up/Taxi	5 minutes
Takeoff	Austere field; 50 ft obstacle, ≤ 4,000 ft.
Climb	To cruise altitude; with range credit
Cruise	At best range speed/altitude (≥ 18,000 ft), 900 n mi
Crescent/Landing	To austere field over 50 ft obstacle in ≤ 4,000 ft
Taxi/Shutdown	5 minutes
Reserves	Sufficient for climb to 3,000 ft and loiter for 45 mins

Table 3: Ferry Mission Requirements

The design and ferry mission profiles for the ZA-21 Shrike are found below in Figure 1. Elements of the mission such as warm-up and takeoff, climb, descent, reserves, and more are labeled on the chart.
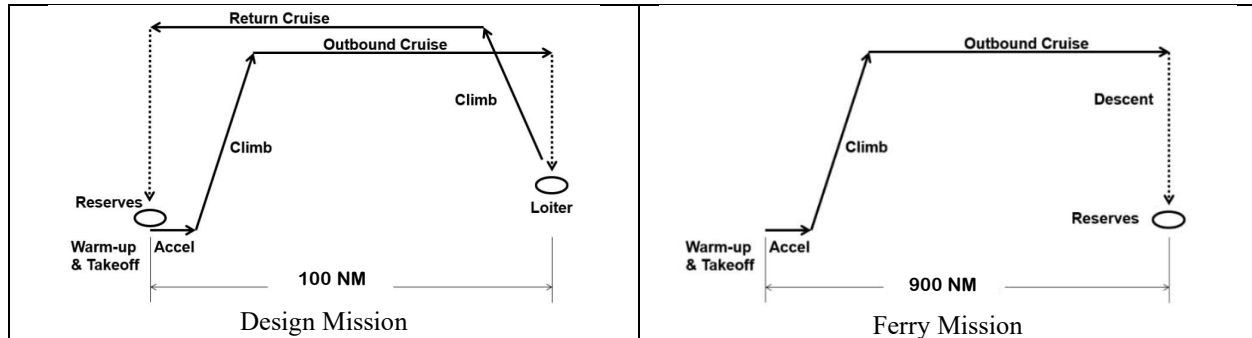
Figure 2: RFP Mission Profiles

IV.   Sizing Analysis

A. Similarity Analysis

The purpose of the similarity analysis was to gain a better understanding of various performance parameters of historical light attack aircraft to guide the design of the ZA-21. The upcoming analysis examines characteristics of aircraft such as aspect ratio, weight fractions, operational ranges, thrust-to-weight (T/W) and wing loading (W/S). Furthermore, the effect of these parameters on one another was examined through trendline analysis.

Historical data plots presented were chosen primarily based on a surface level analysis of the RFP and design solutions that could be predicted to have an impact on said requirements. Some plots were also chosen based on impactful variables and noticeable trend lines that provide meaningful connections between flight parameters.

While researching historical aircraft, detailed information was found for United States military aircraft, but issues arose when pursuing information about aircraft manufactured in other countries, specifically Russia. Several parameters related to aircraft dimensions were not provided such as root chord, tip chord, airfoil type, etc. To determine some unknown dimensions, an analysis of the aircraft's three-view drawing and approximation of values for the aircraft dimensions was completed. Regarding the calculated parameters, issue was taken with values such as taper ratio and fuselage fineness ratio. Again, such calculated parameters depended on aircraft dimensions that were not provided in the initial research.
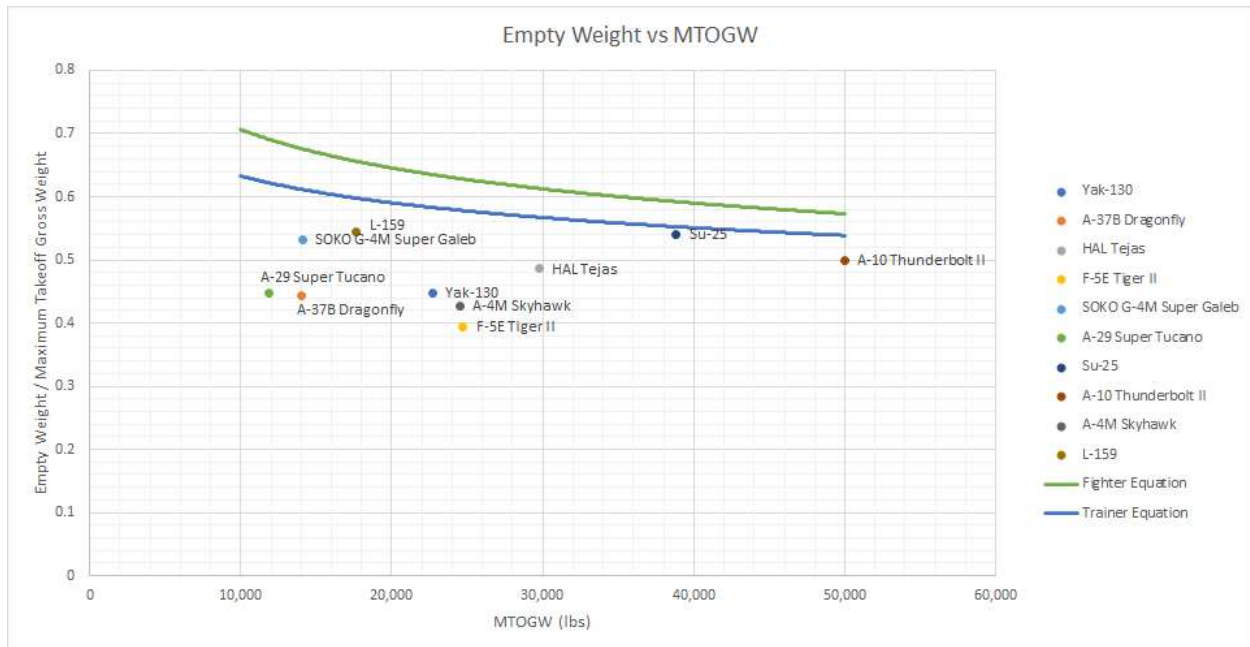
Figure 3: Empty Weight v. MTOGW

The first factor analyzed from similar aircraft was the empty weight fraction in comparison to MTOGW. A lower empty weight fraction allows for greater useable weight capacity, split between both fuel and payload. For the design of the ZA-21, increased payload is important for the aircraft's ability to engage ground targets effectively, and more fuel is desirable for longer loiter times and further operational ranges.

Figure 3 shows the ratio between empty weight and MTOGW among similar light attack aircraft. Overall, empty weight fraction seems to vary little with MTOGW. The applied trendline in the figure are provided by Raymer in Aircraft Design: A Conceptual Approach [25]. Light attack aircraft estimates were not given by Raymer, therefore the trendlines presented are for fighter aircraft and trainer aircraft. Jet fighters and trainers have a less desirable empty weight fraction than light attack aircraft in the specified MTOGW range. Some of the aircraft that are similar to fighters such as the Su-25 have values closer to the trendline. Most of the light attack aircraft have a lower MTOGW and empty weight fraction than a fighter or trainer would.

A trend can be seen in Figure 3 the shows nearly all data points having an W_e fraction from 0.4 - 0.55 regardless of MTOGW. As such, the target empty weight fraction for the design of the ZA-21 was set at 0.5.

Aspect Ratio v. MTOGW - A-10 & Su-25 removed
LAB-7
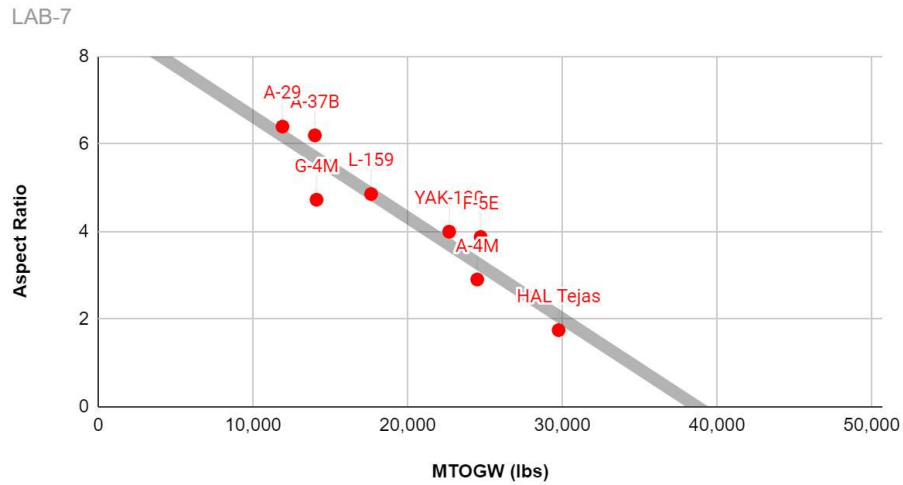
Figure 4: Aspect Ratio v. MTOGW

The next parameter analyzed for similar aircraft was AR and its dependence on MTOGW. Aspect ratio mainly affects aircraft maneuverability and aerodynamic efficiency. The negative effects of both high and low aspect ratios were considered. A low aspect ratio wing would limit the aircraft's payload capabilities whereas a high aspect ratio wing would limit its maneuverability. Figure 4: Aspect Ratio v. MTOGW shows a clear correlation between AR and MTOGW for historical light attack aircraft. Notably, the A-10 and the SU-25 represented outliers and were removed from the trendline analysis. The A-10 and Su-25 are both considered ground attack aircraft, rather than typical light attack aircraft, so their removal is justified.

MTOGW v W/S
LAB-7
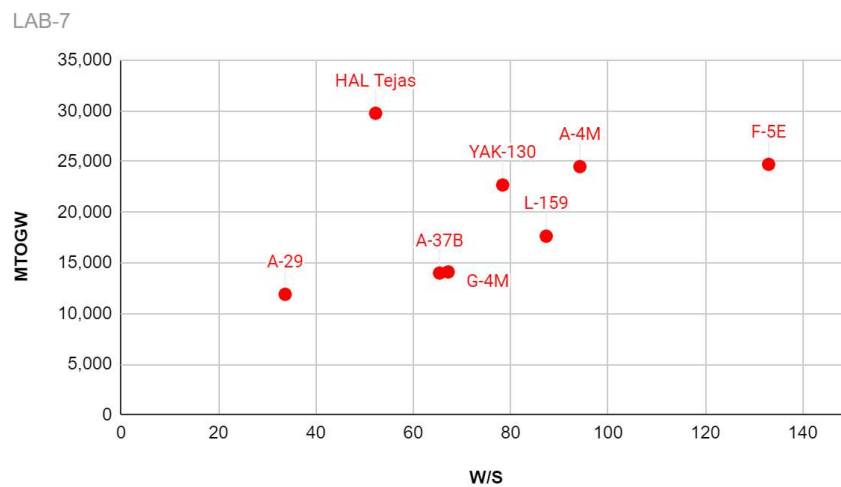
This data in Figure 5 compares the MTOGW and wing loading of the aircraft analyzed. The data provides a range of possible W/S and MTOGW values for the ZA-21. The target range for W/S is 60-100 and the target range for MTOGW is 10,000 lbs to 30,000 lbs.

Fuel Fraction v. MTOGW
LAB-7
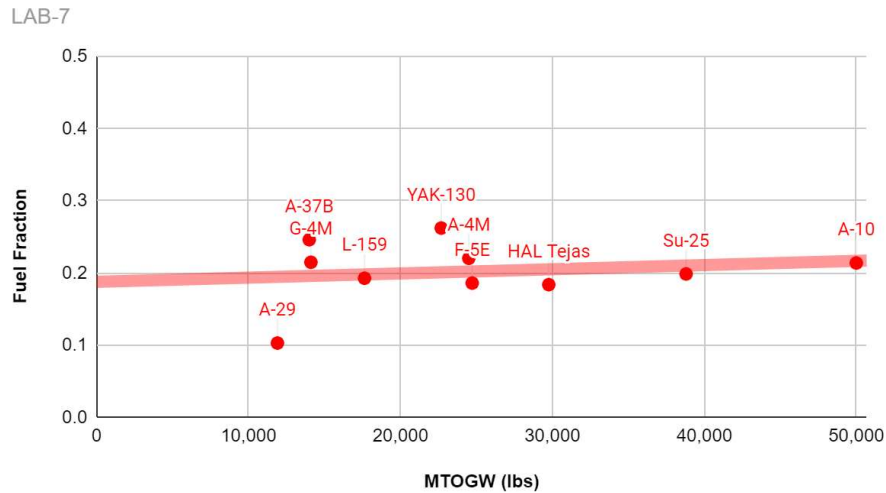
Figure 6: Fuel Fraction v. MTOGW

Figure 6 shows a trendline of about 20% of the MTOGW being reserved for fuel. This value stays relatively constant regardless of the size of the aircraft. For example, the A-10 at 50,000 lbs has the same fuel fraction as the Super Galeb at 15,000 lbs. This shows that fuel weight is a scalar value of the MTOGW generally for a light attack aircraft. While a fuel fraction requirement was not set, the trend above provides guidance for the design of the ZA-21 for appropriate fuel weights.
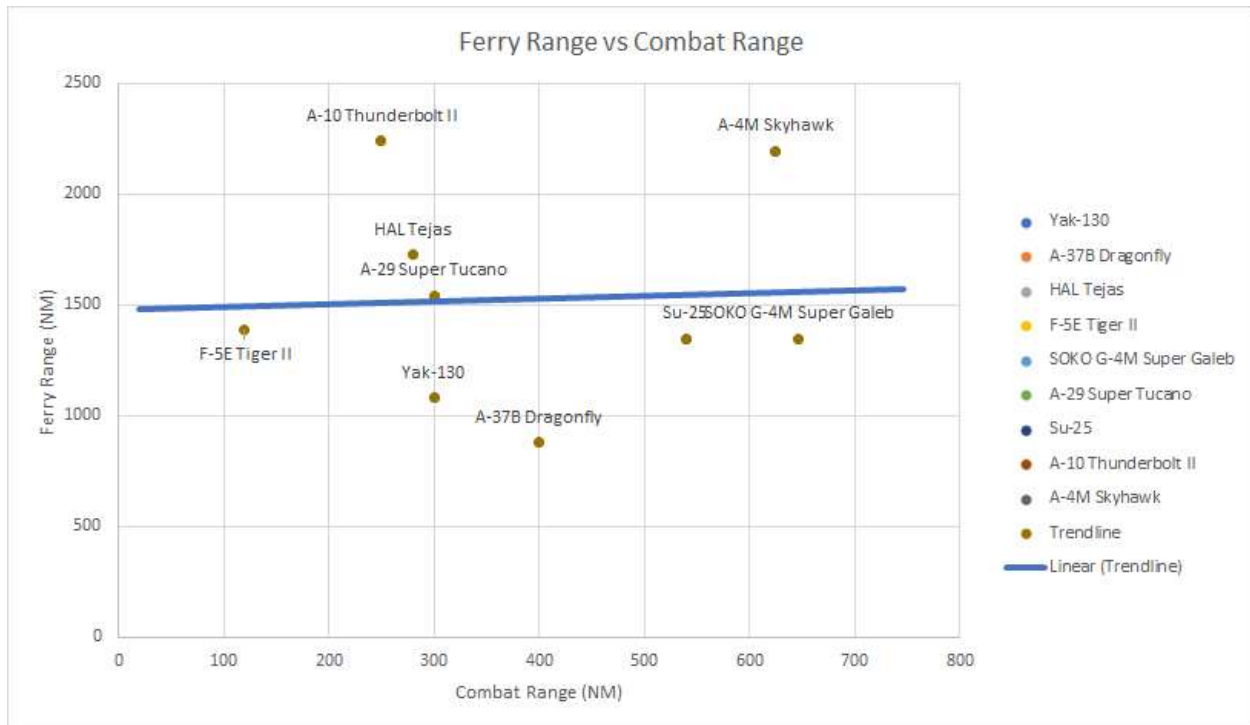
Figure 7: Ferry Range v. Combat Range

Figure 7 depicts the ferry range and combat range of the similar aircraft studied. While there are outliers in the A-10, A-4, and A-37, most aircraft fall along the trendline with a ferry range somewhere near 1,500 NM. As per the RFP [26], the ZA-21 must have a ferry range of 900 NM with reserves.

After examining the performance of the selected group of similar aircraft and referencing their dimensions and design, some conclusions were drawn. The increased maneuverability of the A-37B is attributed to its low wing sweep. Aircraft such as the Yak-130 and the A-4M Skyhawk tout extremely low takeoff and landing distances. Wing loading and thrust to weight ratio are important parameters when analyzing takeoff and landing distance. The A-10 Thunderbolt II is impressive when analyzing survivability and cost to produce. However, the A-10's survivability is based on armor rather than electronic capabilities. In a current day combat situation, armor is not as important as the ability to escape surface-to-air missiles. Advancements in electronics and increased maneuverability can mitigate the risk of the ZA-21 being shot down during combat.

B. Constraint Analysis

T/W and W/S are two of the most important parameters in aircraft design. A lower W/S allows lower takeoff/landing speeds, increased maximum takeoff gross weight (MTOGW), and higher maneuverability. A lower

W/S allows for more payload (armament) on takeoff. A lower W/S allows for more armament or jettisonable fuel tanks for the aircraft. This is proven because a higher W/S at constant wing area will result in a higher MTOGW. However, this must be optimized as an increased MTOGW yields a decreased T/W ratio and therefore decreased maneuverability.
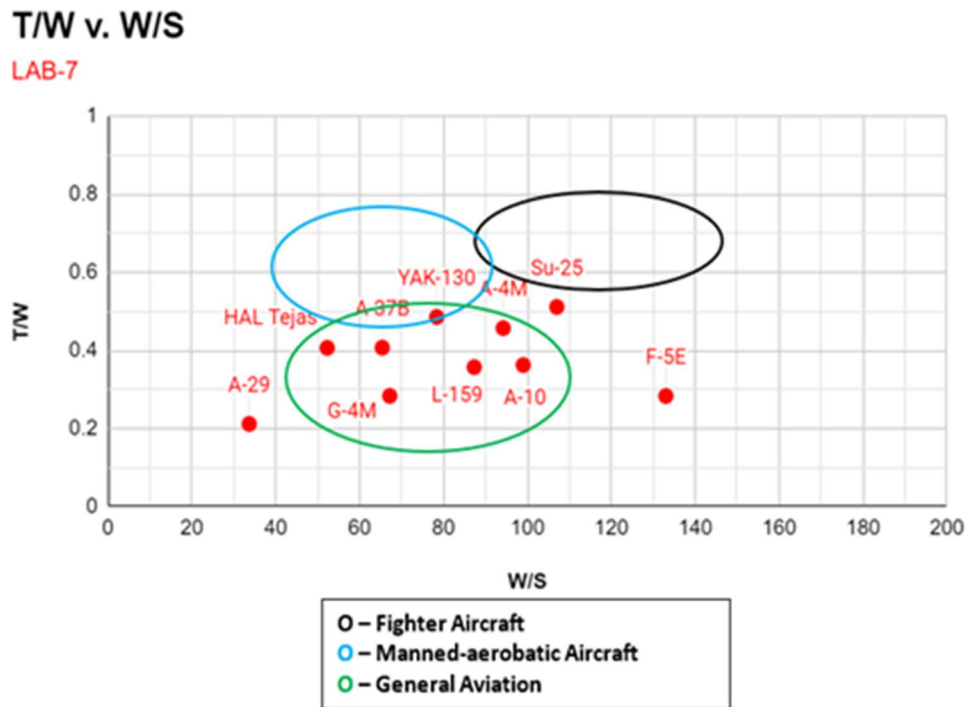
Figure 8: T/W v. W/S Historical Aircraft

Figure 8 is the T/W vs. W/S diagram of initially researched aircraft. These two factors can also be analyzed to form an aircraft constraint diagram (Figure 9) based on the set of requirements below:

- Rate of Climb – minimum 7000 ft/min at sea level

- Sustained Load Factor – minimum 4 g's at sea level

- Takeoff Distance – maximum 2800 ft at SL and 3500 ft at 6000 ft density altitude

- Landing Distance – maximum 2800 ft at SL and 3500 ft at 6000 ft density altitude

The requirements for takeoff and landing distances were established during the system requirements review, and from further discussion, rate of climb and sustained load factor requirements were established based on expected mission profiles and similar aircraft performance as researched during the similarity analysis.
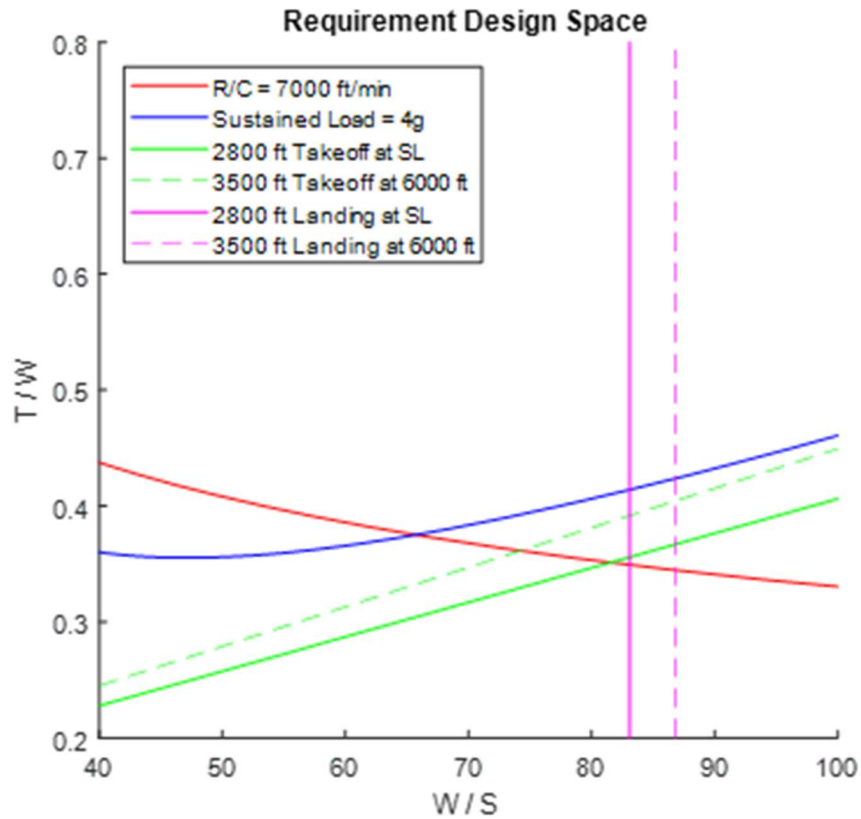
Figure 9: Initial Constraint Analysis

Each of the six design curves, in Figure 9, are determined from equations established using the listed requirements for the aircraft. As is visible in the above plot, the driving constraints for the design space are Sustained Load Factor, Max Rate of Climb, and Landing Distance at 2800 feet density altitude. The feasible design space is shown in Figure 10.
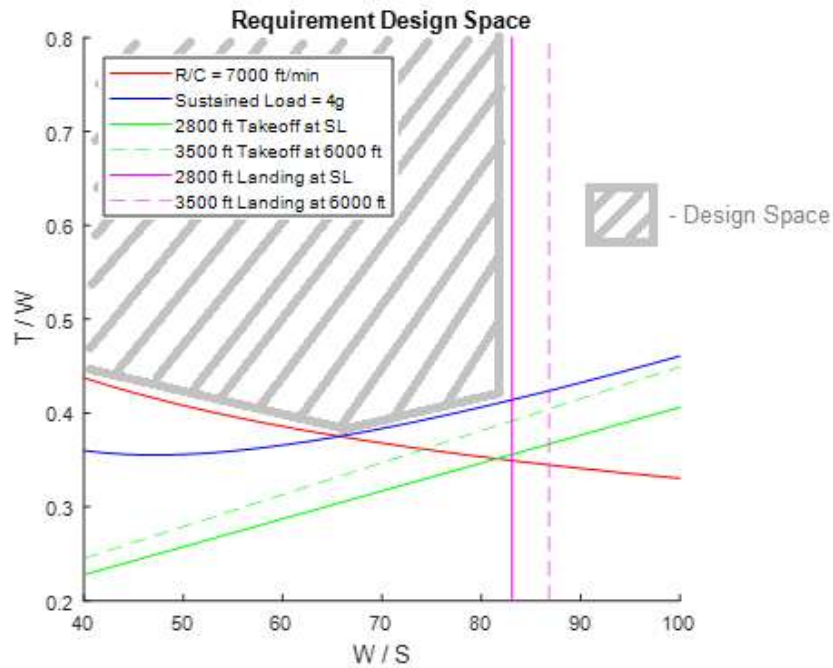
Figure 10: Design Space in Initial Constraint

As seen in Figure 10, the size of the available design space provides a large amount of feasible design possibilities. Additionally, the expected design point within the area of lighter military aircraft without having the greater wing loading and T/W that fighters have. Many of the aircraft researched during the similarity analysis also fit will within this design space.

A few major assumptions were made throughout the constraint analysis. The value of C_{D0} was assumed to be 0.0279. This value was the average of each of the C_{D0} values calculated from the 3-view drawings of historical aircraft. The equation used to calculate each value of C_{D0} was as follows:

$$C_{Do} = C_{fe}\left(\frac{S_{wet}}{S_{ref}}\right)$$

Another assumption made was aspect ratio, AR, which was assumed to be 5. This value was chosen based on historical aircraft data analysis. The takeoff and landing C_{Lmax} values were both assumed to be 1.9 [1]. This value was determined from a University of Texas document that listed typical values of C_{Lmax} for various aircraft classes. LAB-7 estimated the ZA-21 to have a MTOGW of between 20,000 to 30,000 lbs. Looking at trends of T/W, it was seen that a loose majority of similar light attack and ground support aircraft fell in the range of 0.35 to 0.45 for T/W. As seen in Figure 10, the design space supports this T/W range.

C. Constraint Sensitivities Analysis

The following section investigates the sensitivity of the resultant Constraint Diagram to +- 10% changes in the input variables and requirements.
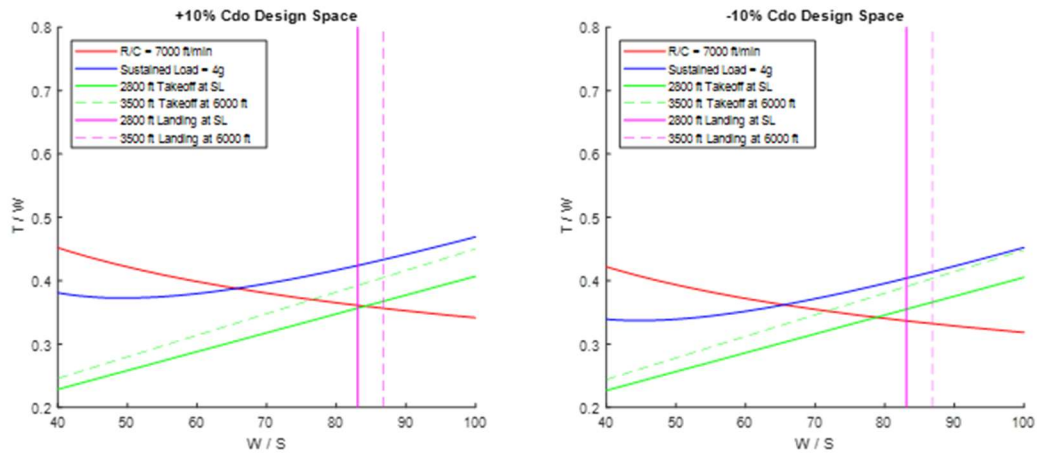
Figure 11: 10% C_{D0} Sensitivity
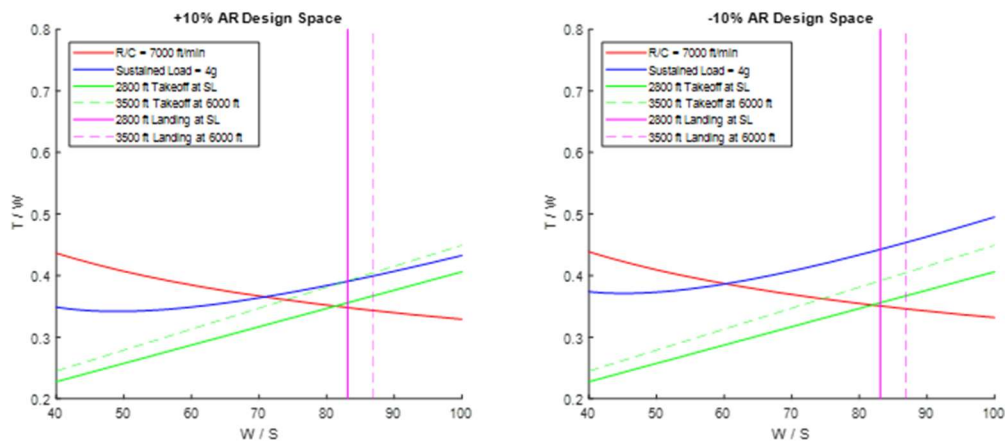
Figure 12: 10% Aspect Ratio Sensitivity
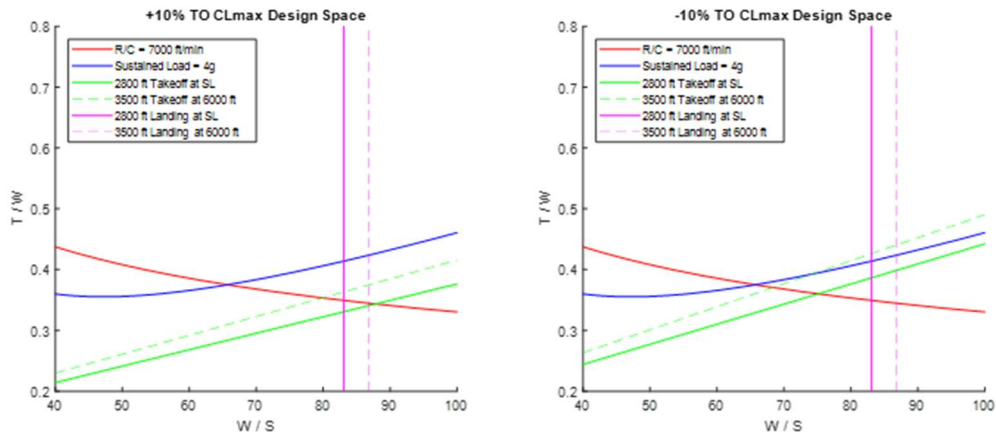
Figure 13: 10% Takeoff C_Lmax Sensitivity
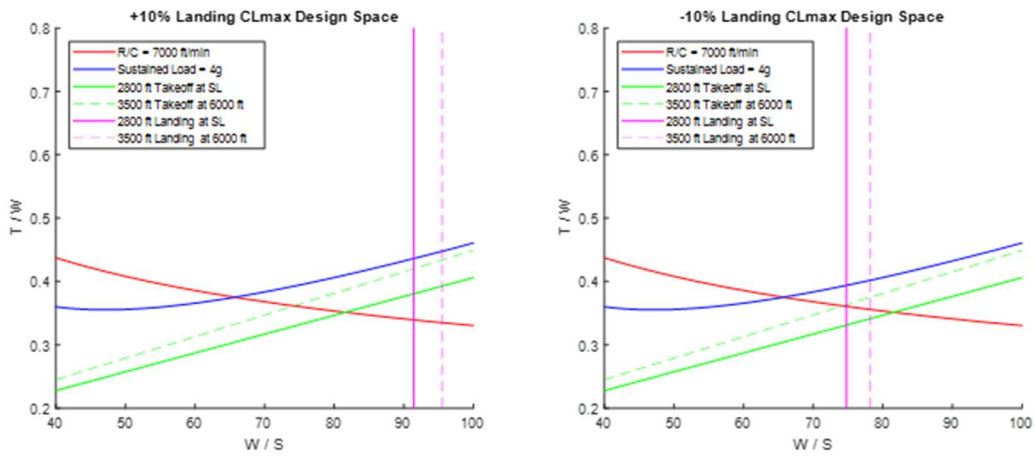
Figure 14: 10% Landing C_Lmax Sensitivity
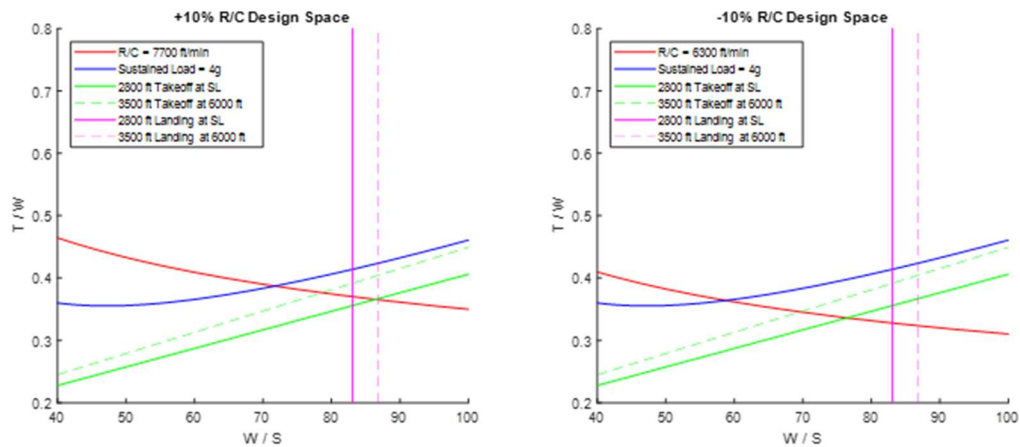
Figure 15: 10% R/C Sensitivity
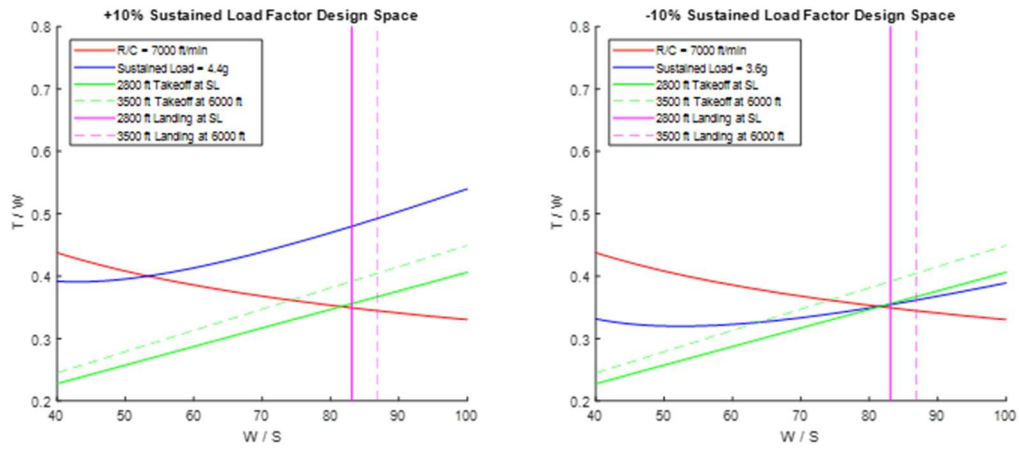
Figure 16: 10% Sustained Load Factor Sensitivity
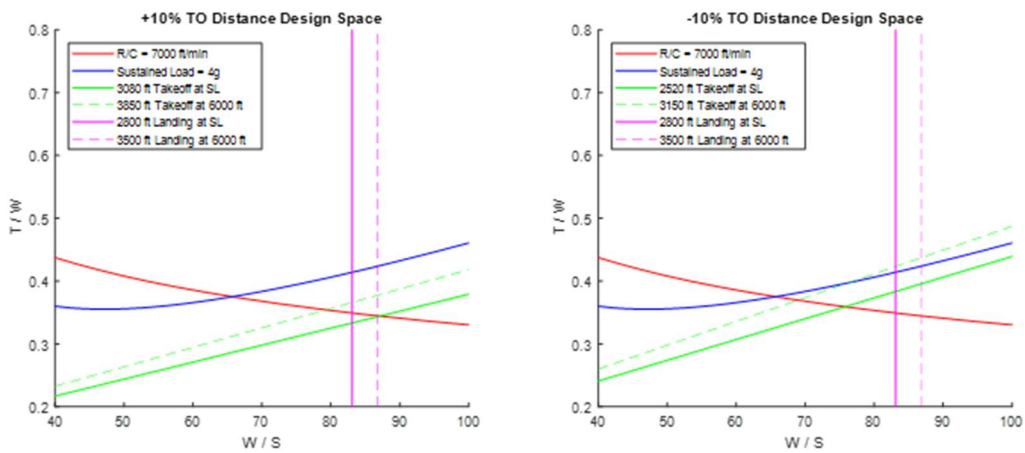
Figure 17: 10% Takeoff Distance Sensitivity
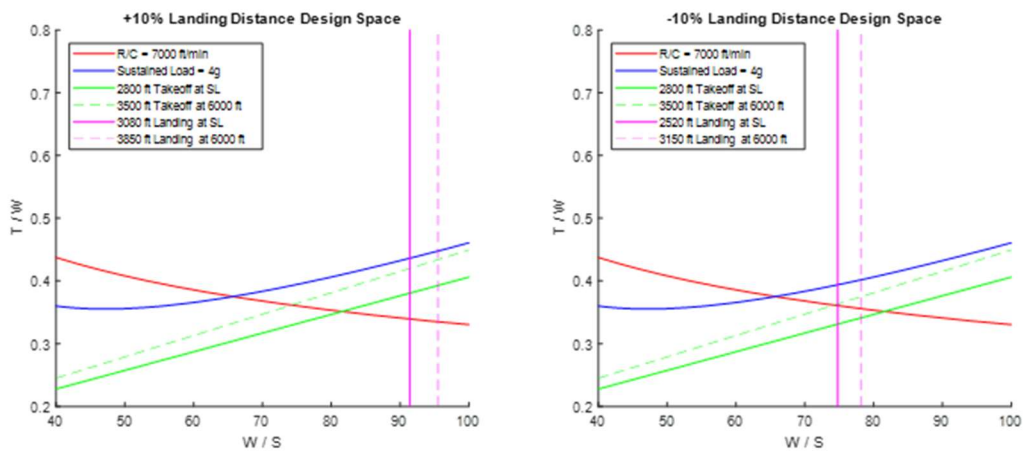
Figure 18: 10% Landing Distance Sensitivity
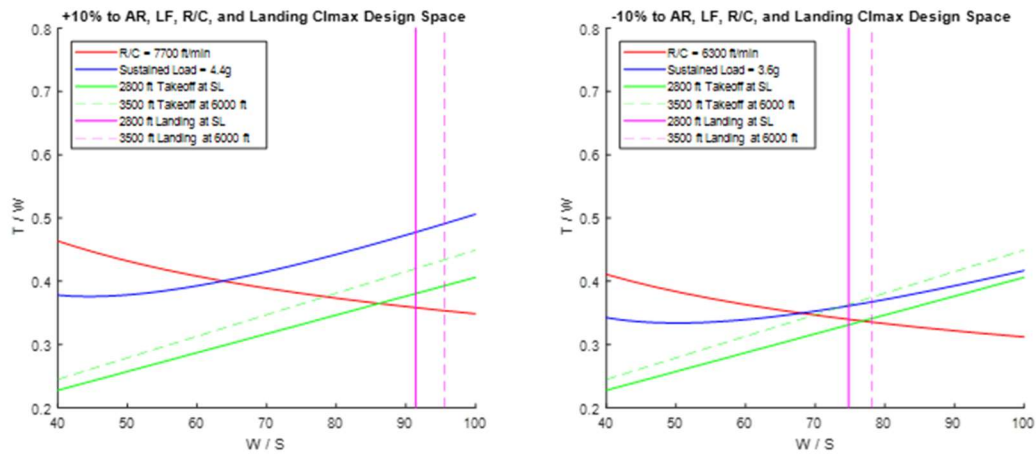
Figure 19: 10% Overall Sensitivity

Based on the analysis of the sensitivities in this section, the largest changes come from adjusting four different variables. These variables include the sustained load factor, the landing distance, the landing C_{Lmax}, and the R/C requirements or input variables. Increasing the sustained load factor closes the design space and resultantly requires a significantly higher thrust to weight ratio. Decreasing the required sustained load factor opens the design space and causes takeoff distance to replace sustained load factor as a limiting factor. Increasing either landing distance or landing C_{Lmax} parameters have the same effect. Increasing these expands the design space, which allows for higher wing loadings. Decreasing both the landing distance or the landing C_{Lmax} has the opposite effect: closing the design space and limiting the craft to lower values of wing loading.

V.   Configuration

A. Design Morphology

The largest components of overall design of the ZA-21 have to do primarily with the weight class of the aircraft. The RFP emphasizes that the aircraft in question should be a "light attack aircraft" which is typically a term reserved for low-weight, ground-support aircraft. Overarching factors affecting weight drastically were of primary concern for early design decisions. Among these, payload limits and engine type were critical for ensuring the aircraft could complete the design mission while remaining inexpensive to build and operate.

For payload, the minimum requirement of 3,000 lbs provided a low-end weight target, but it was still necessary to determine a maximum payload capability in order to properly begin aircraft configuration, as payload weight was one of the largest factors in aircraft sizing. Based on the analysis of similar use-case aircraft, a clear correlation was found between maximum payload weight and the max takeoff gross weight of the aircraft, thus if payload weight were chosen, overall weight could be estimated. After examining typical light attack missions, as well as the capability and typical payloads of similar light attack aircraft, a maximum payload weight of 6,600 lbs was chosen. This was chosen to expand the usability of the aircraft across multiple combat missions, while retaining the small size and low cost of the aircraft. This payload weight fits closely in line with many of the previous submissions for the USAF's Light Attack/Armed Reconnaissance program, as well as the similar aircraft researched and discussed in section IV.

Another major design component considered was engine type selection. The design mission for this aircraft is unique in that it requires extended on-station time, far longer than that of typical combat missions. High performance military turbine engines often do not have the low fuel consumption required to maintain this. Turboprop engines were considered as an alternative; however, it was deemed that the added fuel efficiency was outweighed by the limited performance and thrust ceiling of turboprop engines. Ultimately it was chosen to go with a commercial turbofan engine. These engines are often designed more with fuel efficiency rather than raw performance in mind, however with proper mindfulness, they can be used well in military applications. This provided the ZA-21 with far more fuel-efficient engines for longer loiter times, with little performance loss.

B. External Layout

1. Fuselage

Due to the utilitarian approach of designing an attack aircraft, the structure of the fuselage for the ZA-21 was determined primarily by the arrangement of components within the aircraft. The first factor in this was engines. With a twin engine, over-wing intake design chosen, the aft section of the fuselage was first designed around the width and length of the engine and the required space for the intakes. The center section was then extended forward to make room for the nose, cockpit, and fuel tanks. It was chosen to keep internal fuel within the fuselage only, rather than having small wing-tanks. This allows for better roll authority by keeping this extra mass closer to the aircraft's center of gravity. The overall fuselage structural length is 33.5 ft with a structural height of 5.47 ft. The cockpit bubble extends above this. The rear engine and intake section is 12.64 ft long and 8.56 ft wide while the forward cockpit and nose section is 20.86 ft long and 4.15 ft wide. Overall, the fuselage is fairly straight sectioned with no upward or downward taper at the nose or tail. This was done to ensure the exhaust nozzles of the engine were kept brief and straight, as well as to allow space for the over-wing intakes.

An important consideration of the nose section of the fuselage was pilot viewing angles. Due to the high seating, bubble cockpit, side viewing angles were a non-issue, however the nose cone required a series of redesigns to provide a better pilot viewing angle. This angle can be seen depicted in Figure 20 below:
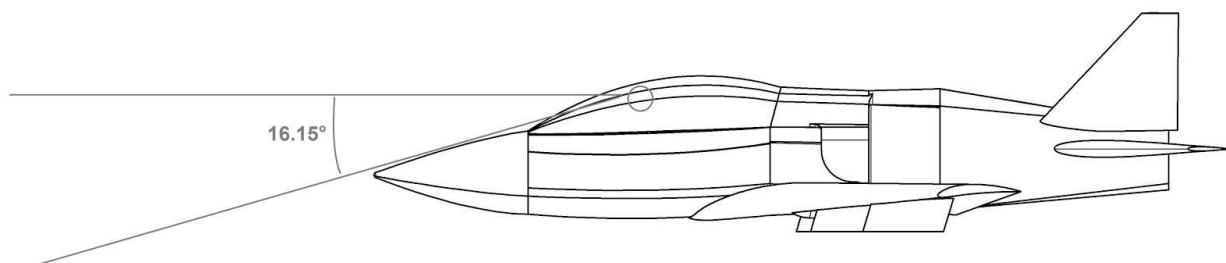
Figure 20: Pilot Viewing Angle

2. Engines

For the ZA-21, a dual engine configuration was chosen. After consideration of both single and dual engine designs, it was determined that two engines would be better primarily for survivability. As a light attack and ground attack aircraft, small arms fire, rockets, and missiles are concerns that must be addressed in design. In the event a

single engine is disabled due to sustained damage, a dual engine configuration allows the Shrike to remain in the air and return to a friendly airfield, saving both valuable lives and resources.

Additionally, the ZA-21 is expected to operate from austere fields. Because of this, it was chosen to mount the engines above the wings. This allows for shorter intake ducts with less weight, and it also protects the engines from foreign object debris during takeoff and landing. Other configurations considered were a single engine with a split intake duct as well as dual engines with under-wing engines, however both of these were determined inadequate for the use case specified by the RFP. Both engines are located in the rear fuselage section, side-by-side exhausting between the outboard horizontal control surfaces. Placing the exhaust between the horizontal control surfaces reduces infrared signature by a small amount and lessens the length and thus weight of the aircraft.

3. Wing

The wing for the ZA-21 was designed primarily from constraint analysis parameters. Based on the required wing loading and selected max takeoff gross weight, a wing area of 275 ft^2 was chosen. Based on analysis of other light attack and ground attack aircraft, an aspect ratio of 5 was also chosen. The high wing area and aspect ratio allow for short takeoffs and landings due to less induced drag and lower wing loading, satisfying austere runway performance.

The main wing has a quarter-chord sweep of 25 degrees. This was done to increase the drag divergence Mach number of the aircraft, allowing for operation at higher speeds. This was necessary to achieve the dash performance desired for mission cruise entry and exit. Additional information on wing parameter selection is available in Section VII.

4. Empennage

For the empennage, a twin-tail configuration was chosen. Other configurations considered were a conventional tail, and an H-tail, however it was determined that a twin-tail would be the best fit for the ZA-21. The nature of a split horizontal tail allows the engine exhausts to fit between, masking some thermal signature. Additionally, having two vertical tails causes both to be shorter than a single conventional tail. This helps to minimize radar cross section. As an added benefit, a twin tail configuration is still capable of limited operation in the event damage is sustained to one vertical tail during combat. The horizontal tail has a 15.51 ft span with a quarter chord sweep of 30 degrees. The horizontal tail has a 5 ft height with a quarter chord sweep of 35 degrees. The vertical

tails are canted at 10 degrees to reduce radar cross section and to provide a slight increase to pitching moment on takeoff. Further analysis of the empennage design can be found in Section X.

5. Weapons Stations

The ZA-21 has a total of seven external weapons stations. Numbered left to right, station 1 is the port wingtip attachment point, stations 2 and 3 are placed under the port wing, station 4 is located on the centerline of the fuselage, stations 5 and 6 are placed under the starboard wing, and station 7 is the starboard wingtip attachment point. Each station aside from wingtip hard-mounts include an Integrated MAU-50/A for arms carriage. Table 4 below supplies pertinent data regarding the locations, weight, and abilities of each station.

Station	1	2	3	4	5	6	7
Pylon Weight (lb)	0	130	130	100	130	130	0
Description	wingtip	underwing	underwing	fuselage	underwing	underwing	wingtip
Chord-wise Location (ft)	24.1	22.3	20.1	19.5	20.1	22.3	24.1
Butt Line Location (ft)	18.5	13	8	0	8	13	18.5
Load Rating (lb)	350	700	1300	1600	1300	700	350

Table 4: Weapons Stations Pertinent Data

6. Integrated Gun

The ZA-21 has an onboard gatling cannon for engaging lightly armored ground targets as well as slow moving air targets such as helicopters. After consideration of multiple cannons, the XM-301 was decided on for its high accuracy, low recoil, and exceptionally low weight. The XM-301 is mounted on the left side of the forward fuselage, next to and below the cockpit. For ammunition loading, storage, and feed system, a modified form of the F-16's rotary storage drum with loading access on the right side of the fuselage. Further information about the gun can be found in Section XIII.

7. 3-view
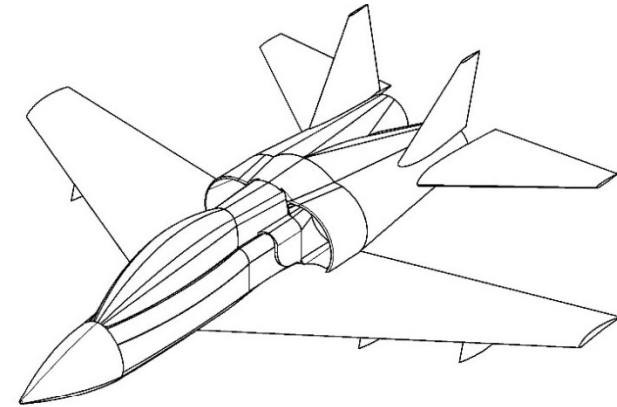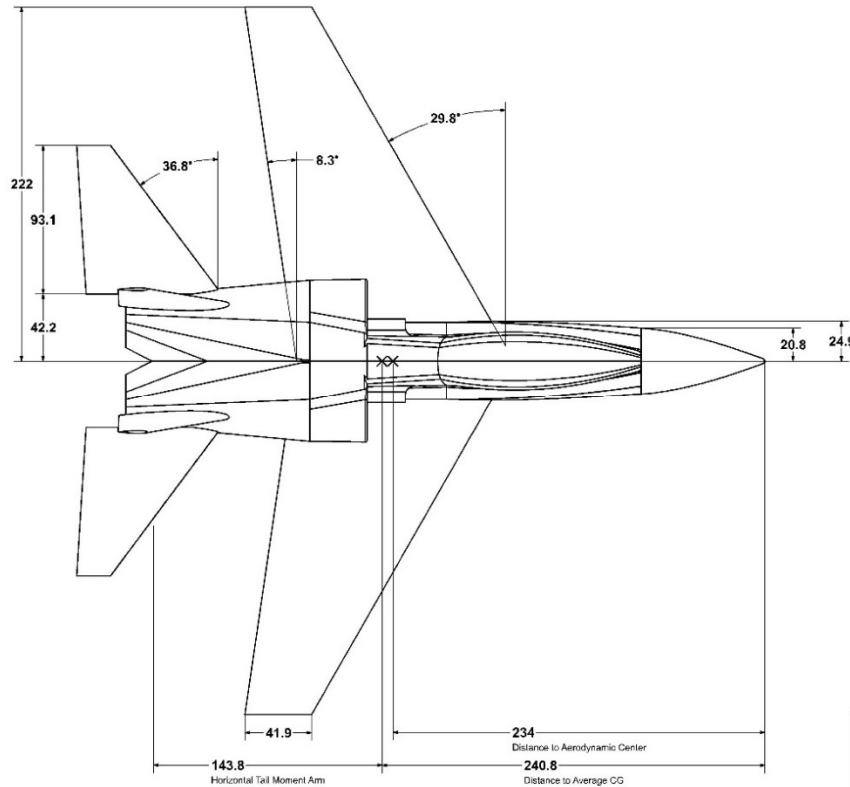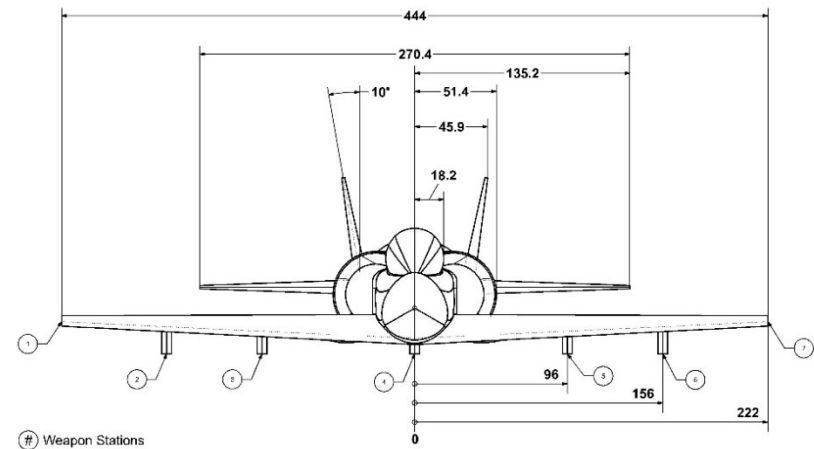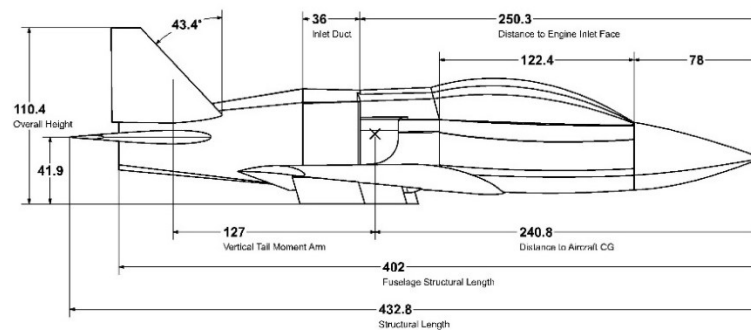
Figure 21: ZA-21 Dimensioned 3-View

C. Payload and Armament

The ZA-21 was designed to carry a variety of weaponry for different mission goals. An overall capability diagram can be found below with designed-to munitions listed for each station. Unlisted arms may still fit the ZA-21 as long as landing gear clearance, ground clearance, and weight limits are met. The operational arms compatible with the Shrike include self-defense air-to-air missiles, ground attack missiles, rocket pods, as well as guided bombs and some cruise missiles. While not applicable to every mission, this variety allows the ZA-21 to effectively execute far more mission classes at a lower operational cost than other aircraft.

	1 (350 lbs)	2 (700 lbs)	3 (1300 lbs)	4 (1600 lbs)	5 (1300 lbs)	6 (700 lbs)	7 (350 lbs)
AIM-9 Sidewinder (LAU-129)	X						X
AIM-120 AMRAAM (LAU-129)		X				X	
7x Hydra 70 Mk 66 (LAU-68)	X	X				X	X
19x Hydra 70 Mk 66 (LAU-61)			X		X		
2x AGM-114 Hellfire (M310)		X				X	
AGM-65H Maverick (LAU-117)		X	X		X	X	
AGM-88 HARM (LAU-118)			X	X	X		
AGM-154 JSOW (BRU-57)				X			
Mk-82 LDGP (MAU-50/A)		X	X	X	X	X	
GBU-38 (MAU-50/A)		X	X	X	X	X	
GBU-12 (MAU-50/A)		X	X	X	X	X	
GBU-16 (MAU-50/A)			X	X	X		
CBU-100 (MAU-50/A)		X	X		X	X	
4x GBU-39 SDB (BRU-61/A)				X			
AN/AAQ-33 Sniper ATP		X	X		X	X	
LANTIRN TP		X	X		X	X	
LANTIRN Nav		X	X		X	X	
AN/ALQ-131 ECM		X	X		X	X	
150 Gal. EXternal Fuel Tank				X			

Figure 22: Weapons Stations Capability Chart

Additionally, for the purpose of the design and ferry missions, as well as for determination of general performance characteristics, a set of nominal design payload configurations have been determined. Outlined below in tables 5 and 6 are the arms layout of the ZA-21 for the design and ferry missions. All performance characteristics are quoted at the design nominal configuration unless otherwise specified.

Design Mission (Nominal) Configuration			
Station	Armament	Arms Weight (lb)	Loaded Weight (lb)
1	Aim-9	188	278
2	LAU-68	247	333
3	AGM-65H	465	600
4	GBU-16	1010	1010
5	AGM-65H	465	600
6	LAU-68	247	333
7	Aim-9	188	278
Cannon	566 rds 20x102mm	300	300
Total:	-	3110	3732
		Delta Cdo:	0.01124

Table 5: Design Mission (Nominal) Payload Configuration

Ferry Configuration			
Station	Armament	Arms Weight (lb)	Loaded Weight (lb)
1	Aim-9	188	278
2	LAU-68	247	333
3	Mk-82 LDGP	502	502
4	-	0	0
5	Mk-82 LDGP	502	552
6	LAU-68	247	333
7	Aim-9	188	278
Cannon	566 rds 20x102mm	300	300
Total:	-	2174	2576
		Delta Cdo:	0.00760

Table 6: Ferry Mission Payload Configuration

Drag estimations for hanging stores were based on estimations in Raymer [25] as well as the 2009 Weapons File from the Air Force Air Armament Center (source). Drag for the pylons themselves were based on scaled sizing and drag of the hanging stores pylons for the A-10 Thunderbolt II.

D. Internal Layout

Internal layout was done using Siemens NX 3-D modeling software. Primary systems and their associated volumes were modeled in general form and placed within the aircraft. Smaller components such as individual avionics components or engine components were grouped into larger labeled volumes. The two images below outline the location of various internal elements, as well as depicting their approximate volumes.
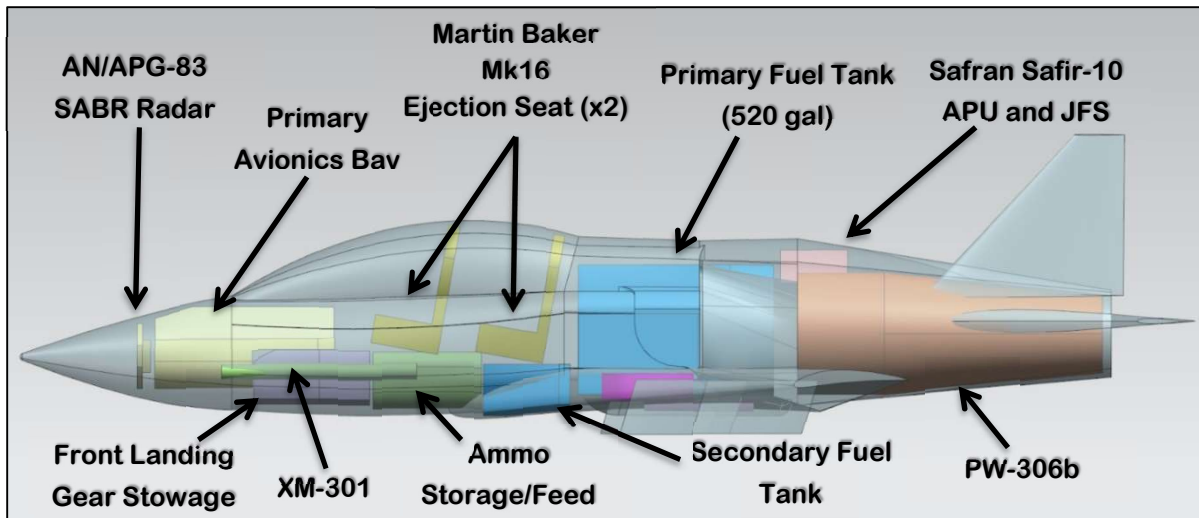
Figure 23: Internal Layout Side View
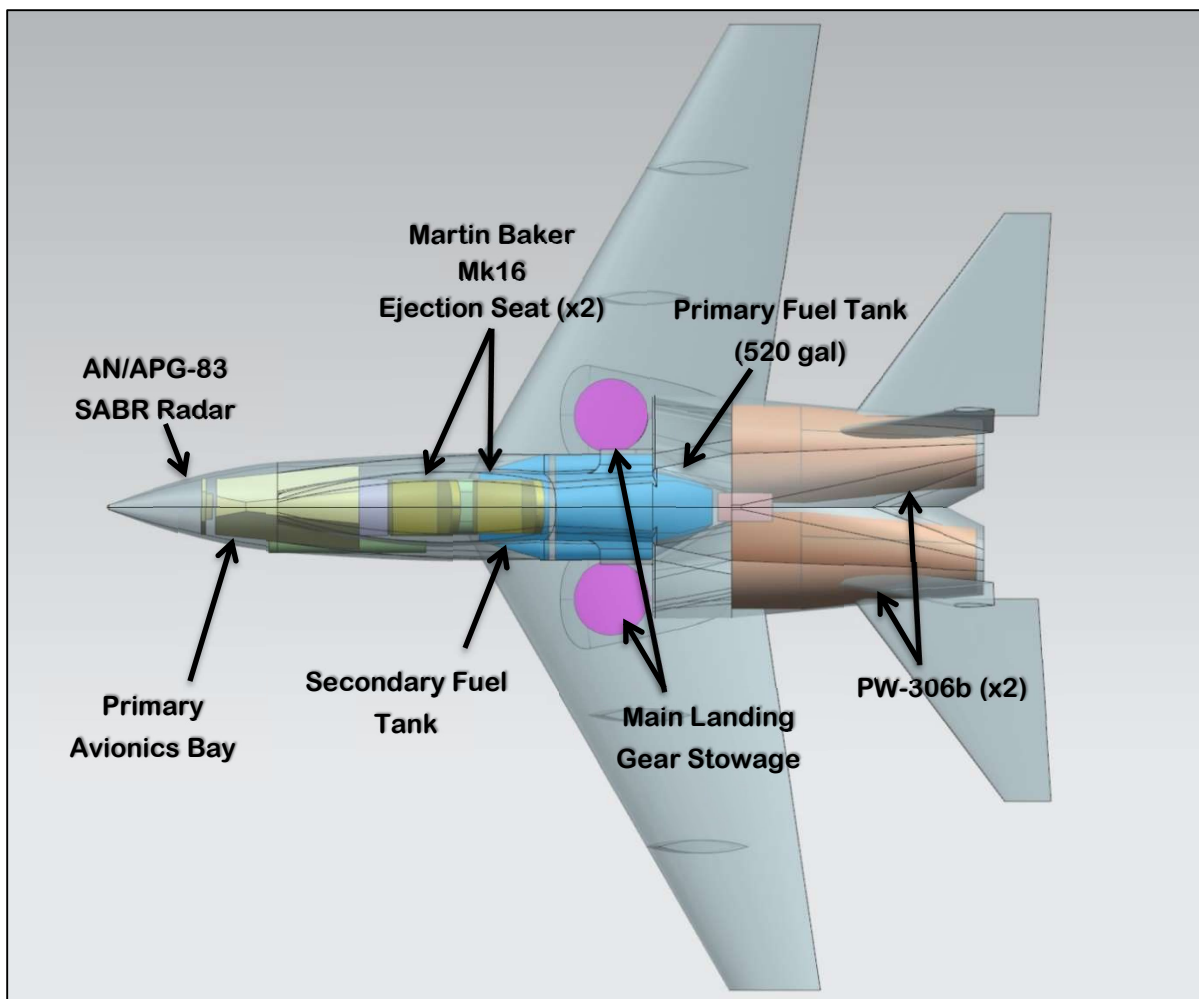
Figure 24: Internal Layout Top View

VI.   Propulsion

Figure 25: Pratt and Whitney 306b

A. Engine Selection

  Many engines within similar aircraft, shown in Table 7, were investigated as potentials for the engine of the

ZA-21. The main parameters looked at were size, thrust, and survivability.

Engine	Manufacturer	Thrust (Uninstalled, lbf) / Per Engine	SFC (lb/(lbf*h))	Weight (lbs)	Length (in)	Diameter (in)	Bypass Ratio
HTF5000	Honeywell Aerospace	5,000	0.42	1534	92.4	34.2	4.4
TFE731-5BR	Honeywell Aerospace	4,750	0.517	899	49.7	39.4	2.8
AI-222	Ivchenko-Progress	5,553	0.66	970	77.17	25.2	1.19
Adour	Turbomeca-Rolls Royce	6,000	0.81	1,784	114	22.3	0.8
J47-GE-7	GE Aerospace	5,970	1.014	2,554	145	36.75	0
F124-GA-200	Honeywell Aerospace	6,300	0.78	1,050	102.1	36	0.49
F3-IHI-30	Ishikawajima-Harima	3,680	0.7	750	79	25	0.9
M88-2	Snecma	11,200	0.782	1,978	139.3	27.4	0.3
PW306b	Pratt and Whitney	5,922	0.402	1,151	81.2	44	4.5
TF34	GE Aerospace	9,275	0.363	1,478	100	52.2	6.5

Table 7: Engine Considerations

The need for either one or two engines was discussed. Twin and single engine configurations were considered. Twin engines provide a level of survivability that is unattainable with a single engine and were therefore chosen. To maintain a proper thrust to weight as determined by the sizing analysis in Section IV, the engine(s) had to produce at least 12,000 pounds of thrust before installation corrections. Table 7 shows the engines considered for the ZA-21 Shrike along with the most pertinent characteristics of each engine as it applies to the design process.

The preliminary engine choice was the Honeywell F124-GA-200. This engine had mostly ideal specifications: thrust, weight, BPR. All requirements were met except one, specific fuel consumption. After early iteration design, it was discovered that the engine consumed too much fuel to complete the required design mission. Even though this engine was used on some of the other aircraft researched during sizing analysis, it was found that none of said aircraft could meet the fuel consumption requirements of the design mission. The Shrike with the F124-GA-200 could complete the given ferry mission successfully, but the loiter time requirement in the design mission made this engine choice illogical. After further review, it was determined that the high specific fuel consumption of 0.78 was the limiting factor, and a new engine must be selected.

Engine selection then changed to a higher bypass, lower SFC engine. The list of potential engines was examined again to find a suitable engine. The option of single versus dual engine configurations was re-evaluated, however the same determination of a twin-engine design was made. Because the engine reconfiguration started with SFC, a maximum SFC of 0.5 was set in order to meet the mission requirements. With the new internal requirement of under 0.5 SFC, two potential engines from the original list remained: the HTF5000 and PW-306b.

While neither engine was perfectly ideal in terms of thrust, an alternative route could be considered. Using parameters set by Raymer [25], the engines could be scaled up in size as long as thrust to weight was kept the same. Using this procedure, the SFC will remain the same while increasing both the thrust and weight. The primary downfall of "rubbering" an engine in this way is that the development cost of the modified engine increases. To match the thrust performance of the previous engines, the target thrust for a single engine was 6300 lbs. This led to a large disparity between the two remaining engine options. The HTF5000 needed about a 20% increase in thrust and weight, this engine quickly became a non-option as it was extremely heavy and would cost too much to upgrade the engine. This left the group with one engine to use: the PW-306b. The engine was able to meet the internal requirement of 6300 lbs

of thrust with a ~6% increase to thrust to weight. Therefore, a twin layout of the PW-306b was selected as the new configuration moving forward.

B. Engine Performance

Thrust		General Engine Information	
6,300	lbs (uninstalled)	Pressure Ratio	15.5
5,411.7	lbs (installed)	Bypass Ratio	4.5
10,823.4	Tot lbs (installed)	Inlet Temp (K)	1,445
		SFC (lb/lbf-hr)	0.407
Engine Specs		T/W	5.15
2	Engines		
81.2	Length (in)	*Thrust and Weight Before Scaling	
6.77	Length (ft)	5,933	Thrust (lbs)
38.2	Diameter (in) FAN	1,151	Weight (lbs)
3.18	D (ft) FAN	6.19%	Upscale
7.96	Area (ft^2) FAN		
1,222.35	Weight/Engine (lbs)*		

Table 8: Basic PW306b Datasheet

The Pratt and Whitney 306b is a medium bypass turbofan engine. While this engine is primarily used for business jet applications, the specifications of the PW306b provide an adequate solution to the propulsion problem. The length of the engine is within the initial guess' on the length of the aircraft. Since the reevaluation of the engine took place, the width was a changing factor in the design. As explained in the last section, the engine ultimately needed a larger bypass ratio to achieve the necessary fuel consumption. To compensate for the larger bypass ratio, the width of the aircraft needed to be wider, as well as the inlet (covered in the next section).

The base thrust of the engine was 5,933 lbs which was slightly below the thrust needed for the mission requirements. As covered quickly in the last section, the engine would have to be upscaled to be able to meet mission requirements. The target thrust was 6,300 lbs which led to an upscaling of 6% on the engine. The weight of each engine then was increased from 1,151 lbs to 1,222 lbs.

While the thrust of the engine is 6,300 lbs, the aircraft inlets have installed thrust corrections that lower the overall thrust the engines can produce. There are five thrust corrections: pressure recovery, bleed extraction, engine

bleed, engine power extraction and inlet distortion. Engine bleed, engine power extraction, and inlet distortion are all assumed to be zero due to the manufacturer nozzle design being the one used. That leaves the two primary thrust corrections to be pressure recovery and bleed extraction. The equation for percent thrust loss in pressure recovery are as follows: $\% \, Thrust \, Loss = C_{RAM} \left[\left(\frac{P_1}{P_0} \right)_{ref} - \left(\frac{P_1}{P_0} \right)_{actual} \right] * 100$. The variable C_{RAM} in the equation is 1.35 for subsonic flight. The equation for bleed extraction is as follows: $\% \, Thrust \, Loss = C_{BLEED} \left(\frac{Bleed \, Mass \, Flow}{Engine \, Mass \, Flow} \right) * 100$. Raymer [25] says for initial estimates, C_{BLEED}, can be estimated to be 2. Bleed mass flow can be estimated to be 1-5% of the mass flow. 1% being a straight duct and 5% being an S duct, since the Shrike uses something in between, a 3% bleed flow was estimated. Thus, pressure recovery loss is ~8.1% and bleed extraction is ~6%. These results in an 14.1% loss in installed thrust when compared to the base thrust of the engine. This leaves the aircraft with ~5,411 lbs of thrust per engine resulting in a total net thrust of ~10,823 lbs of thrust. This gives the aircraft of a thrust to weight of 0.49 during the design mission. Using liberal estimates for the installed thrust losses, the total net thrust of the aircraft can be up to ~12,000 lbs of thrust, which would be more than enough thrust for any given mission and give pilots more thrust to work with. Using the installed thrust value, the Shrike's thrust and SFC values at altitude can be estimated. In Figure 26 the thrust capability at each altitude is shown. In Figure 27 the SFC of the Shrike is shown.
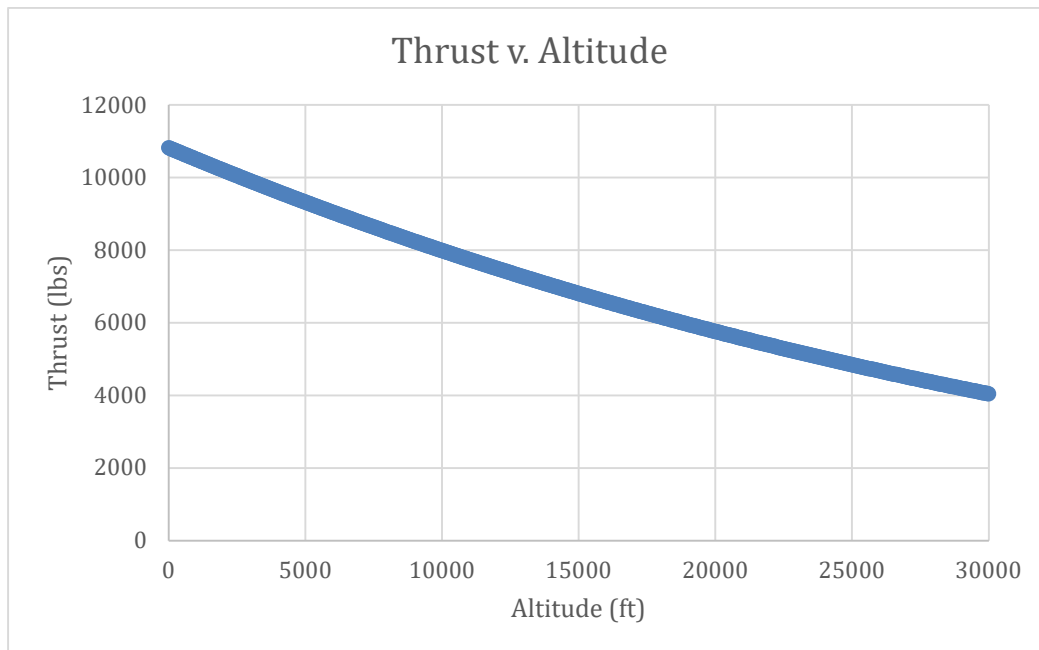
Figure 26: Thrust Available per Altitude
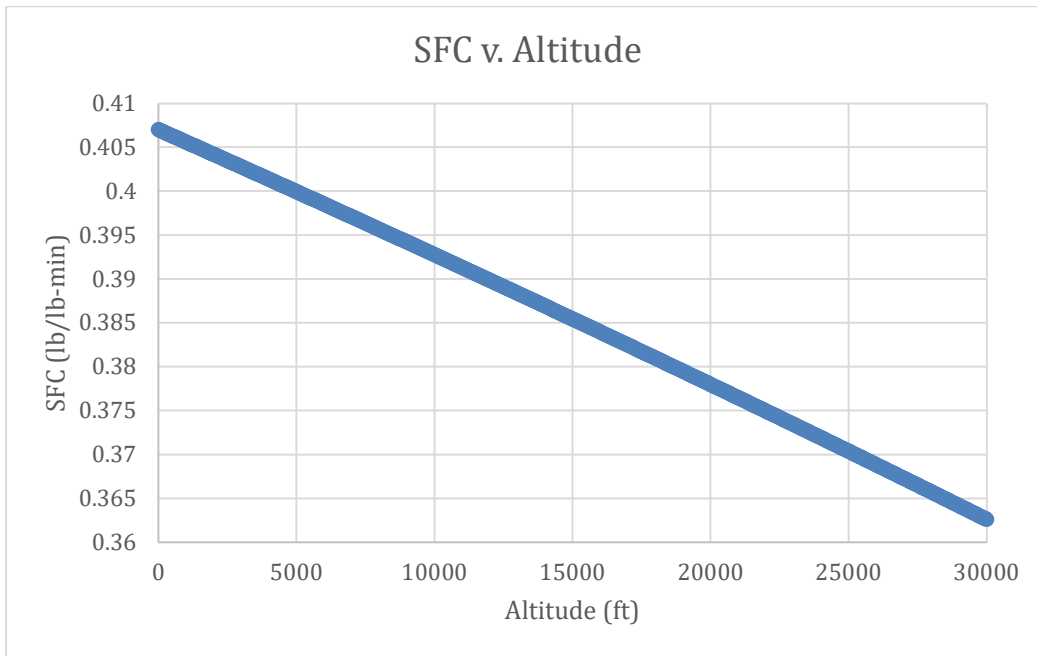
Figure 27: Engine SFC per Altitude

C. Inlet and Capture Area
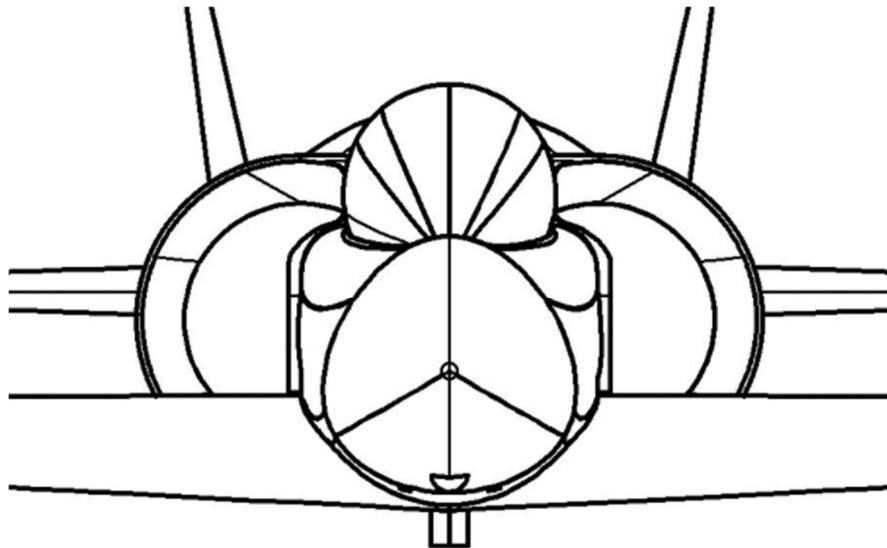
Figure 28: Inlet Front Face

The inlet area of the Shrike is determined from the capture area of the engine. The capture area can be calculated several different ways, however for the sake of simplicity, it was calculated using an equation of capture area over mass flow equals a constant provided by Raymer [25]. The ratio between capture area over mass flow is 0.025. Using this ratio, the capture area was found. This ratio changes with speeds over Mach 1, but because the Shrike

will not be experiencing those speeds, the ratio remains the same. The inlet area must be bigger than the smallest capture area so that engines can achieve maximum rated thrust. The mass flow for the engine is not given, so using parameters set by Raymer [25] we are able to find the mass flow of the engine. Raymer [25] gives the explanation "if mass flow is not known, it can be estimated to be 26 times the square of the engine front-face diameter in feet." This gives a clear path to calculating the mass flow, which was determined to be ~263 lbs/s. After finding the mass flow, and setting the ratio to be 0.025, the capture area is estimated to be 6.59 ft^2. The inlet of the engine has an area of 7.59 ft^2. Note that the capture area is a minimum the inlet area can be to get the full amount of thrust for the engine.

The engine placement on the aircraft is to be embedded in the fuselage for maximum protection from enemy fire. This required an analysis and implementation of heat shields so the extreme heat of the engine would not damage other components of the fuselage. This also required clever designing of the inlets to fit on the aircraft. The CAD team worked with the propulsion team to shape the inlet around the aircraft to keep it tight to the aircraft while providing an area adequate for the capture area. The exhaust area was designed with maximum thrust in mind. Since the aircraft will not exceed the speed of sound, this simplifies the exhaust design process. Raymer [25] states that the exhaust for non-supersonic planes can have an exhaust area of 0.3 to 0.5 of the capture areas. This was set at 0.4 and the resultant area was calculated to be ~4 ft^2. With the aircraft designed around the engines, and the engine configuration having all necessary stipulations met, the ZA-21 has enough power to complete even the most arduous missions required according to the AIAA RFP.

VII.   **Aerodynamics**

A. **Airfoil Selection**

The initial step towards aerodynamic design after general wing outline was the determination of the airfoil shape. When an airfoil was chosen, it was important to consider the airfoil's effect on negative pitch coefficient, structural weight of the wing, lift, drag, and critical Mach number. All these characteristics are directly related to the type, thickness, and camber of the airfoil. Camber provides lift at zero angle of attack and increases the maximum lift of an airfoil but also increases drag and pitching moments [25 pp. 56]. Increased lift from the introduction of camber reduces stalling speed and the required takeoff speed, thus reducing the takeoff distance. Therefore, camber is instrumental in meeting the takeoff requirement of 4,000 feet. Airfoil thickness ratio has a direct effect on drag, lift,

stall, and structural weight of the wing. Stall is of lesser concern when selecting an airfoil for the Shrike because stall characteristics of lower-aspect-ratio and highly swept wings are dominated by three-dimensional effects [1 pp. 68]. For low-aspect-ratio wings, a lower thickness ratio increases the stall angle, maximum lift coefficient, and structural weight of the wing [25 pp. 69]. Drag increases as thickness ratio increases due to separation. Four-digit NACA airfoils and supercritical airfoils provide the capabilities to maximize the previously discussed aerodynamic characteristics. Supercritical airfoils are rarely used in military aircraft but will be considered due to their ability to delay shock formation on the upper-surface, increasing the critical Mach number of the wing and avoiding nose-down "Mach tuck" [25 pp. 65].

Five airfoils were chosen for analysis: NACA 2415, NACA 4412, NACA 4415, NACA 6412, and SC(2)-0714. The airfoils were analyzed at a Reynold's number of 3 million in XFLR5; a software using the vortex lattice method. XFLR5 assumes time independent, incompressible flow which results in limitations at speeds near Mach 1.
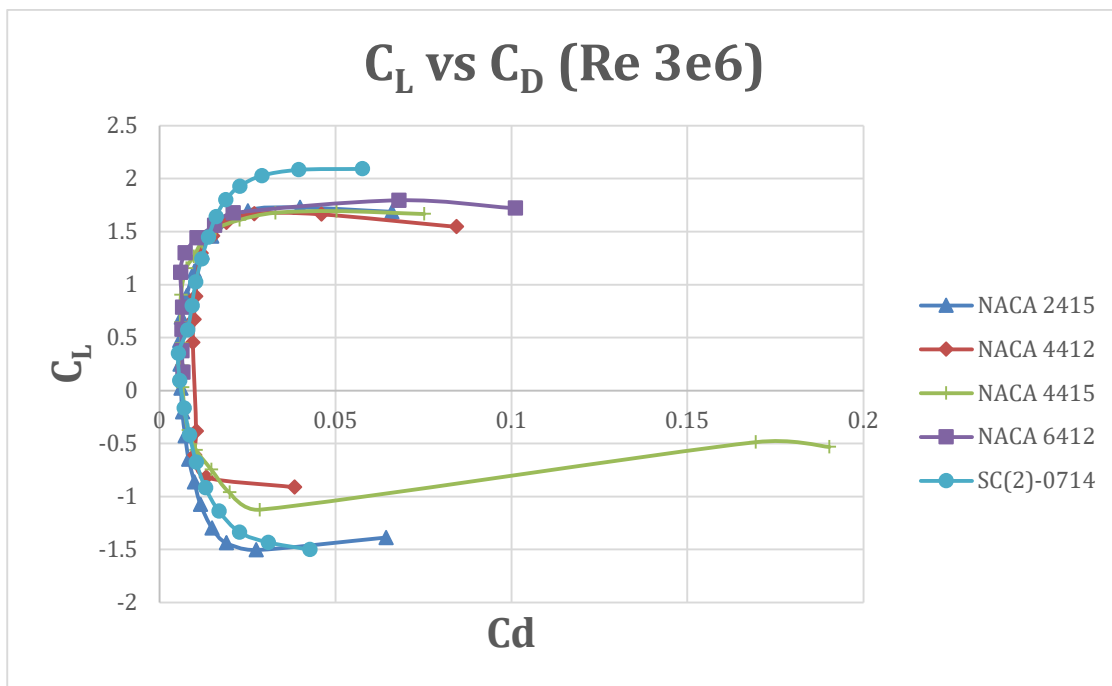
Figure 29: C_L v. C_D Plot
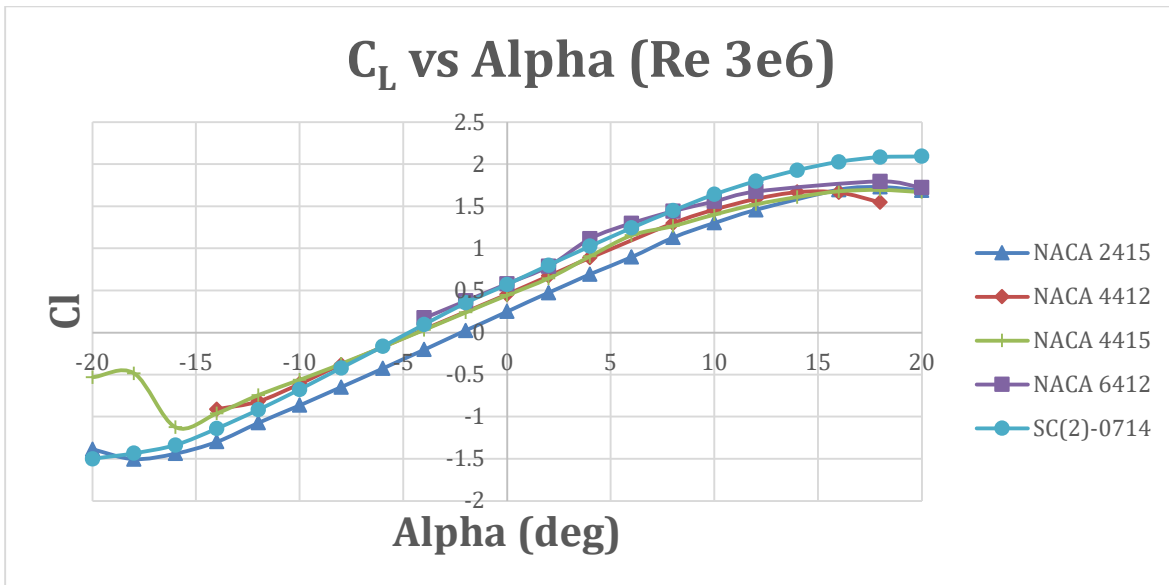
Figure 30: C_L v. Alpha Plot
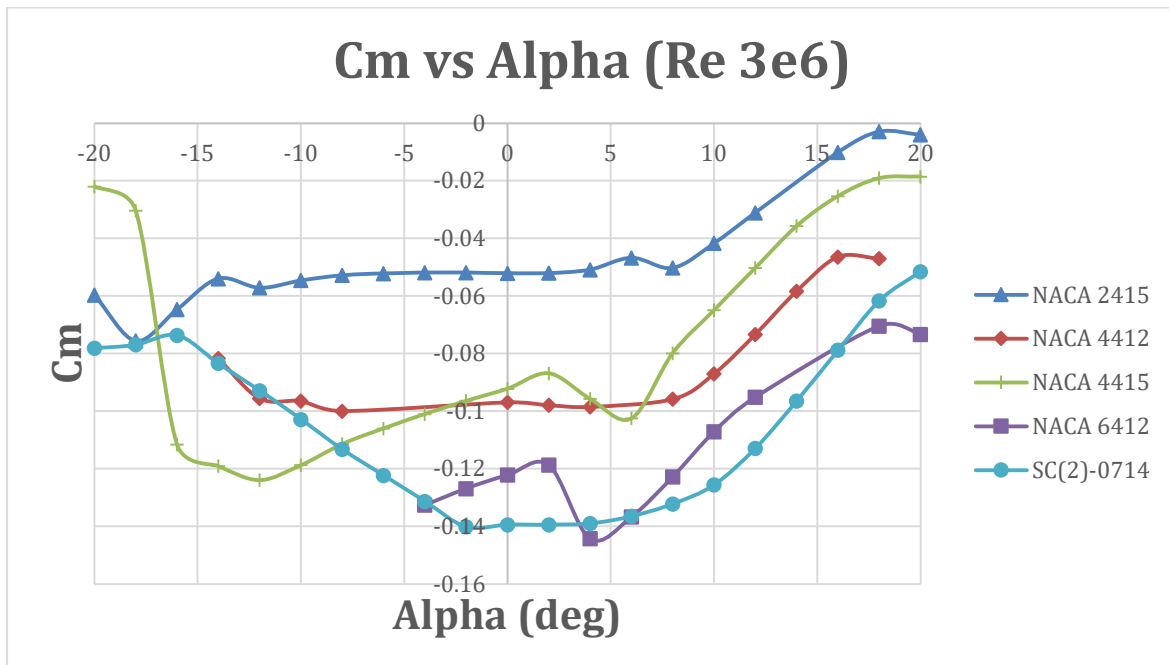
Figure 31: Cm v. Alpha Plot
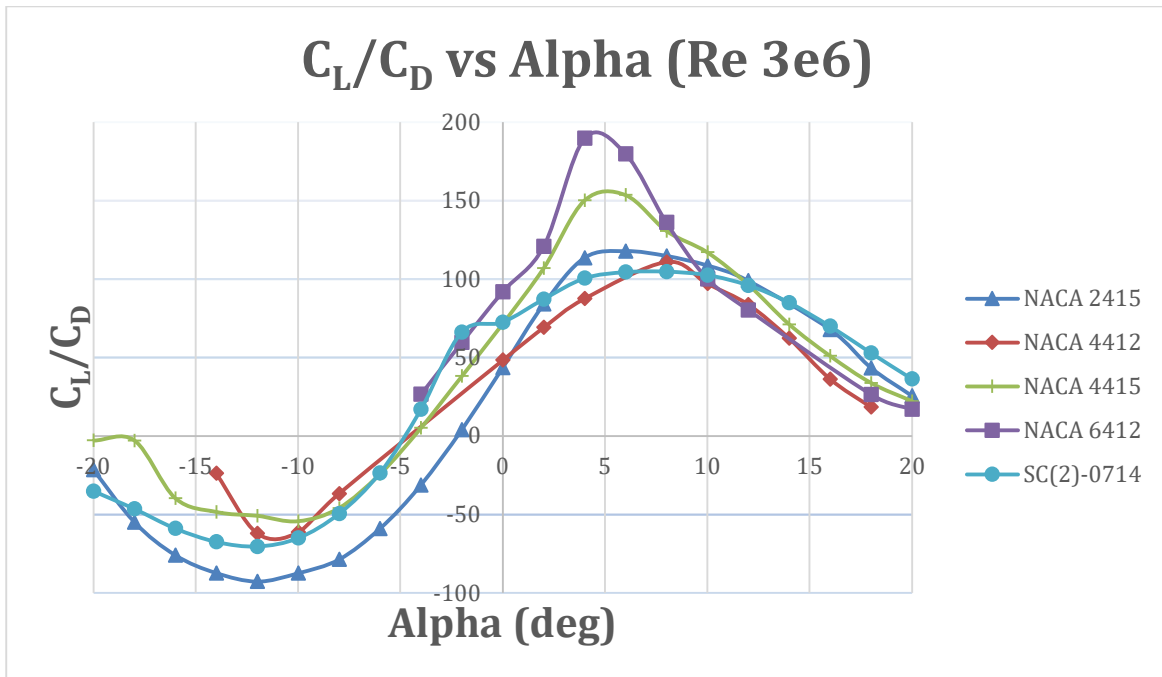
Figure 32: C_L/C_D v. Alpha Plot

The airfoils shown in the figures above highlight the high and low ends of the previously discussed aerodynamic characteristics (camber, and thickness) and include a supercritical airfoil for comparison to the traditional four-digit NACA airfoils. Limiting the negative pitch coefficient is essential in maintaining the stability of the aircraft due to the size constraints of the horizontal stabilizer. The NACA 6412 and SC(2)-0714 reach maximum pitch coefficient values of $C_m = -0.14012$ and $C_m = -0.14422$, respectively. For comparison, the previously discussed airfoils have pitch coefficients, at minimum, 40.16% higher than the NACA 4412 and were therefore eliminated from consideration. The minimal camber of the NACA 2415 limits the airfoil's coefficient of lift at $\alpha = 0$ therefore increasing the takeoff distance of the aircraft if chosen. The remaining airfoils (NACA 4412 and NACA 4415) have similar aerodynamic characteristics. As stated above, for low-aspect-ratio wings, a lower thickness ratio increases the stall angle, maximum lift coefficient, and structural weight of the wing. Therefore, the NACA 4412 airfoil was selected for use on the ZA-21. The NACA 4412 is shown below in Figure 33.
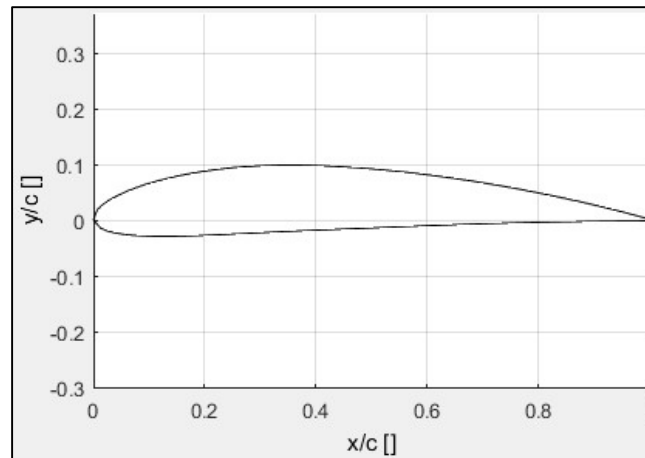
Figure 33: NACA 4412 – Max Thickness 12% at 30% chord, Max Camber 4% at 40% Chord

B. Wing Design

Wing design parameters were chosen with consideration to trade studies and historical aircraft. Parameters such as wing area, aspect ratio, quarter chord sweep angle, and wing twist were of utmost importance during the early design phase. An extensive sizing analysis was conducted to select the wing loading and max takeoff gross weight of the aircraft. From the sizing analysis, a plot of max takeoff gross weight versus aspect ratio was created as shown in Figure 7. Based on the trend line of the plot, an aspect ratio of 5 was chosen. Additionally, a wing area of 275 ft^2 was attained from the max takeoff gross weight and wing loading values determined.

Quarter chord sweep angle and wing twist were chosen to optimize the stall and maneuverability characteristics of the aircraft. Adding sweep to the wing is essential when approaching near-supersonic speeds to delay the formation of shocks. Per Raymer [25 pp. 82] Figure 4.21, a quarter chord sweep angle of 25 degrees is appropriate for a wing with an aspect ratio of 5, approaching transonic speeds. Dihedral is added in addition to wing sweep to improve the lateral stability of the aircraft. To avoid tip stall and improve overall stall characteristics, wing twist is added. The wing should be twisted to create a negative angle compared to the root airfoil. Per Raymer [25 pp. 86] -3 degrees of twist provides adequate stall characteristics. No incidence angle was added to maintain a balance between aircraft lift versus drag and the pilot's visibility. Setting the wing incidence angle to -3 degrees would optimize the lift versus drag curve but sacrifice crucial pilot visibility.

Parameter	Value
Wing Area	275 ft^2
Aspect Ratio	5
c/4 Sweep	25 deg
Twist	-3 deg
Wingspan	37 ft
Taper Ratio	0.308
Dihedral	3 deg
Tip Chord	3.5 ft
Root Chord	11.4 ft

Table 9: Wing Design Characteristics

C. Aircraft Aerodynamic Characteristics

Aircraft aerodynamics were analyzed for steady level flight using VSPAERO, a vortex lattice solver. Steady level flight is defined at Mach 0.70 at 30,000 feet. Because of the limitations of VSPAERO, simulations were run at Mach 0 and then scaled up using the lift-curve slope vs Mach number chart provided by Raymer [25 pp. 399]. The corresponding graphs are provided below in Figures 38, 39, and 40.
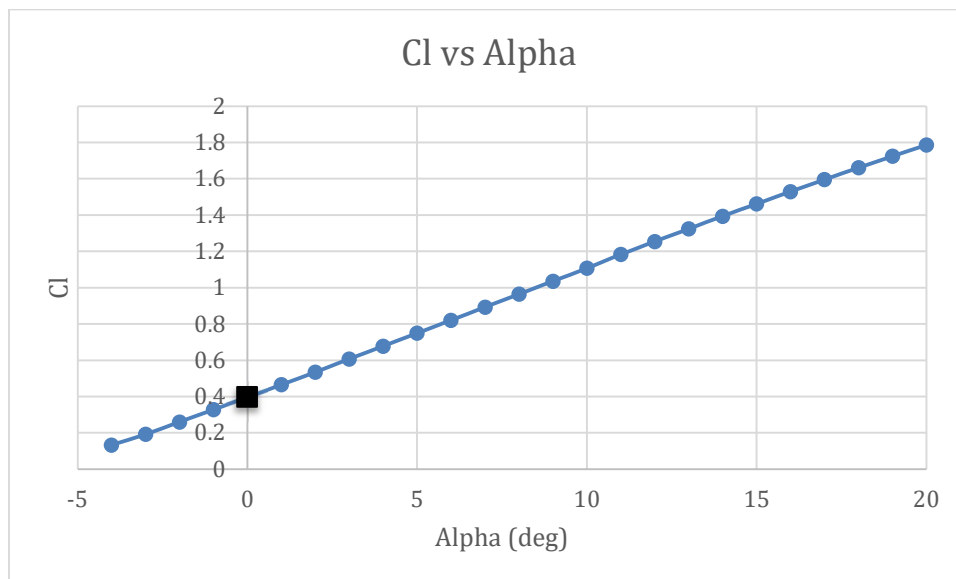
Figure 34: Cruise C_L v. Alpha

L/D vs Alpha
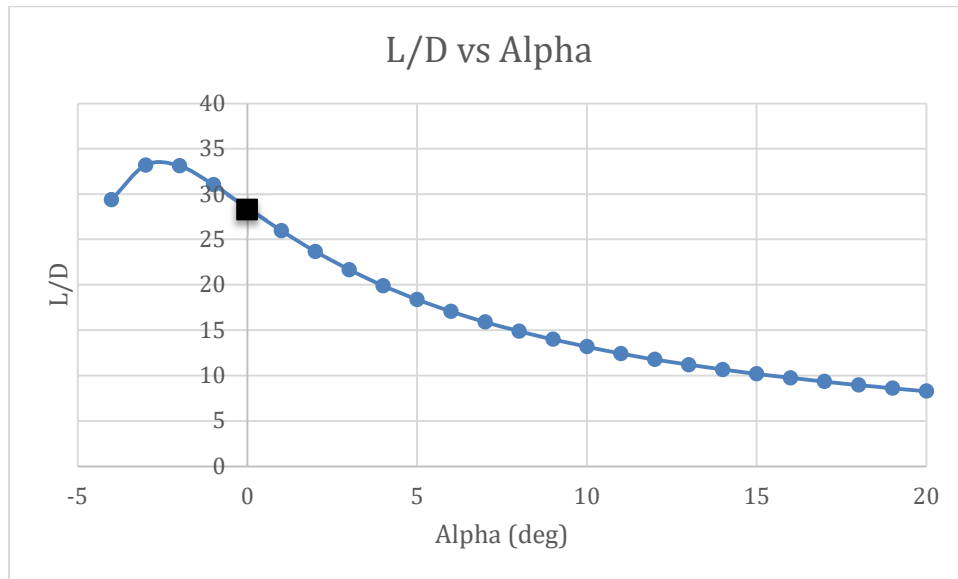
Figure 35: Cruise L/D v. Alpha

Cl vs Cd
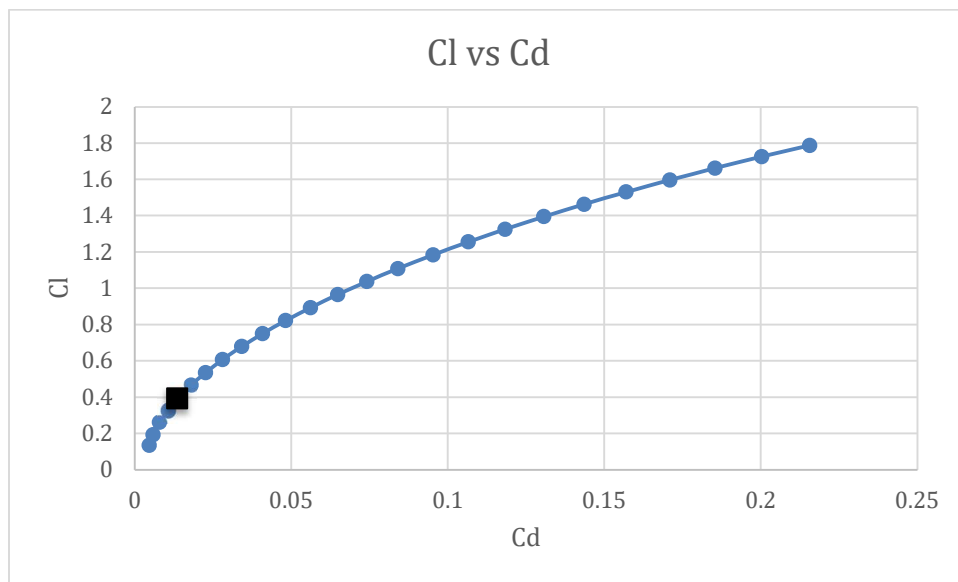
Figure 36: Cruise Drag Polar

To determine the C_L and L/D for steady level flight, these characteristics were analyzed at α = 0 deg. Under cruise conditions C_L = 0.40 and L/D = 28.50. The previously mentioned values are represented by a black rectangle in Figure 34, Figure 35, and Figure 36. The coefficient of lift and lift to drag are sufficient for the Shrike to sustain steady level flight.

Takeoff and landing conditions were analyzed using XFLR5, a vortex lattice solver. XFLR5 allows for the creation of basic leading edge and trailing edge flaps. Both leading edge and trailing edge flaps were used to represent the actual flap configuration composed of a slotted trailing edge flap and leading-edge flap. The leading-edge flap and

trailing edge slotted flap are set at 10 degrees for takeoff and 15 degrees for landing. Takeoff and landing conditions are represented at Mach 0.176 and an average Reynold's number of 30,000,000. The results are displayed in Figure 37 and Figure 38 below. The black rectangle on both figures is indicative of target performance values.
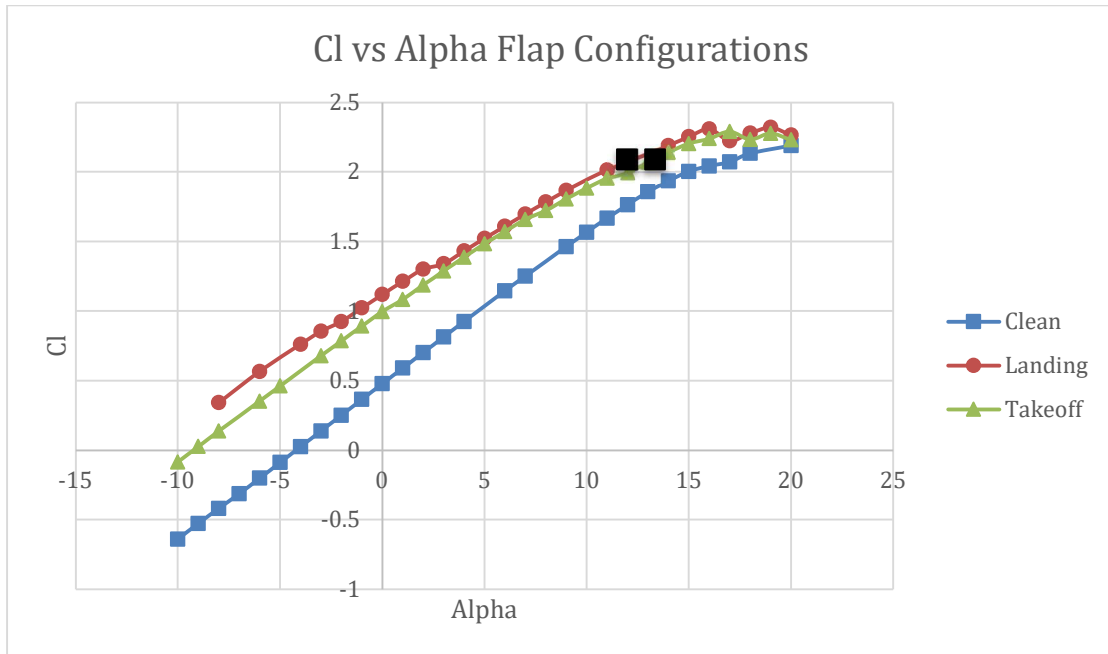
Figure 37: Takeoff and Landing C_L v. Alpha
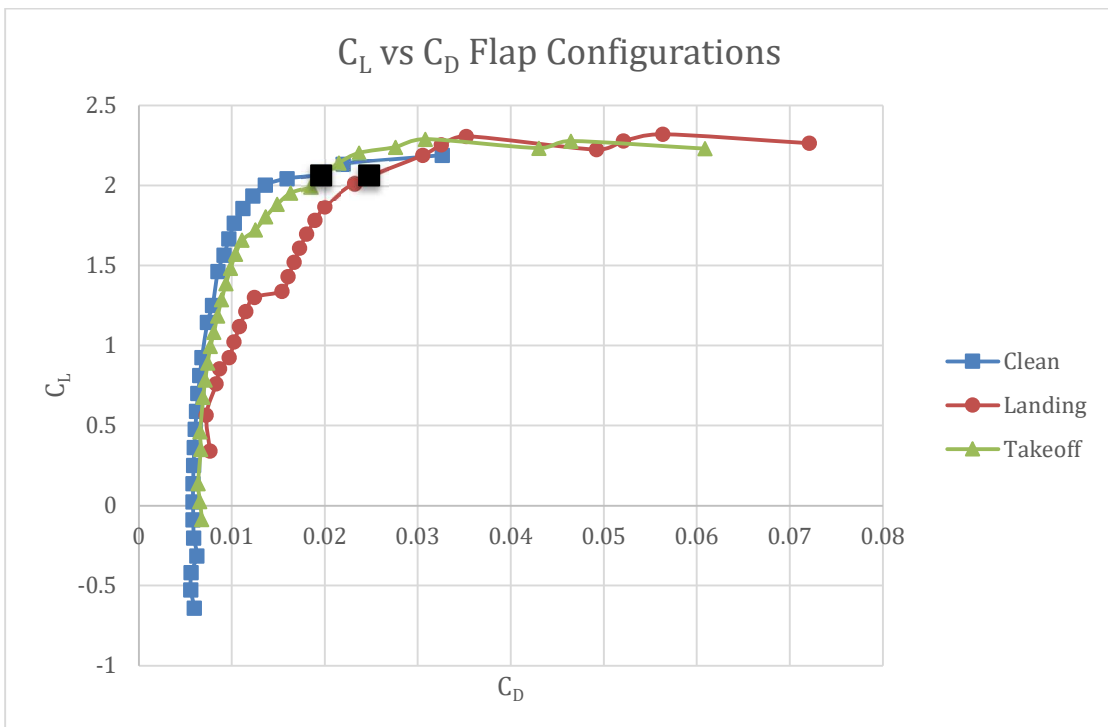
Figure 38: Takeoff and Landing Drag Polars

D. High Lift Devices

The design of high lift devices was driven by the landing and takeoff distance requirement. Performance designated a C_L of 2.06 as essential to landing and taking off in less than 4,000 feet. A slotted trailing edge flap and leading-edge flap were chosen as the Shrike's high lift devices. The slotted trailing edge flap is the main actor in increasing the C_{Lmax} while maintaining a similar angle of attack. It is important to note the increase in drag due to the trailing edge flap. The leading-edge flap is crucial in delaying stalling effects while slightly increasing the C_{Lmax} of the aircraft during takeoff and landing.

The standard configurations within XFLR5 were used to size the high lift devices. The leading-edge flap is hinged at 20% of the chord at an angle of 10 degrees for takeoff and 15 degrees for landing. The trailing edge slotted flap is hinged at 80% of the chord at an angle of 10 degrees for takeoff and 15 degrees for landing. A sample of the flap configuration is provided below in Figure 39.
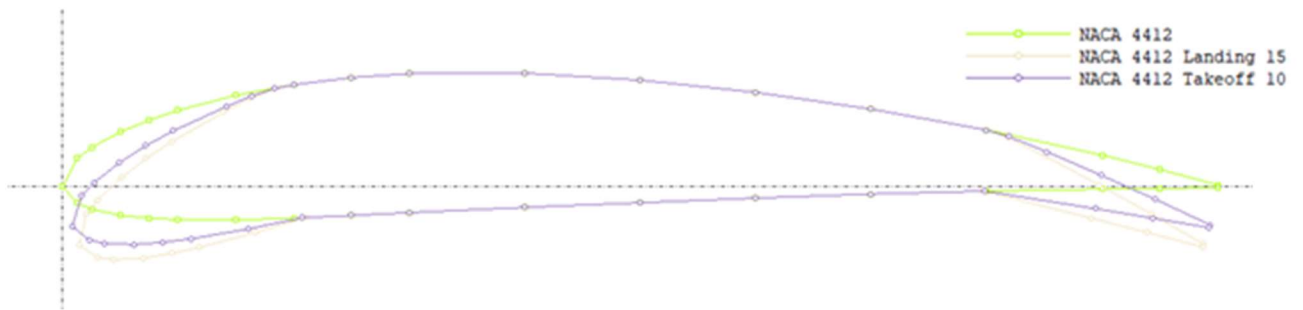
Figure 39: High Lift Devices Configuration

Figures 41 and 42 are a verification of each configuration of the landing and takeoff configurations within XFLR5. The dimensions of the high lift devices are shown below in Table 10.

Dimension	Units	Value
Total TE Slotted Flap Span	ft	19.16
Total LE Flap Span	ft	31.24
Flapped Area (TE Slotted Flap)	ft^2	140.68
Flapped Area (LE Flap)	ft^2	174.86
Hinge Angle	degrees	10.8

Table 10: High Lift Devices Dimensions

E. Control Surface CAD Layout

Figure 40: Aileron, Elevator, and Flaps Overlay
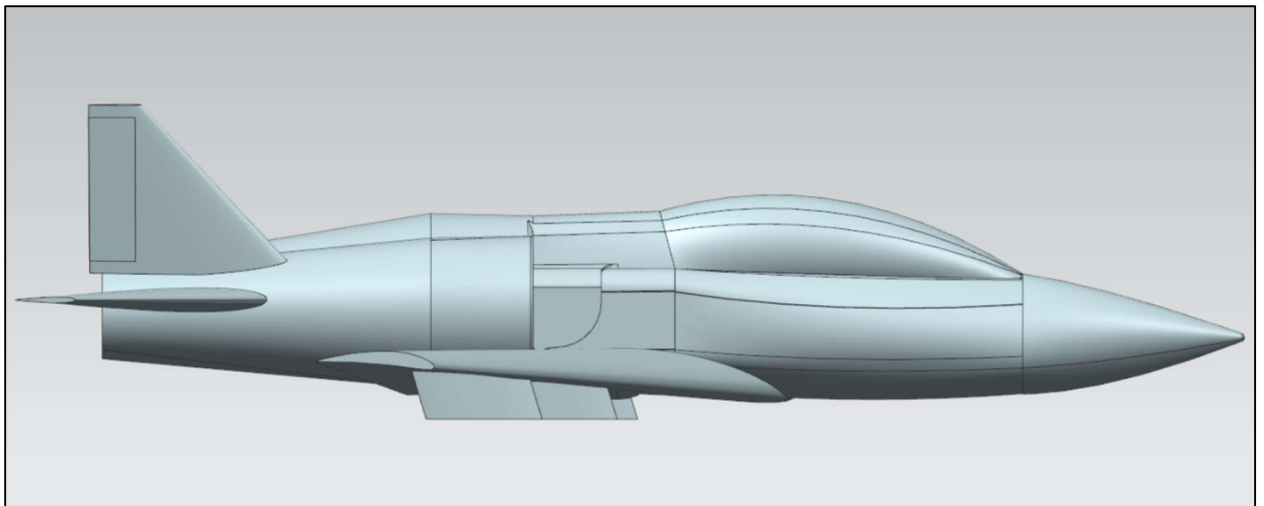
Figure 41: Rudder Overlay

F. Drag Analysis

Parasitic drag was calculated for cruise conditions using Raymer's RDS student software. RDS employs the component buildup method of estimating the subsonic parasite drag of each component using a calculated flat-plate skin friction coefficient and a component form factor [25 pp. 417]. Estimating parasitic drag is especially important

during cruise. Increased values of drag are detrimental to the endurance and speed of an aircraft. Cruise conditions for the simulation are Mach 0.70 at an altitude of 30,000 feet. Drag was minimized at cruise conditions. The resulting drag buildup values are provided below in Table 11 and Table 12. The two tables represent the drag buildup for the design and ferry mission configurations. Contribution to drag from pylons, stores, and launchers are estimated using two sources, including an air force weapons file [2] and a source on predicting drag of installed stores [28].

Component	S-wet (ft^2)	FF	Q	Cd0	Contribution (%)
Wing	428.3	1.454	1.0	0.00603	23.33
Horizontal Tail	139.5	1.387	1.0	0.00202	7.81
Vertical Tail	39.0	1.408	1.0	0.00118	4.56
Fuselage	609.0	1.129	1.0	0.00538	20.81
Pylons, Stores, Launchers	-	-	1.0	0.01124	43.48

Table 11: Parasitic Drag Buildup Design Mission

Component	S-wet (ft^2)	FF	Q	Cd0	Contribution (%)
Wing	428.3	1.454	1.0	0.00603	27.15
Horizontal Tail	139.5	1.387	1.0	0.00202	9.10
Vertical Tail	39.0	1.408	1.0	0.00118	5.31
Fuselage	609.0	1.129	1.0	0.00538	24.22
Pylons, Stores, Launchers	-	-	1.0	0.0076	34.22

Table 12: Drag Buildup Ferry Mission

Additional forms of drag were addressed for the cruise segment of both missions. Induced drag was calculated as the square of the lift coefficient per Raymer [25 pp. 442]. A lift coefficient of 0.40 was assumed based on previous aerodynamic calculations. Leakage drag was estimated as 10% of total parasitic drag per Table 12.8 [25 pp. 431]. Total drag buildup calculations are shown in Tables 12 and 13.

Drag Type	C_{d0}	C_{di}	C_{dleak}	C_{dtot}
Value	0.02585	0.16	.002585	0.1884

Table 13: Drag Buildup Totals – Design Mission

Drag Type	C_{d0}	C_{di}	C_{dleak}	C_{dtot}
Value	0.02221	0.16	.002221	0.184431

Table 14: Drag Buildup Totals – Ferry Mission

Takeoff and landing see the addition of flap drag due to the separated flow above the flap. Flap drag was estimated using Equation 12.61 as provided by Raymer [25 pp. 452]. Flap deflection was assumed at 65 degrees for landing and 30 degrees for takeoff. Drag buildup was calculated for the design and ferry missions for landing and takeoff in Table 15 and Table 16 below.

Component	Landing	Takeoff
Flap ΔC_d	0.1186	0.0431
Non-Flap Total C_d	0.1884	0.1884
Total C_d	0.3070	0.2316

Table 15: Takeoff and Landing Drag - Design Mission

Component	Landing	Takeoff
Flap ΔC_d	0.1186	0.0431
Non-Flap Total C_d	0.1844	0.1844
Total C_d	0.3034	0.2279

Table 16: Takeoff and Landing Drag - Ferry Mission

G. Aerodynamic Characteristic Outline

Provided in Table 17 and Table 18 are the prominent aerodynamic characteristics for the design and ferry missions.

Characteristic	Cruise	Landing	Takeoff
α (deg)	0	12	13
C_L	0.40	2.06	2.06
C_{dtot}	0.1884	0.3070	0.2316

Table 17: Key Aerodynamic Characteristics – Design Mission

Characteristic	Cruise	Landing	Takeoff
α (deg)	0	12	13
C_L	0.40	2.06	2.06
C_{dtot}	0.1884	0.3034	0.2279

Table 18: Key Aerodynamic Characteristics – Ferry Mission

VIII. Performance Characteristics

A. Takeoff and Landing Performance

Per the RFP, the LAB-7 ZA-21 Shrike must be capable of taking off and landing at density altitudes of 0ft and 6000 ft in equal to or less than 4000 ft clearing a 50 ft obstacle. Using aircraft takeoff and landing equations highlighted in Raymer [25], the following plots in Figure 46 could be created. The takeoff distance calculation involves a sum of the ground roll, transition, and air run distances. It was also calculated using a TOGW not including a typical 5 min, 10% mil power warm-up/taxi. This typical warm-up/taxi yields a fuel loss of about ~36 lbs, therefore reducing aircraft weight and takeoff distance required.

The maximum and minimum weight used for landing performance calculations was the aircraft MTOGW (24,853 lbs) and the aircraft's EW (13,653 lbs) to showcase the extremes of flight. The total landing distance includes a landing air run, transition, and braking distance of the aircraft. It should be noted that at typical mission approach weights, more specifically the design and ferry mission, that the aircraft is well below the RFP required landing distance.
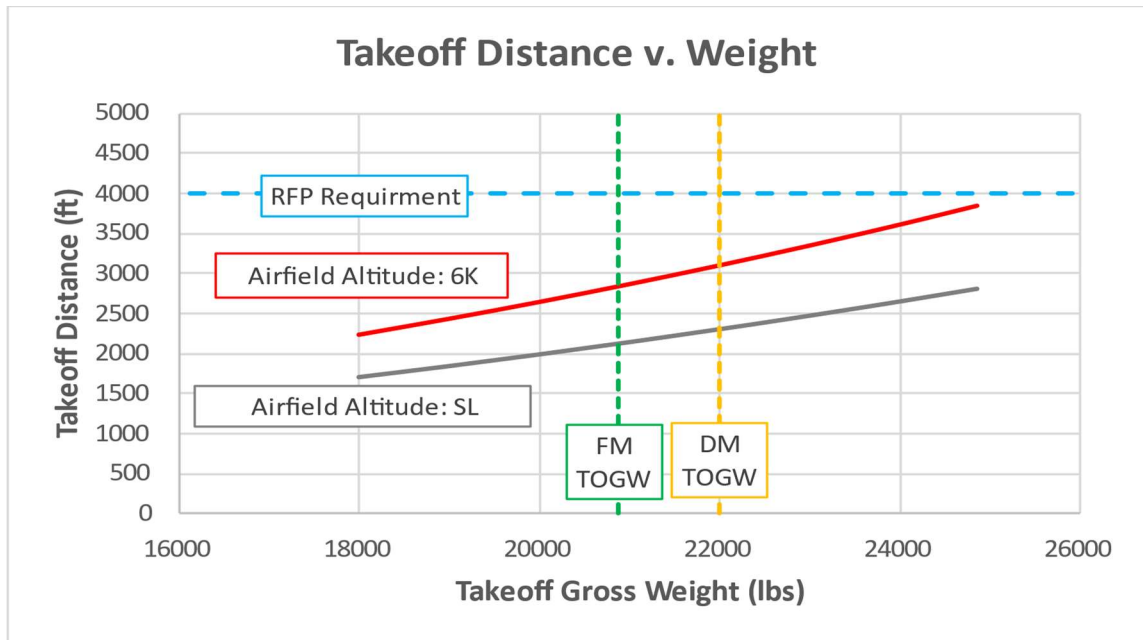
Figure 42: TO Distance v. Weight
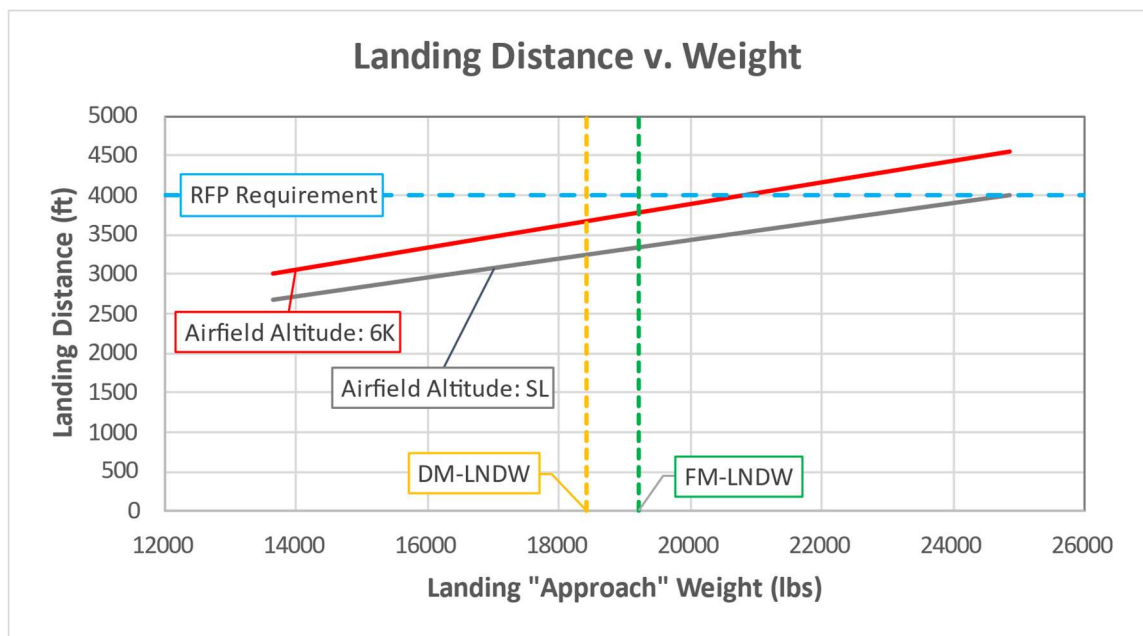
Figure 43: Landing Distance v. Weight

B. Flight Ceilings

The ZA-21's flight ceilings were calculated based on a climb schedule derived from the design mission's return climb segment. The parameters for this climb can be seen in section IX-A-10. The aircraft was configured at a basic flight design gross weight of 19,885lbs which includes a full design mission payload (see Section V-C). The

process used to calculate the ceilings began by deriving a linear relationship between R/C at SL and R/C at another

altitude and calculating the altitudes for the different ceiling types.

Ceilings		
Ceiling Type	**Units**	**Altitude**
Absolute	ft	48,600
Service	ft	48,100
Cruise	ft	47,200
Combat	ft	46,200

Table 19: Flight Ceilings

C. Flight Envelope

The ZA-21's Flight Envelope was calculated at BFDGW = 19,885lbs and performance load factor of n=1.
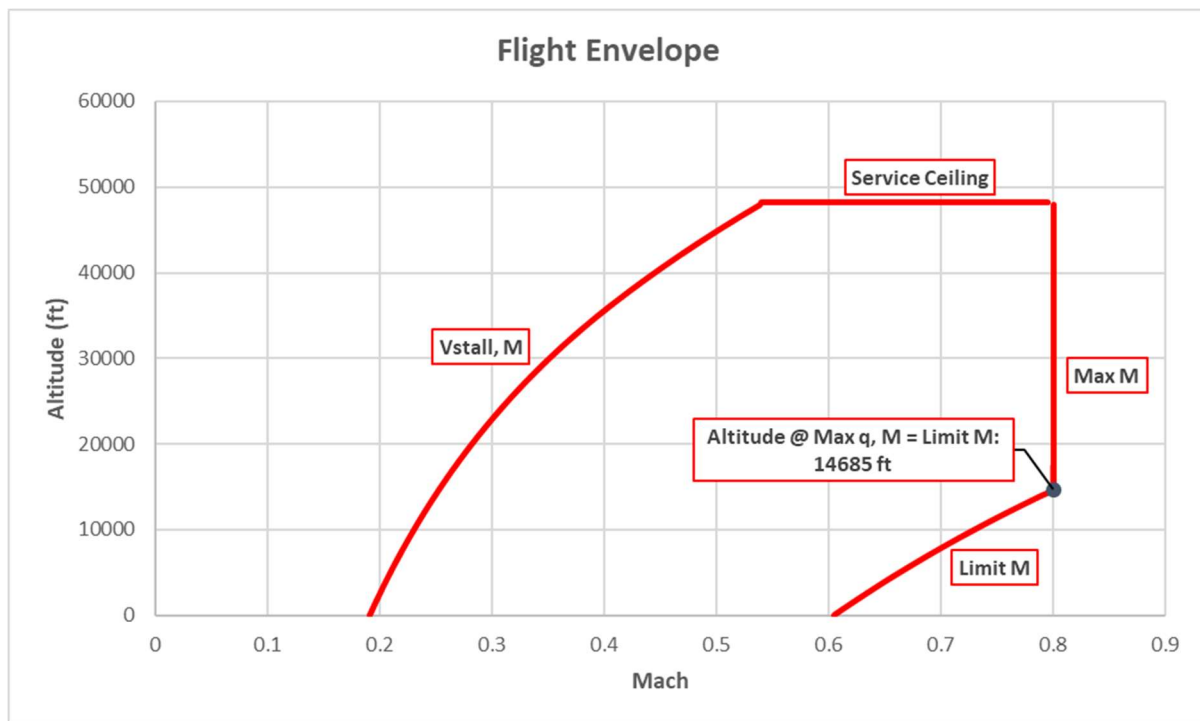
Figure 44: Flight Envelope

D. Maneuver Diagram

The ZA-21's Maneuver Diagram was calculated at BFDGW = 19,885lbs, performance load factor of n=1

and a maneuver altitude of 3000 ft.
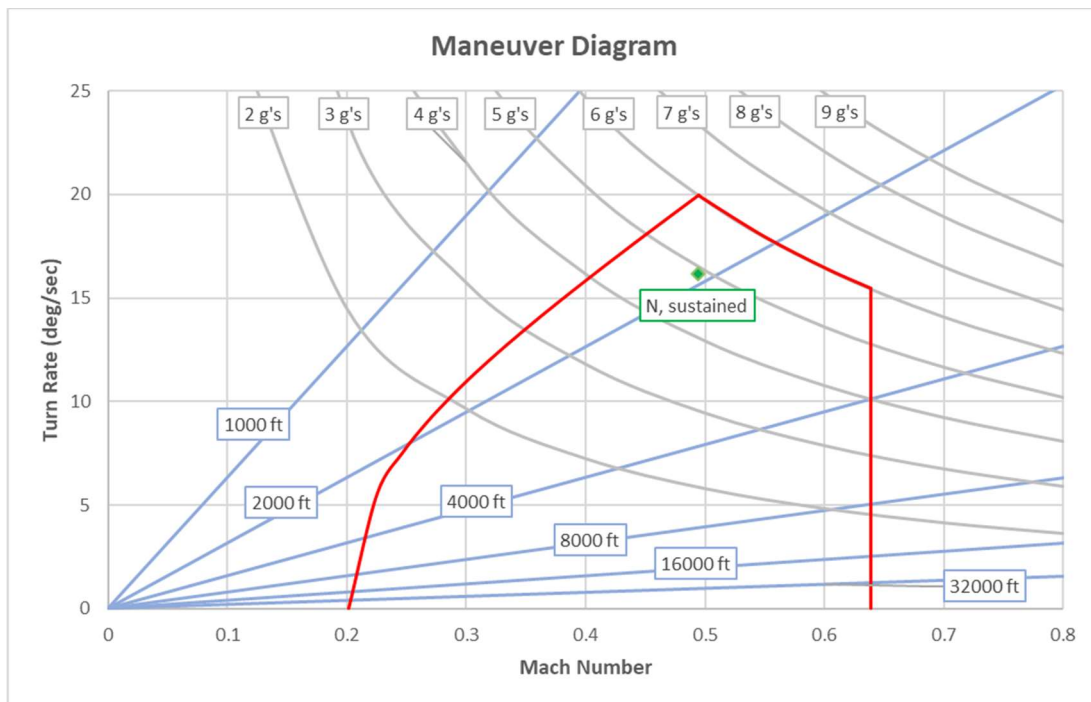
Figure 45: Maneuver Diagram

E. Engine-Out on Cruise Performance

On a single engine, at 30,000 ft in the configuration outlined below, the ZA-21 can cruise 1,350 NM. This distance is more than enough to return safely to the base of departure and/or continue combat.

To calculate the single engine (engine out) performance of the ZA-21, a basic taxi-TO-acceleration-climb-cruise-descent/landing mission was performed. In this case, no T/F/D was credited toward the descent/landing segment. The aircraft was configured with full design mission payload and 62% fuel (2600lbs) yielding a TOGW of 20,385lbs. The initial fuel weight of 2600lbs was used to simulate mid-flight fuel conditions that might be experienced post combat damage.

The cruise segment, where the engine out simulation began, was performed at 30,000 ft. Using the T,D v. Mach figure below, a constant cruise Mach of 0.65 was determined. To simulate a single engine out, the thrust available and resultant fuel usage for the entirety of the cruise segment was cut in half (T_A = 2,024lbs).
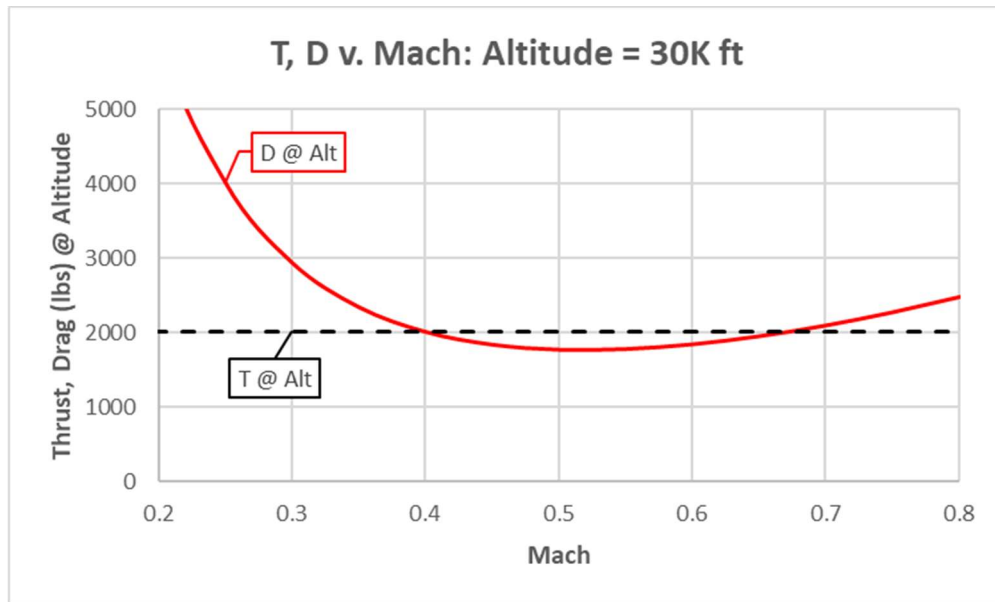
Figure 46: T, D v. Mach @ 30K ft

Airfield Altitude: Sea Level			
Cruise Altitude (ft)		30,000	
Cruise Mach		0.650	
Cruise Type	**Time (min)**	**Fuel (lbs)**	**Distance (NM)**
Constant Altitude	211.5	2352.0	1350.0

Table 20: Engine-Out Cruise Performance

Airfield Altitude: Sea Level			
Engine-Out Mission TFD	**Time (min)**	**Fuel (lbs)**	**Distance (NM)**
Total:	221.1	2555.9	1375.5
Final Aircraft Weight (lbs)	**17,829**		

Table 21: Engine Out Total TFD and Aircraft Weight

F. Other Key Aircraft Performance Parameters

To showcase the ZA-21's best endurance, range, and loiter performance, a plot of three key performance coefficients was created below. The maximum of each coefficient yields the Mach for optimal performance. C_L/C_D showcases the endurance of ZA-21, as at its maximum drag is at a minimum and therefore fuel consumption is as well. $C_L^{0.5}/C_D$ indicates the range of the aircraft and $C_L^{1.5}/C_D$ yields the loiter performance. To perform the calculations, the aircraft was configured as follows: BFDGW = 19,885lbs, load factor = 1, and an altitude of 30,000 ft. The maximum's, and therefore optimal speed for performance, for each coefficient is shown in the table below.
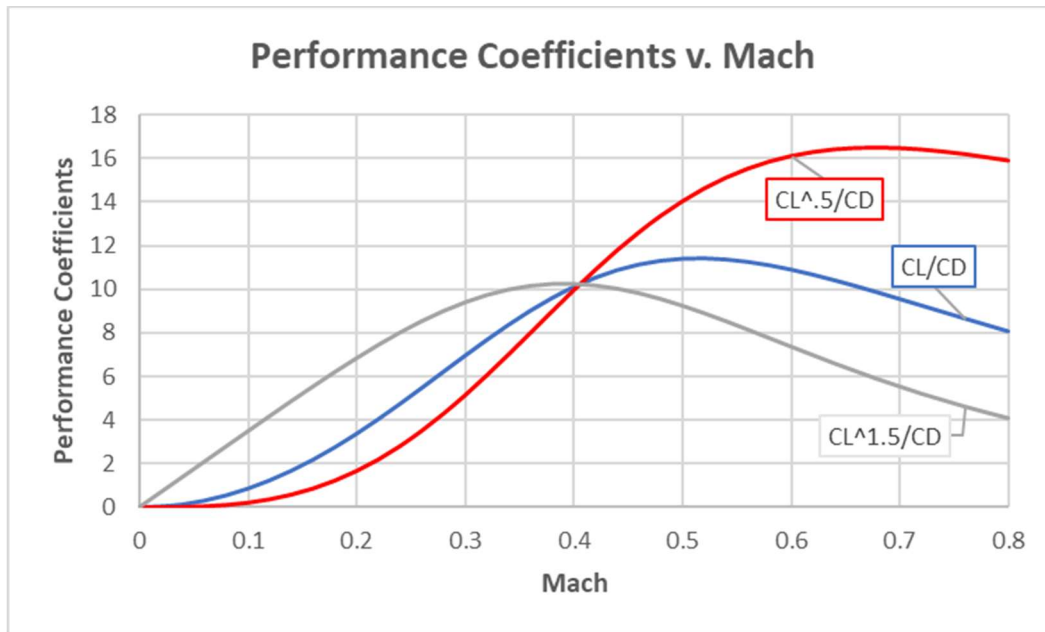
Figure 47: Performance Coefficients v. Mach

Key Aircraft Performance Parameters			
Parameter	**Units**	**Value**	**Mach**
$(C_L/C_D)_{MAX}$	-	11.4	0.51
$(C_L^{0.5}/C_D)_{MAX}$	-	10.2	0.38
$(C_L^{1.5}/C_D)_{MAX}$	-	16.5	0.66

Table 22: Key Aircraft Performance Parameters

As seen below, the max KEAS and max Mach were parameters that were decided upon based on the needs of the RFP missions and requirements. These parameters then led to a calculated max q, or dynamic pressure, value of 541lb/ft^2. At this point, max q, the aerodynamic structural load on the aircraft is directly proportional. This also leads to a maximum dive speed, which changes at different flight conditions, of 0.80.

The divergence Mach number is the speed at which the air moving over the wing begins to separate and form shocks, significantly increases the amount of drag force on the aircraft. This parameter greatly limits the capabilities of the aircraft, however for this case does not affect the needed performance capabilities of the ZA-21. As seen below the drag divergence Mach number is 0.81 which is greater than the max Mach of the aircraft.

Other Aircraft Performance Parameters		
Parameter	**Units**	**Value**
Max KEAS	knots	400
Max Mach	-	0.80
Max q	lb/ft^2	541
Dive Speed, Mach	-	0.80
Divergence Mach	-	0.81

Table 23: Key A/C Performance Parameters

IX. Mission Performance

A. Design Mission

1. Design Mission Performance Requirements

To analyze the design mission performance of the aircraft, an excel workbook was created using equations and assumptions from Raymer [25]. The use of these equations and assumptions will be noted in the relevant mission segment. The configuration for this design mission is separated into its defined categories: Weights (Section XII-C), Payload (Section V-C) and Aerodynamics (Section VII-A).

According to the RFP, the aircraft must be capable of landing and taking off in ≤ 4,000 ft with a 50 ft obstacle at a density altitude up to 6,000 ft on austere fields, as well as carry a minimum of 3,000 lbs of expendable armament. Additionally, the RFP states that the design mission segments include a 5 min. warm up/taxi, takeoff, a climb to ≥ 10,000 ft, a 100 NM cruise, a descent to 3000 ft completed within 20 minutes of initial climb, a 4 hour loiter, another climb to ≥ 10,000 ft, a return-to-base 100 NM cruise, a descent/landing, a 5 min. taxi/shutdown, and enough reserve fuel sufficient for a climb to 3,000 ft and a 45 min loiter. This is also outlined in Section III of the report.

2. Warm-up/Taxi

Airfield Altitude: Sea Level			
Warm-up Ground Rules	**Time (min)**	**Fuel (lbs)**	**Distance (NM)**
5 minutes at 10% power for taxi	5.0	36.7	0.0

Table 24: DM Warm-up TFD

The ground rules were decided on for the mission as they are typical values for a military warm-up and taxi.

3. Takeoff

Airfield Altitude: Sea Level			
Takeoff Speeds (KTAS)			
Stall	Rotation	Takeoff	Obstacle
107.0	112.3	117.7	128.4
Total Takeoff Distance (ft)			
2,309			
Time (min)		**Fuel (lbs)**	**Distance (NM)**
0.5		36.7	0.0

Table 25: DM Takeoff Performance

The rotation, takeoff, and obstacle velocities were calculated at 1.05x, 1.10x, and 1.20x stall velocity respectively. To calculate the takeoff ground roll distance, a coefficient of rolling resistance had to be decided on. For the case of a typical mission being performed from austere fields, a worst-case coefficient of 0.05 was used – assuming poor and/or friction-high runway conditions. A typical takeoff time of 5 minutes was also assumed for this mission segment.

4. Outbound Acceleration to Climb

Airfield Altitude: Sea Level			
Initial Mach	0.194		
Final Mach	0.632		
Acceleration Type	**Time (min)**	**Fuel (lbs)**	**Distance (NM)**
Level Acceleration	0.7	50.9	3.3

Table 26: DM Outbound Acceleration Performance

5. Outbound Climb

Airfield Altitude: Sea Level			
Initial Altitude (ft)	50	Initial Mach	0.632
Final Altitude (ft)	30,000	Final Mach	0.709
Climb Type	**Time (min)**	**Fuel (lbs)**	**Distance (NM)**
Constant 417 KTAS	0.7	50.92	3.3

Table 27: DM Outbound Climb Performance

6. Outbound Cruise

Airfield Altitude: Sea Level			
Cruise Altitude (ft)		30,000	
Cruise Mach		0.709	
Cruise Type	**Time (min)**	**Fuel (lbs)**	**Distance (NM)**
Constant Altitude	14.4	190.9	100.0

Table 28: DM Outbound Cruise Performance

The outbound cruise was performed at max range factor mach. Furthermore, as cruise distance was known, the final aircraft weight for the segment could be calculated using the Breguet range equation. Subtracting this from the initial aircraft weight for the segment yields fuel used.

7. Descent

Airfield Altitude: Sea Level			
Initial Altitude (ft)	30,000	Descent Mach	0.709
Final Altitude (ft)	3,000		
Climb Type	**Time (min)**	**Fuel (lbs)**	**Distance (NM)**
Enroute Descent	4.1	13.3	30.4

Table 29: DM Descent Performance

An enroute descent at a constant Mach (cruise Mach) was performed so that the 20 minute "cruise + descent" requirement set by the RFP could be met. The total time, from end of the outbound climb, for the cruise and descent segments was 18.5 minutes.

8. Loiter

Airfield Altitude: Sea Level			
On Station Loiter, No Drops	**Time (min)**	**Fuel (lbs)**	**Distance (NM)**
Loiter	240.0	2844.5	0.0

Table 30: DM Loiter TFD

The loiter segment was performed at maximum efficiency factor Mach to yield the best fuel performance for the segment. Furthermore, as loiter time was known, the final aircraft weight for the segment could be calculated using the Breguet range equation. Subtracting this from the initial aircraft weight for the segment yields fuel used.

9. Return Acceleration to Climb

Airfield Altitude: Sea Level			
Initial Mach	0.308		
Final Mach	0.588		
Acceleration Type	**Time (min)**	**Fuel (lbs)**	**Distance (NM)**
Level Acceleration	0.4	26.8	2.0

Table 31: DM Return Acceleration Performance

10. Return Climb

Airfield Altitude: Sea Level			
Initial Altitude (ft)	3,000	Initial Mach	0.588
Final Altitude (ft)	30,000	Final Mach	0.653
Climb Type	**Time (min)**	**Fuel (lbs)**	**Distance (NM)**
Constant 417 KTAS	3.1	75.1	19.0

Table 32: DM Return Climb Performance

11. Return Cruise

Airfield Altitude: Sea Level			
Cruise Altitude (ft)		30,000	
Cruise Mach		0.653	
Cruise Type	**Time (min)**	**Fuel (lbs)**	**Distance (NM)**
Constant Altitude	16.9	191.4	100.0

Table 33: DM Return Cruise Performance

The return cruise was also performed at max range factor mach. Again, as cruise distance was known, the final aircraft weight for the segment could be calculated using the Breguet range equation which in turn yields the fuel used for the segment.

12. Descent/Landing

Airfield Altitude: Sea Level			
Landing Speeds (KTAS)			
Stall	Approach	Flare	Touchdown
98.0	117.6	112.6	107.7
Total Landing Distance (ft)			
3,251			
Time (min)		**Fuel (lbs)**	**Distance (NM)**
0.0		0.0	0.0

Table 34: DM Descent/Landing Performance

The approach, flare, and touchdown velocities were calculated at 1.20x, 1.15x, and 1.10x stall velocity, respectively. To calculate the braking ground roll distance, a coefficient of braking had to be decided on. For the case of the typical mission being performed off austere fields, a worst-case coefficient of 0.3 was used – assuming poor runway conditions.

13. Taxi/Shutdown

Airfield Altitude: Sea Level			
Shutdown Ground Rules	**Time (min)**	**Fuel (lbs)**	**Distance (NM)**
5 minutes at 10% power for shutdown	5.0	36.7	0.0

Table 35: DM Taxi/Shutdown TFD

The ground rules were decided on for the mission as they are typical values for a military taxi and shutdown.

14. Fuel Reserves

Airfield Altitude: Sea Level			
Reserves	**Time (min)**	**Fuel (lbs)**	**Distance (NM)**
Constant 186 KTAS Climb + 45min 3K Loiter	45.3	503.0	0.9

Table 36: DM Fuel Reserves TFD

15. Design Mission Total TFD and Aircraft Weight

Airfield Altitude: Sea Level			
Design Mission TFD	**Time (min)**	**Fuel (lbs)**	**Distance (NM)**
Total:	294.0	4,101	289.5
Final Aircraft Weight (lbs)	**17,884** (using Reserves)		

Table 37: DM Total TFD and Aircraft Weight

16. Design Mission Time History Summary

Mission Leg		FLIGHT CONDITIONS			INCREMENTAL			TOTAL		
		Aircraft Weight (lb)	Altitude (ft)	Speed (Mach)	Time (min)	Fuel (lb)	Distance (NM)	Time (min)	Fuel (lb)	Distance (NM)
		XX,XXX.Y	XX,XXX	X.YYYY	XXX.YY	XX,XXX.Y	XXX.Y	XXX.YY	XX,XXX.Y	XXX.Y
1 Warm-up & Taxi	Initial Conditions	21,985	0	0.000	5.0	36.7	0.0	5.0	36.7	0.0
	Final Conditions	21,948	0	0.000						
2 Takeoff	Initial Conditions	21,948	0	0.000	0.5	36.7	0.0	5.5	73.4	0.0
	Final Conditions	21,912	50	0.194						
3 Accel to Climb Speed	Initial Conditions	21,912	50	0.194	0.7	50.9	3.3	6.2	124.3	3.3
	Final Conditions	21,861	50	0.632						
4 Climb to Altitude	Initial Conditions	21,861	50	0.632	3.9	94.5	26.3	10.1	218.9	29.6
	Final Conditions	21,766	30,000	0.709						
5 Outbound Cruise	Initial Conditions	21,766	30,000	0.709	14.4	190.9	100.0	24.4	409.8	129.6
	Final Conditions	21,575	30,000	0.709						
6 Descent	Initial Conditions	21,575	30,000	0.709	4.2	13.3	30.4	28.6	423.1	159.9
	Final Conditions	21,562	3,000	0.709						
7 Loiter	Initial Conditions	21,562	3,000	0.308	240.0	2,844.5	0.0	268.6	3,267.6	159.9
	Final Conditions	18,717	3,000	0.308						
8 Accel to Climb Speed	Initial Conditions	18,717	3,000	0.308	0.4	26.8	2.0	269.0	3,294.4	161.9
	Final Conditions	18,691	3,000	0.588						
9 Climb to Altitude	Initial Conditions	18,691	3,000	0.588	3.1	75.1	19.1	272.1	3,369.6	181.0
	Final Conditions	18,615	30,000	0.653						
10 Return Cruise	Initial Conditions	18,615	30,000	0.653	16.9	191.4	108.5	289.0	3,561.0	289.5
	Final Conditions	18,424	30,000	0.653						
11 Descent / Landing	Initial Conditions	18,424	30,000	0.163	0.0	0.0	0.0	289.0	3,561.0	289.5
	Final Conditions	18,424	0	0.000						
12 Taxi & Shutdown	Initial Conditions	18,424	0	0.000	5.0	36.7	0.0	294.0	3,597.7	289.5
	Final Conditions	18,387	0	0.000						
13 Reserves Climb	Initial Conditions	18,387	0	0.282	0.3	22.2	0.9		3,619.9	
	Final Conditions	18,365	3,000	0.285						
14 Reserves Loiter	Initial Conditions	18,365	3,000	0.285	45.0	480.8	0.0		4,100.7	
	Final Conditions	17,884	3,000	0.285						

Table 38: DM Segmented Flight Conditions and TFD Summary

B. Ferry Mission

1. Ferry Mission Performance Requirements

Again, to analyze the ferry mission performance of the aircraft, the same excel workbook method was used as in the design mission. Regarding the equations and assumptions used, the same reasonings/equations were used throughout the ferry mission as they were in the comparable mission segment of the design mission unless otherwise stated. The configuration for this ferry mission is separated into its defined categories: Weights (Section XII-C), Payload (Section V-C) and Aerodynamics (Section VII-A).

The same requirements from the RFP apply to this mission as they did to the design mission except for the following ferry mission specific exceptions. The ferry mission will include a full crew (2 persons) and a payload near 60% of the payload requirement (3000 lbs). It is stated that the ferry mission segments include a 5 min. warm up/taxi, takeoff, a climb to ≥ 18,000 ft, a 900 NM cruise at best range speed, a descent/landing, a 5 min. taxi/shutdown, and enough fuel sufficient for a climb to 3000 ft and a 45 min loiter. This is also outlined in Section III of the report.

2. Warm-up/Taxi

Airfield Altitude: Sea Level			
Warm-up Ground Rules	**Time (min)**	**Fuel (lbs)**	**Distance (NM)**
5 minutes at 10% power for taxi	5.0	36.7	0.0

Table 39: FM Warm-up TFD

3. Takeoff

Airfield Altitude: Sea Level			
Takeoff Speeds (KTAS)			
Stall	Rotation	Takeoff	Obstacle
104.2	101.3	114.6	125.1
Total Takeoff Distance (ft)			
2,128			
Time (min)	**Fuel (lbs)**	**Distance (NM)**	
0.5	36.7	0.0	

Table 40: FM Takeoff Performance

4. Acceleration to Climb

Airfield Altitude: Sea Level			
Initial Mach	0.189		
Final Mach	0.638		
Acceleration Type	**Time (min)**	**Fuel (lbs)**	**Distance (NM)**
Level Acceleration	0.6	47.5	3.0

Table 41: FM Acceleration Performance

5. Climb

Airfield Altitude: Sea Level			
Initial Altitude (ft)	50	Initial Mach	0.638
Final Altitude (ft)	30,000	Final Mach	0.716
Climb Type	**Time (min)**	**Fuel (lbs)**	**Distance (NM)**
Constant 421 KTAS	3.3	80.8	22.5

Table 42: FM Climb Performance

6. Cruise

Airfield Altitude: Sea Level			
Cruise Altitude (ft)		30,000	
Cruise Mach		0.716	
Cruise Type	**Time (min)**	**Fuel (lbs)**	**Distance (NM)**
Constant Altitude	128.0	1455.9	900.0

Table 43: FM Cruise Performance

7. Descent/Landing

Airfield Altitude: Sea Level			
Landing Speeds (KTAS)			
Stall	Approach	Flare	Touchdown
100.1	120.1	115.0	110.1
Total Landing Distance (ft)			
3,344			
Time (min)	**Fuel (lbs)**		**Distance (NM)**
0.0	0.0		0.0

Table 44: FM Landing Performance

8. Taxi/Shutdown

Airfield Altitude: Sea Level			
Shutdown Ground Rules	**Time (min)**	**Fuel (lbs)**	**Distance (NM)**
5 minutes at 10% power for shutdown	5.0	36.7	0.0

Table 45: FM Shutdown TFD

9. Fuel Reserves

Airfield Altitude: Sea Level			
Reserves	**Time (min)**	**Fuel (lbs)**	**Distance (NM)**
Constant 186 KTAS Climb + 45min 3K Loiter	45.3	489.2	1.0

Table 46: FM Fuel Reserves TFD

10. Ferry Mission Total TFD and Aircraft Weight

Airfield Altitude: Sea Level			
Ferry Mission TFD	**Time (min)**	**Fuel (lbs)**	**Distance (NM)**
Total:	142.4	2,183	925.6
Final Aircraft Weight (lbs)	**18,696** (using Reserves)		

Table 47: FM Total TFD and Aircraft Weight

11. Ferry Mission Time History Summary

		FERRY MISSION TIME HISTORY SUMMARY								
		FLIGHT CONDITIONS			INCREMENTAL			TOTAL		
Mission Leg		**Aircraft Weight**	**Altitude**	**Speed**	**Time**	**Fuel**	**Distance**	**Time**	**Fuel**	**Distance**
		(lb)	**(ft)**	**(Mach)**	**(min)**	**(lb)**	**(NM)**	**(min)**	**(lb)**	**(NM)**
		XX,XXX.Y	XX,XXX	X.YYYY	XXX.YY	XX,XXX.Y	XXX.Y	XXX.YY	XX,XXX.Y	XXX.Y
1 Warm-up & Taxi	Initial Conditions	20,879.0	0	0.0000	5.00	36.7	0.0	5.00	36.7	0.0
	Final Conditions	20,842.3	0	0.0000						
2 Takeoff	Initial Conditions	20,842.3	0	0.0000	0.50	36.7	0.0	5.50	73.4	0.0
	Final Conditions	20,805.6	50	0.1891						
3 Accel to Climb Speed	Initial Conditions	20,805.6	50	0.1891	0.65	47.5	3.0	6.15	121.0	3.0
	Final Conditions	20,758.0	50	0.6379						
4 Climb to Altitude	Initial Conditions	20,758.0	50	0.6379	3.30	80.8	22.5	9.45	201.8	25.6
	Final Conditions	20,677.2	30000	0.7159						
5 Outbound Cruise	Initial Conditions	20,677.2	30,000	0.7159	127.99	1,455.9	900.0	137.44	1,657.7	925.6
	Final Conditions	19,221.3	30,000	0.7159						
6 Descent / Landing	Initial Conditions	19,221.3	30,000	0.0000	0.00	0.0	0.0	137.44	1,657.7	925.6
	Final Conditions	19,221.3	0	0.0000						
7 Taxi & Shutdown	Initial Conditions	19,221.3	0	0.0000	5.00	36.7	0.0	142.44	1,694.4	925.6
	Final Conditions	19,184.6	0	0.0000						
8 Reserves Climb	Initial Conditions	19,184.6	0	0.2986	0.33	21.8	1.0		1,716.1	
	Final Conditions	19,162.9	3,000	0.3017						
9 Reserves Loiter	Initial Conditions	19,162.9	3,000	0.3017	45.00	467.4	0.0		2,183.5	
	Final Conditions	18,695.5	3,000	0.3017						

Table 48: FM Segmented Flight Conditions and TFD Summary

X.   Stability and Control

The LAB-7 ZA-21 Shrike is an attack aircraft, designating it as a Class IV, high maneuverability aircraft. Within the category A nonterminal flight phases, the ZA-21 Shrike will conduct ground attack and weapon delivery/launch. Category A flight phases require rapid maneuvering, precision tracking, or precise flight-path control. Within the category B nonterminal flight phases, the ZA-21 Shrike will complete climb, cruise, loiter, and descent segments. Category B flight phases employ gradual maneuvers without precision tracking and may require accurate light-path control. Similar to category B flight phases, category C terminal flight phases include gradual maneuvers but require accurate flight-path control. The ZA-21 Shrike completes three category C flight phases, takeoff, approach, and landing. The ZA-21 Shrike is designed to and meets the satisfactory degree of suitability. The level defined as satisfactory signifies flying qualities that are clearly adequate for the mission flight phase. To meet this, the desired performance must be met with minimal pilot compensation.

A.   Empennage Design

A trade study was conducted to weigh out the benefits of several empennage configurations. The configurations under consideration were twin tail, conventional, H-tail, cruciform, and T-tail. The QFD ranking scale was used to choose the best configuration for the ZA-21 design based on several categories. Cost, size, stability, weight, and survivability were chosen as categories of interest from least to most important, respectively.

Type	Weight of Importance	Twin Tail	Conventional	H-Tail	Cruciform	T-Tail
Stability	3	4	2	5	1	3
Size	2	2	5	1	4	3
Weight	4	3	5	1	4	2
Survivability	5	5	3	4	2	1
Cost	1	3	5	2	4	1
Total	-	56	56	43	41	29

Table 49: Empennage Configuration Trade Study

The trade study resulted in a tie between two configurations, twin tail and conventional. The twin tail ultimately prevailed due to its performance in the most important category, survivability.

B. Empennage Sizing

The volume coefficient and distance between a quarter of the main wings and tails mean aerodynamic center were essential in the sizing of the horizontal and vertical stabilizers. There are ample examples of the previously mentioned parameters in historical aircraft. Data was collected on the A-4M Skyhawk, A-37B Dragonfly, and Yak-130 to portray values for the previously mentioned characteristics on similar aircraft.

Parameter	Units	A-4M Skyhawk	A-37B Dragonfly	Yak-130
I_{HT}	ft	16.69	14.77	11.5
I_{VT}	ft	14.17	14.46	10.45
C_{HT}	-	0.2689	0.5771	0.3532
C_{VT}	-	0.0936	0.0333	0.0591

Table 50: Plane Parameter Comparison

Volume coefficients were chosen to stay within the range of the similar aircraft. Span, l_{HT}, and l_{VT} were optimized based on the volume coefficients. Subsequent calculations were performed to obtain the remaining horizontal and vertical tail characteristics. The final selection made for the horizontal and vertical tails is the NACA 0010 airfoil. The NACA 0010 is a symmetrical airfoil of 10% thickness, 2% less than the thickness of the main wing to avoid detrimental stalling of the stabilizers before the main wing. The symmetry and thickness of the airfoil provide optimal performance at the near-transonic speeds of the design and ferry missions.

Characteristic	Units	Horizontal Tail	Vertical Tail
b	ft	15.51	5.00
λ	-	0.25	0.25
S	ft^2	68.75	19.23
AR	-	3.50	1.30
$\Lambda_{c/4}$	deg	30	35
Canted Angle	deg	-	10
I_{HT}	ft	12.50	-
I_{VT}	ft	-	11.10
Volume Coefficients	-	0.386	0.042

Table 51: Horizontal and Vertical Tail Characteristics

C. Control Surface Sizing

Control surface sizing was dictated by historical aircraft and data provided by Raymer [25]. The ZA-21 employs ailerons, a rudder, and an elevator to establish and maintain attitude of the aircraft throughout the duration of flight. The relevant characteristics for each control surface are provided in Table 51 below.

Characteristic	Units	Aileron	Rudder	Elevator
Span	ft	4.63	4.25	5.71
Span Ratio	-	0.25	0.85	0.75
Chord	ft	1.48	1.35	1.55
Chord Ratio	-	0.20	0.35	0.35
Area	ft^2	6.85	5.72	8.85
Deflection	deg	+/- 25	+/- 25	+/- 25
Hinge Angle	deg	10.8	0	9.6

Table 52: Aileron, Rudder, and Elevator Characteristics

D. Longitudinal Static Stability

Calculating the longitudinal static stability derivatives is essential to proving the Shrike's horizontal tail configuration can effectively oppose the pitching moment created by the wing, fuselage, and engines. The longitudinal static stability derivatives were calculated using the framework provided by Raymer [25]. The resulting derivative values are highlighted below Table 52.

Derivative	$C_{L\alpha}$	Cm_{α}	$Cm_{\delta e}$	ε_{α}
Value	4.71	-0.339	-0.849	0.48

Table 53: Longitudinal Static Stability Derivatives

The negative value of $C_{m\alpha}$ indicates the aircraft's ability to generate moments that oppose any change in angle of attack. Additionally, a negative $C_{m\alpha}$ proves that the Shrike is longitudinally statically stable. The negative value of $C_{m\delta e}$ indicates that the elevator adds to the opposition of the pitching moment when it is pitched upward.

Characteristic	Units	Value
Neutral Point, % MAC	%	38.1
Neutral Point Fuselage Station	in	247.90
CG	in	240.80
CG, % MAC	%	30.90
Static Margin	%	7.20
Aerodynamic Center	in	234.00

Table 54: Key Stability Parameters

The methods defined in Raymer [25 pp. 592-593] were used to find the aircraft's neutral point and static margin. Static margin is represented as the distance in percent MAC from the neutral point to the CG. Verifying the CG was ahead of the neutral point was essential in ensuring the overall stability of the aircraft.

E. Lateral Static and Dynamic Stability:

LAB-7 used the United States Air Force Stability and Control Digital DATCOM to analyze the lateral-directional static and dynamic stability of the Shrike. The resulting values are displayed below Table 54. The positive value for the yawing moment coefficient ($C_{n\beta}$) indicates the aircraft's ability to provide a restoring moment. The negative value for the rolling moment coefficient ($C_{L\beta}$) represents the aircraft's ability to resist positive sideslip and restore the aircraft to level flight. The additional dynamic stability derivatives are further proof of the Shrike's lateral-directional stability.

Derivative	$C_{n\beta}$	$C_{L\beta}$	C_{np}	C_{Lp}	C_{yp}	C_{nr}	C_{Lr}
Value	0.000346	-0.000823	-0.000272	-0.00583	-0.000456	-0.000546	0.00107

Table 55: Lateral-Directional Static and Dynamic Stability Derivatives

XI.   Structures and Loads

A. Loads

1. V-n Diagram
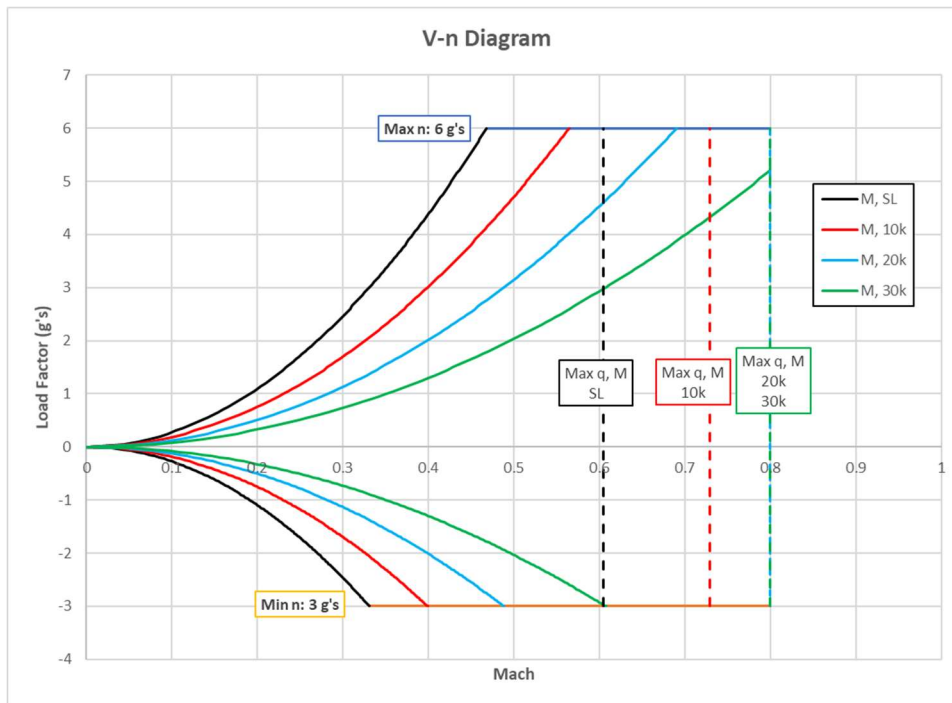
Figure 48: V-n Diagram

2. Wing Loading

With an ultimate load factor of 9 G's, and a MTOGW of roughly 25,000 pounds. It is estimated that the maximum load the wings could undergo would be:

$$Maximum\ Load\ Per\ Wing = \frac{MTOGW * Ultimate\ Load\ Factor}{number\ of\ wings} = \frac{25,000 * 9}{2} = 112,500\ lbf$$

The figures below utilize the value of 112,500 pounds for the load applied to the bottom of the wing. This should give an accurate representation of the amount of deformation and stress the wing would undergo during flight. While it is unlikely that the aircraft will ever experience this true amount of force directly on the wings because other surfaces of the aircraft will also produce lift. For the sake of these FEM analysis however, it was important to show forces that could have even the slightest potential to be encountered to ensure the structural integrity of the aircraft.
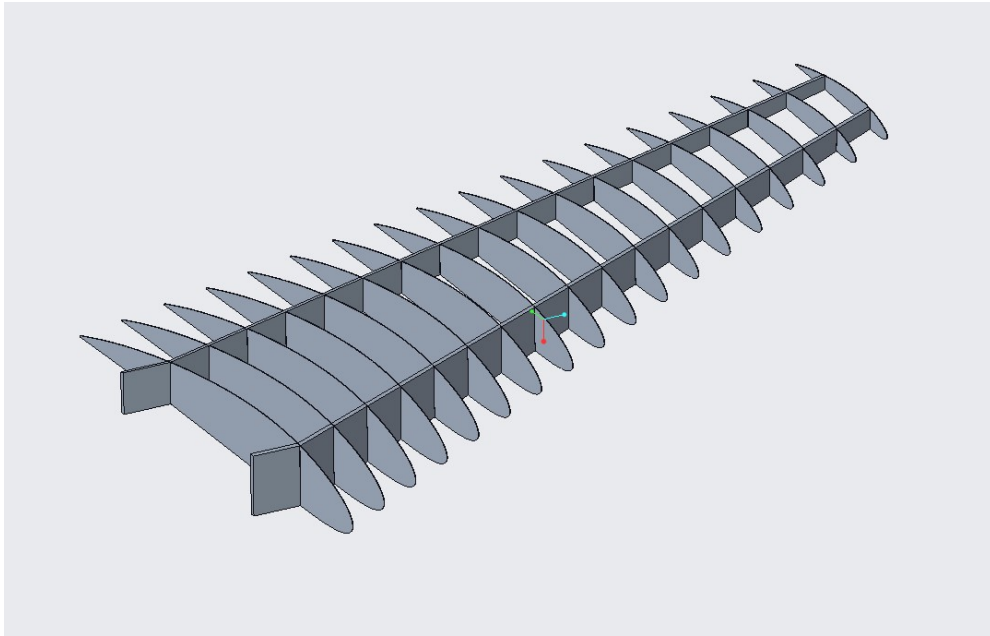
Figure 49: Wing Skeletal Structure Model

The structural layout of the wing shown above uses two spars, and includes ribs placed 300 mm apart. The ribs themselves are 5 mm in thickness. This layout was used as it provided strong results in terms of low stress load as well as rigidity with some deflection allowed. The spars are 30 mm thick and are placed with respect to hinge line for surface control placement, as well as at the ideal structural stability point.
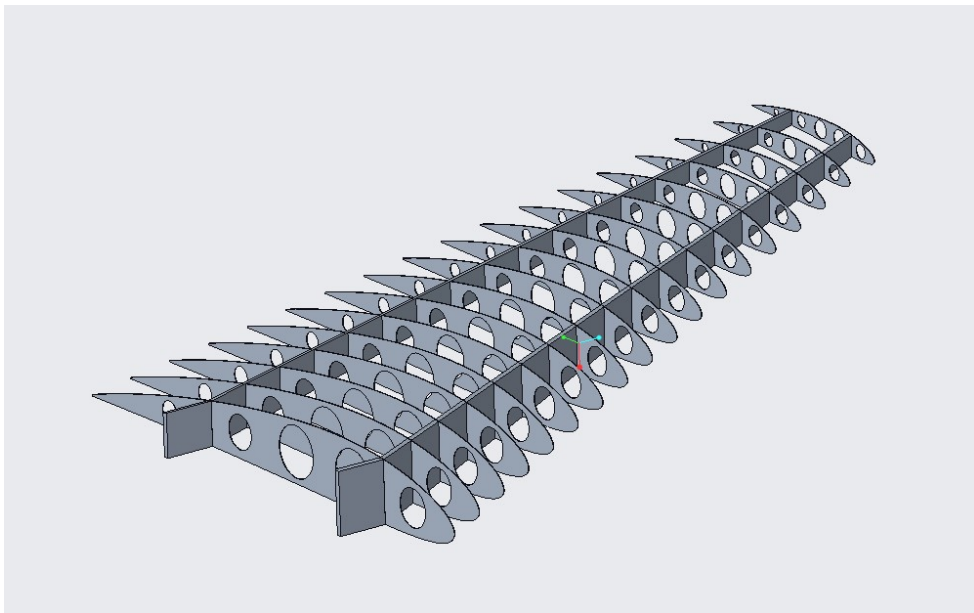
Figure 50: Prototype Lightweight Wing Structure

A light-weight version of the wing was created, but due to the limited capabilities of the Creo Simulate software, which was used, the structure was unable to be tested. However, after reviewing the stress points of the non-lightweight wing it would likely suffice as the removal of material in the ribs would not be cause for structural failure.
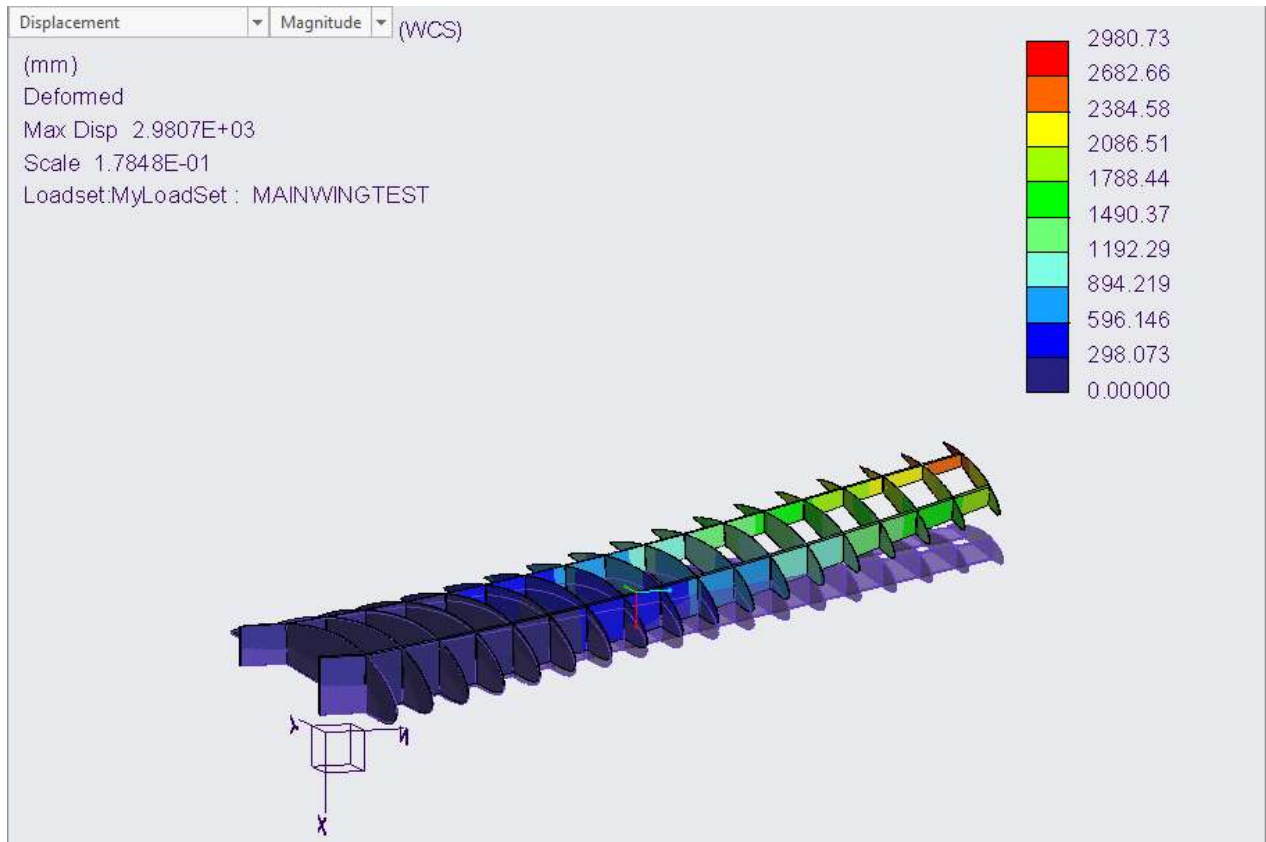
Figure 51: Wing Displacement Under Max Load

3. Shear Stress Forces
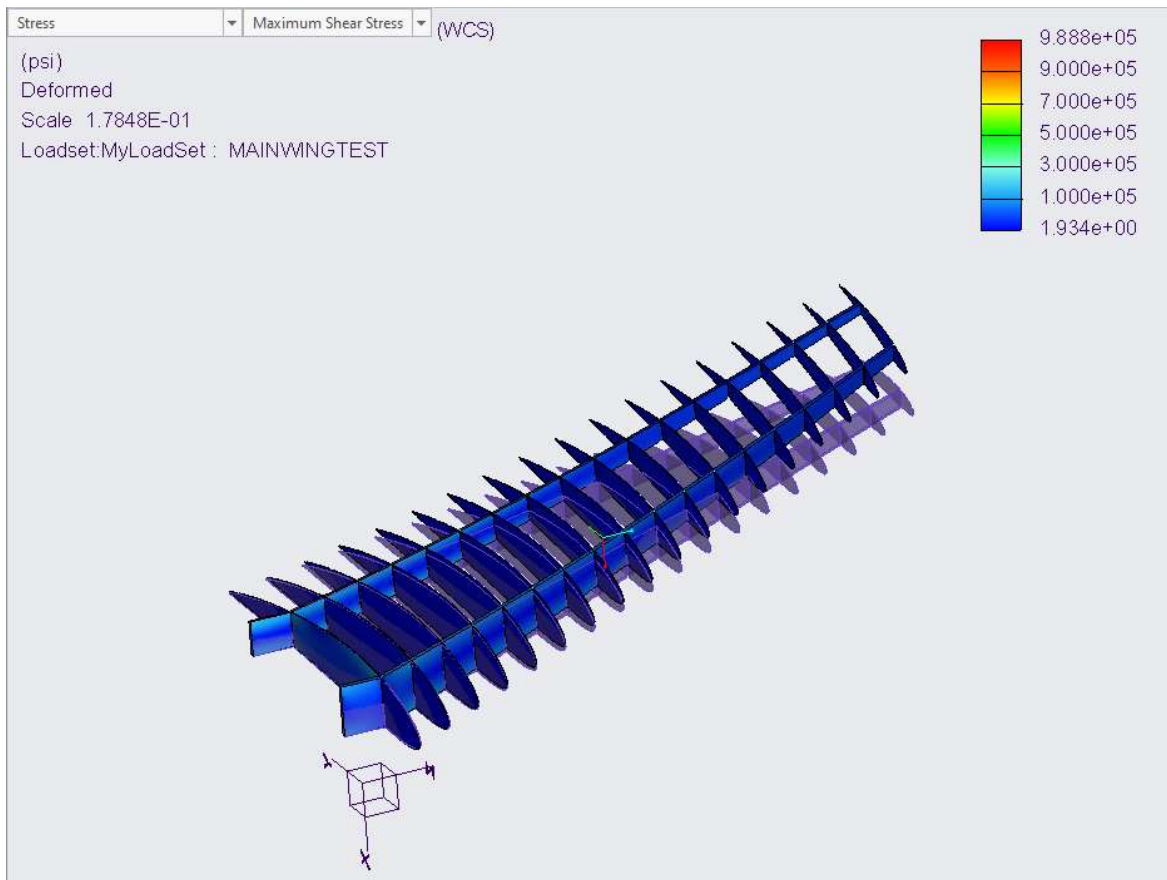
Figure 52: Maximum Shear Stress Representation

Above, the maximum shear stress distribution of the model can be seen under load. As it can be seen, the amount of stress in the member is minimal in relation to the material's maximum stress point. As was stated above, this amount of load is highly unlikely in real flight but gives more peace of mind knowing that the wing can withstand an extreme amount of load without breaking.

4. Load Paths
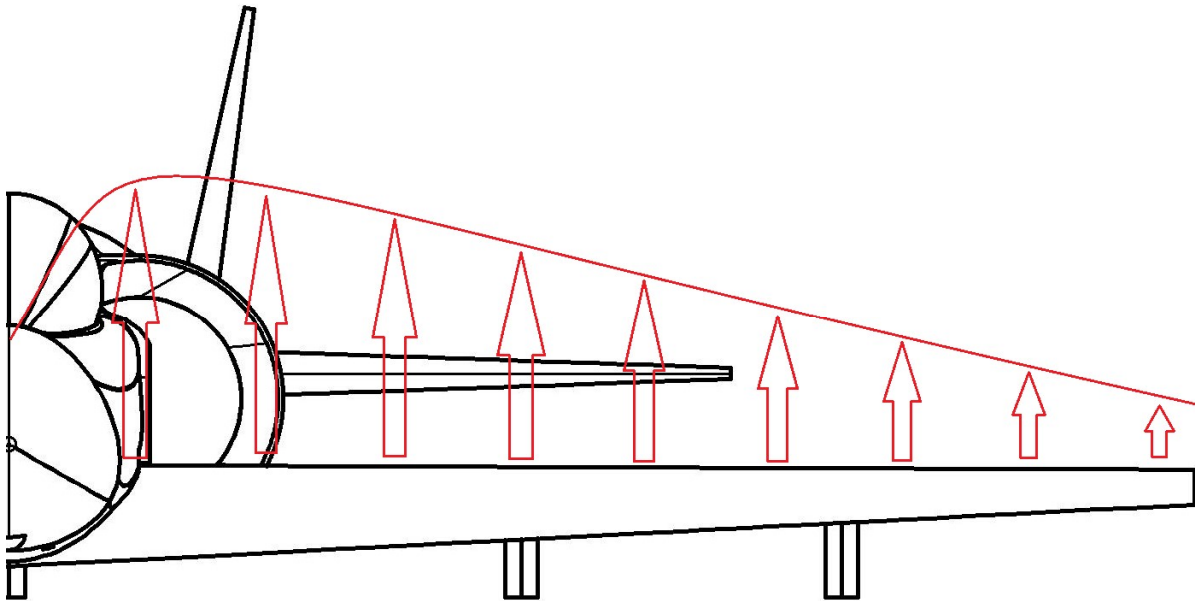
Figure 53: Wing Lift Load Path

The wing lift loading of the aircraft is a non-uniform distributed load. The wingtips will not produce the levels of lift that will be produced at the areas of the wing with larger chord length. The figure above shows a representation of how the lift load is distributed along the aircraft wing. Lift will drop off once the wing intersects with the fuselage but will not go to zero due to the small lift forces generated by the fuselage body.

B. Material Selection

1. Fuselage

To stand up to the rigors of combat, the fuselage must have the highest degree of strength, durability, and protection for the aircraft's most critical systems. The frame of the fuselage will utilize the aluminum alloy Al 2024, the T3 variant, which has high strength and excellent fatigue resistance. The downside to the material is its low corrosion resistance but due to the frame's location inside the aircraft, that risk should be minimized as well as applying an anodized coat or a thin layer of high purity aluminum to reduce the risk further. The external skin of the fuselage will utilize a carbon epoxy composite. The material is strong, stiff, and lightweight and is used commonly amongst aircraft in every sector. To ensure the protection of the crew of the aircraft, resin impregnated Kevlar® 49 will line the cockpit to provide a high degree of survivability for the aircrew in a situation of heavy enemy fire.

This choice in material around the cockpit was between the aforementioned material and titanium, like that used in the A-10's titanium bathtub. With small gaps between the equipment around the front of the aircraft, Kevlar® seemed to be the better choice to achieve strength in thinner sheets. Titanium's impressive capabilities of high strength with low density will not be skipped up on as Titanium 4-4-2 will be used for the fuselage wingbox support. Finally, for the fuselage, the radome requires a material to allow electromagnetic waves to pass through from the radar. The best material for this is S-glass fiberglass which accounts for electromagnetic waves to pass though as well as being high in strength and durability. The chosen materials and their properties are listed in the following table, Table 56.

Part	Material	Density	Young's Modulus	Tensile Strength	Yield Strength	Elongation
-	-	g/m³	GPa	MPa	MPa	%
Frame	Al 2024-T3	2.78	73	415	275	12.5
Fuselage Skin	Carbon/Epoxy Composite	1.60	83	600	595	0
Cockpit Lining	Kevlar® 49	1.44	124	3600	3000	2.4
Wingbox	Ti-4-4-2	4.60	114	1138	1035	12
Nose Cone	S-Glass	2.49	90	4750	3920	0

Table 56: Fuselage Material Properties

2. Wing

The wing needs to meet similar requirements as the fuselage in being strong and durable to handle enemy weapons fire as well as stressed caused by aerodynamic forces. The frame will be the same as that found in the fuselage, utilizing Al 2024-T3 for its fatigue resistance against flexing. The skin of the wing will be comprised of another carbon composite, but instead of epoxy, it will be made of Carbon/BMI, BMI standing for Bismaleimide. With a tensile and yield strength of 744 and 730 MPa, respectively, all at a density of 1.25 g/cm³, this material has increased strength at a lighter weight compared to the epoxy composite found in the fuselage. A Young's Modulus of 56.3 GPa allows for a higher degree of flexibility as well for the wing. These same materials will be used for the empennage design as well.

3. Landing Gear

A material with high strength, fatigue resistance, and toughness is required for the landing gear. Due to this, 300M steel is the preferred material, increasing the strength already provided by its derivative, AISI 4340 steel [30]. This does come with an increased price of about $20 per foot of a 1.25-inch diameter piece for reference, according

to TW Metals and their online price calculator [29], but since it is for the landing gear which will be operating from austere fields, the slight price hike in a stronger, more resilient material is justified.

C. Landing Gear

1. Landing Gear Design

When designing a landing gear system, the first step, before any measurements can be done, is to decide on a configuration for the aircraft in development. This configuration includes the general wheel placement and the gear's ability to be actuated, considering the advantages and disadvantages of each possible combination. A quick decision can be on whether the gear is to be retractable or if it is fixed. Due to the missions at hand, a high subsonic or near transonic speed is required for the aircraft. This higher speed can produce a greater parasitic drag on any surface that is not designed for low drag or lift. This factor of drag, as well as weight, cost, and maintenance, are the primary considerations when deciding between a fixed and retractable gear. In the case previously stated, a fixed gear performs poorly when it comes to drag and, despite having on average a lower weight, cost, and maintenance, the selection of this fixed configuration is overwhelmed by the negative aspect of the drag produced in-flight. Thus, a retractable gear was selected based on this factor as well as considering the selection of historical aircraft and their decision on using retractable gears.

With retraction decided, the next order of business was the general wheel placement for the aircraft. The most common types of landing gear configurations are the tricycle undercarriage, popular with the considered historical aircraft, a bicycle arrangement, see in the AV-8B Harrier, and conventional landing gear, or "taildragger" which was widely used with propeller aircraft. With these three configurations, it can be graded on several factors, such as stability, visibility for the pilots, weight, steering authority, and ease of takeoff. A quality function deployment, QFD, analysis can be applied to discover which configuration is best for the aircraft being designed and can be found in Table 57.

Type	Weight of Importance	Tricycle	Bicycle	Taildragger
Stability	3	3	2	1
Visibility	2	3	2	1
Weight	4	2	1	3
Steering Authority	1	3	2	1
Ease of Takeoff	5	3	1	2
Total	-	41	21	28

Table 57: Landing Gear Configuration QFD Analysis

From this analysis, the tricycle configuration is the best choice for the aircraft being designed. Surprisingly, taildragger is a second pick but due to its exclusive use with propeller-driven aircraft, a bicycle configuration would have till been considered before a taildragger was selected. The next step is to then calculate the exact position for the gear based on the selection of a tricycle configuration, which allows for the best operation on the ground of those considered.

2. Landing Gear Configuration

With the trade study completed to decide on configuration, steps can be made to determine the position of the nose and main landing gear. Once the weight of the aircraft had been decided, with the information of the most forward and aft center of gravity locations, the down position of the gear can be decided to ensure stability on taxi, takeoff, and landing. The location of the landing gear, stability on the ground, and sizing of critical parts were aided by the calculations provided by Raymer in the Landing Gear and Subsystems section [25]. Knowing the down positions of the nose and main gear, MTOGW, empty weight, and center of gravity positions, Raymer [25] provides approximation equations to determine the loads on each landing gear strut. With this value for load per strut, it is possible to determine the size and number of tires needed as well as the tire pressure needed to operate on an austere field of CBR 5. Additionally, from the load per strut, the shock absorber for each strut can be sized to allow for a safe operating range when landing. Finally, deriving the value for stall speed allows for the approximation of brake disc size while also considering the number of braked wheels. The results of these calculations for the landing gear can be found in the following table, Table 58.

Gear	Distance From Nose	Height	From Center-line	Wheels per Strut	Tire Size	Tire Pressure	Max Load per Strut	Shock Absorber Length	Shock Absorber Diameter	Shock Absorber Stroke Length	Brake Disc Size
-	ft	ft	ft	-	in x in	psi	lbs	ft	in	in	in
Nose	6.61	4.00	0.00	2	22 x 6.5	68.00	7,685	2.30	3.03	11.00	-
Main	22.85	4.00	5.68	1	34 x 10.5	77.00	10,583	2.30	3.56	11.00	12.00

Table 58: Landing Gear Specifications

From the landing gear specifications above in Table 58, a tailstrike angle can be calculated at 21.45 degrees, which is sufficient to prevent tail strikes on takeoff and landing. The overturn angle was determined prior to placement but can be calculated to be 55 degrees, more than enough to allow for a high degree of stability on the ground. For the shock absorbers, oleopneumatic type shocks with metered orifices were selected due to their high efficiency in transferring loads to the airframe, the dimensions of which are also seen in Table 58. With the loads on each strut, position, and shock absorbers calculated, tires can be selected for the nose and main landing gear. For the nose, a strut with two wheels was ideal to handle the braking load specified in Table 58 and Goodyear's 222K68-2 Aircraft Rib tires are perfect to fit that role. Rated to handle 2,800 lbs of load each in taxiing, the maximum static load on the nose strut when taxiing is 4,732 lbs, the tire can handle 4,200 lbs when braking after landing or an aborted takeoff. This allows for 868 lbs and 715 lbs of margin to the maximum loads of the tire on taxiing and braking, respectively. For the main landing struts, a single tire was needed for each to handle the maximum load of 10,583 lbs, that tire being the Goodyear 347K08T1 Flight Leader tire, which is rated at 10,870 lbs, allowing for a margin of 287 lbs. These tires additionally were selected for their noticeably low rated tire pressures of 68 and 80 psi, allowing the tires to operate near their rated pressures and allow the aircraft to have enough of a contact patch to operate from an austere airfield with a CBR of 5 without damaging the surface.

The extension and retraction of the gear will be done using hydraulic pressure from localized hydraulic pumps driven by electric motors. Due to the position of the nose landing gear and how close it is to the nose cone of the aircraft, the actuation system for the nose gear will retract rearward into the fuselage, just under the feet of the front seat. This requires the use of an extension handle to allow the gear to be fully extended as the drag from the air can possibly keep the gear from locking in the case of a hydraulic failure. The main gear will fold forward into a wing

protrusion under the intake of the engine, thus allowing for minimal disruption in airflow over the top of the wing, outboard of the engines.

D. Service Life

Per the RFP, the ZA-21 Shrike must be capable of performing 15,000 flight hours over 25 years. Annually, this is 600 hours yielding approximately 122 design missions or 252 ferry missions. In a typical year, one can speculate 60% of the hours to be for training, 10% for FM type missions, and the remaining 30% for DM type missions. This is the equivalent 360 training hours, 60 FM hours, and 180 DM hours. Certain design aspects of the ZA-21 were chosen with this requirement in mind, such as the twin vertical tail, wing rib spacing, and off-the-shelf parts. The number of flights before certain primary structures fail can be estimated using Goodman's criterion, however this is where the off-the-shelf parts and easily available materials make for the longevity of this program.

XII. Mass Properties

A. Weight Build-up

The method for determining the weight budget of the ZA-21 was a list of equations derived for fighter aircraft provided in Raymer [25]. Raymer mentions multiple methods to determine these weight estimations, but for the case of LAB-7, the method of approximating the weights via general rule of thumb ideas was used for initial weight estimations. Original static estimations were used, such as 9 lb/ft^2 for the main wing, and other general assumptions for fighters were used for initial weight estimation of the aircraft in order to get sizing more pinpointed.

After initial estimations for sections were made and the design became more concrete, the statistical weights method was then used. This method is a more refined estimate, which utilizes statistical equations based on regression analysis. Every feature of the aircraft which can have a weight estimation is featured in the weight budget and using these sophisticated equations, the aircraft empty weight can be accurately estimated.

Once weight estimates are determined, component locations were then estimated based upon general geometric layout of the ZA-21. Due to the symmetric nature of the aircraft, the only location considered has been along the X axis. The X starting location is the nose tip of the aircraft and runs parallel to the ground. Over the course of the designing of the aircraft, these locations were optimized and updated to better signify the actual locations of the components.

In order to account for all unknown weight values, a fudge factor was used. This fudge factor was a percentage of the empty weight that would be added on top of the empty weight of the aircraft in order to account for unforeseen additional weights not included in the weight budget. Raymer [25] specifies this fudge factor as being between 3-15% to allow for additional weight growth. The rule of thumb that was followed was 6%, which is what was recommended as being a good middle of the road value. This increased empty weight by 773 pounds but gave peace of mind and growth safety in the weight budget.

THIS SPACE INTENTIONALLY LEFT BLANK

	Weight (lbs)	Location (ft)	Moment (ft*lbs)				
Structures	**4,895.85**	**20.28**	**102,764.91**	**%We Allowance (Fudge Factor)**	**6**		
Horiz. Tail	190.51	29.7	5,658.17	Empty Weight Allowance	773	20.15	15,572.47
Vert. Tail	337.44	29.7	10,021.95				
Fuselage	1,693.35	22.33	37,818.06				
Canopy	350	12	4,200.00	**TOTALS**	**Weight (lbs)**	**Location (ft)**	**Moment (ft*lbs)**
Main Land Gear	689.14	21.92	15,106.04				
Nose Land Gear	242.1	7.04	1,704.41	**Total Weight Empty**	**13,653**	**20.15**	**275,113.62**
Propulsion	**3,567.92**	**-**	**88,386.47**	**Useful Load**	**11,200.00**	**-**	**224,278.00**
Engine	2,444.00	26	63,544.00	Crew	350	12	4,200.00
Firewall	21.47	20.8	446.58	Max Fuel	4,200.00	19.2	80,640.00
Engine Mounts	48.04	26	1,249.09	Oil	50	26	1,300.00
Engine Section	29.42	26	765.03	Max Payload	6,600.00	20.93	138,138.00
Air Induction Sys	293	22.3	6,533.96	Design Payload (alternate)	3,732.00	20.93	78,110.76
Tailpipe	67.05	32	2,145.73	Ferry Payload (alternate)	2,626.00	20.93	54.962.18
Oil Cooling	76.86	26	1,998.24				
Engine Controls	42.76	23.8	1,017.68				
Engine Starter	31.78	26	826.33				
Fuel System/Tanks	513.53	19.2	9,859.83				
Equipment	**4,416.68**		**68,353.44**				
Flight Controls	1,068.31	26.5	28,310.27				
Instruments	160.29	7.5	1,202.18				
Electrical	822.02	15.1	12,412.47				
Gun	330	10.1	3,333.00				
Avionics	778.54	5.7	4,437.69				
Air Conditioning/ Anti-Ice	195.95	19	3,723.10				
Handling Gear	6.36	10.8	68.72				
Pylons	620	20.93	12,976.60				
Furnishing/ Equipment	435.2	12	5,222.40				

Table 59: Weight Budget Statement

B. Center of Gravity

The center of gravity was estimated using a simple method. The location column signifies the estimated CG of each component on the weight budget in terms of the X axis (along the length of the aircraft). By estimating the CG of each component and calculating the moments of each component, then summing each of these moments, the CG can be determined by dividing the moment sum by the weight sum.

$$Aircraft\ CG = \frac{\sum_{each\ component}^{total\ components}(component\ CG\ location * component\ weight)(ft * lbs)}{\sum component\ weights\ (lbs)}$$

Figure 54: CG Calculation Equation

Using this method, many CG values can be determined. This method was especially useful in determining locations that relied on CG positioning, such as the placement of the main wing and landing gear locations.

C. CG Travel with Weapon Loading

Using the general method of estimating CG from the above section, it is possible to determine the CG travel from loading weapons on wing pylons. In order to minimize CG shift, the pylons were placed in positions along the wing which would minimize that shift. To find the smallest shift in CG, the CG is first calculated for the aircraft without the wings being placed in order to determine the non-wing CG location of the aircraft. Once this location is determined, the wing is placed on that exact location, so the addition of the wing does not shift the CG of the aircraft as well as having the wing directly at the location of the CG. Pylon are placed accordingly with the wing, so the addition of payload will minimally affect the CG shift when weapons are loaded and unloaded.

Using this method, it can be seen in the table below how the CG shifts between the different weapon configurations in each mission loadout.

CG Confgiuration	Sum of Moments (ft*lbs)	Sum of Weights (lbs)	Est. CG from Nose (ft)
Empty Weight	275,077.29	13,653.28	20.15
Max Takeoff Gross Weight	499,391.62	24,853.28	20.09
Design Mission TOGW	439,364.38	21,985.28	19.98
Ferry Mission TOGW	416,215.80	20,879.28	19.93
Basic Flight Design Gross Weight	399,044.38	19,885.28	20.07

Table 60: CG Locations of Each Configuration

D. Flight CG Envelope

The method used to create the CG envelope was similar to finding CG in the previous sections. First limits must be set for the forward and aft positions of the aircraft CG. Normally the forward CG limit is set by elevator effectiveness and the aft CG limit is set by directional stability values, according to Raymer [25]. These values were outside of the scope and level of detail to be completed in this design phase and instead, Raymer suggests that the FWD and AFT CG limits can be estimating using an old rule of thumb that the limits shall not be separated by more than 8% MAC.

In order to find these limits, it would be necessary to convert the existing CG of the aircraft to %MAC. This was done by utilizing values known as the Leading Edge MAC (LEMAC) and Trailing Edge MAC (TEMAC). These values were an X position value for the location at the edges of the wing at the MAC location. To convert our CG value into a %MAC, the following equation supplied by FlightLiteracy.com [8] was used:

$$CG\ inches\ \%MAC = \frac{Distance\ aft\ of\ LEMAC * 100}{MAC}$$

Figure 55: CG Inches %MAC Equation [8]

Using the above equation, the CG was converted to %MAC and knowing the 8% MAC rule of thumb, +/-4% was done on that number to establish the FWD and AFT limits. Using this method, those limits were then converted back into X axis coordinates and the CG envelope plots can be created.
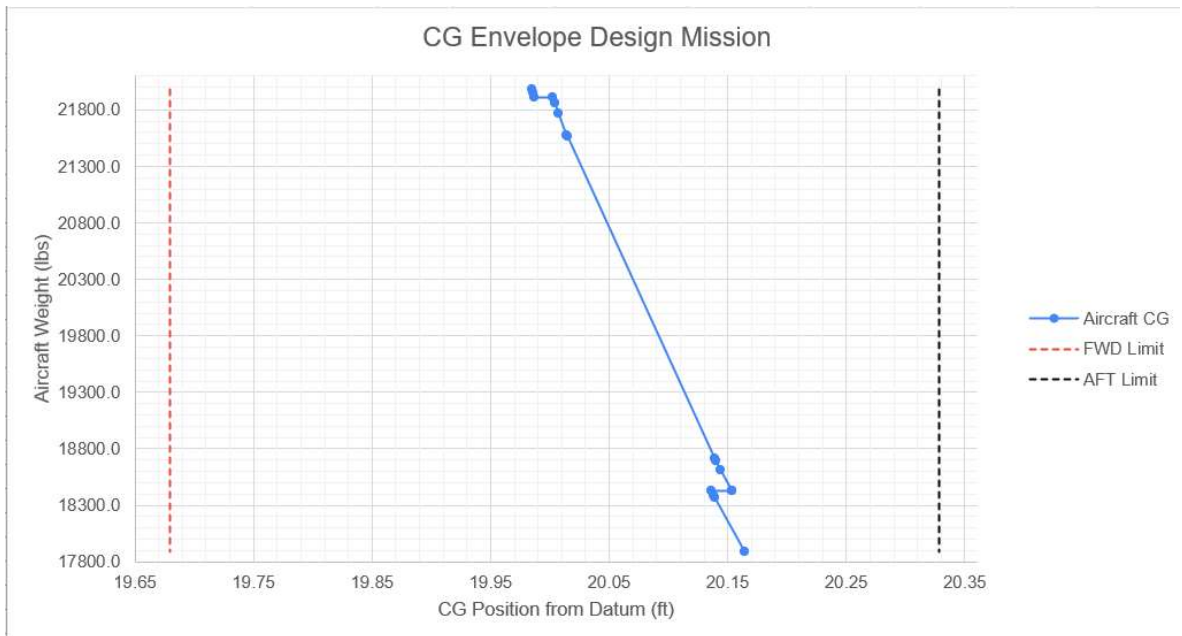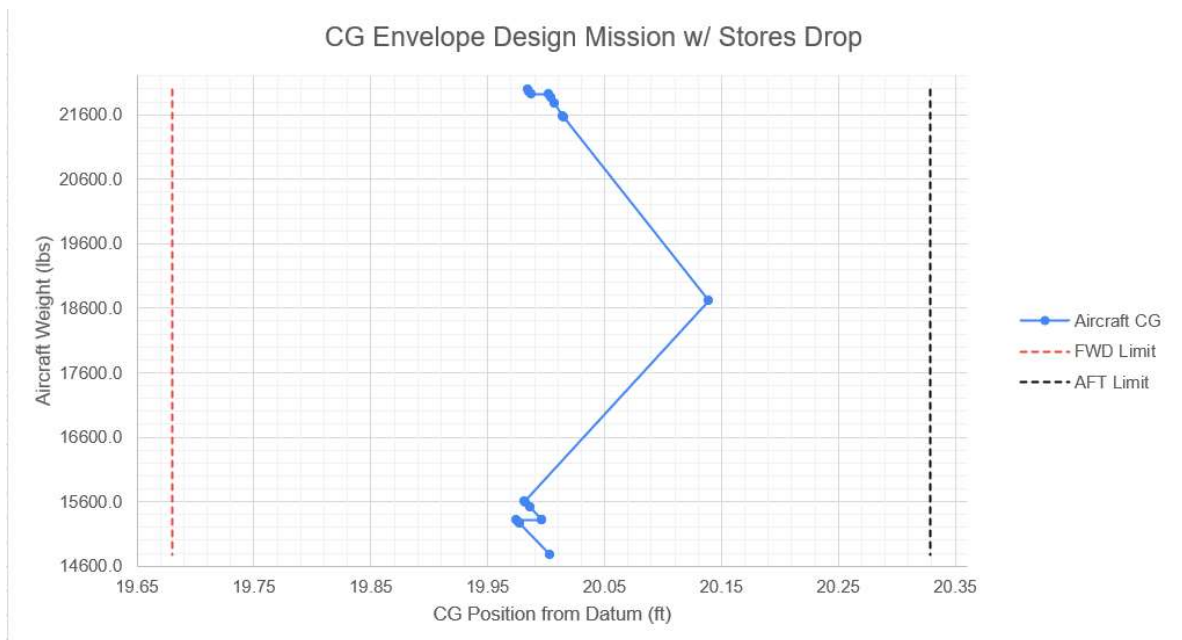
Figure 56: CG Envelope for Design Mission

Figure 57: CG Envelope for Design Mission w/ Stores Drop
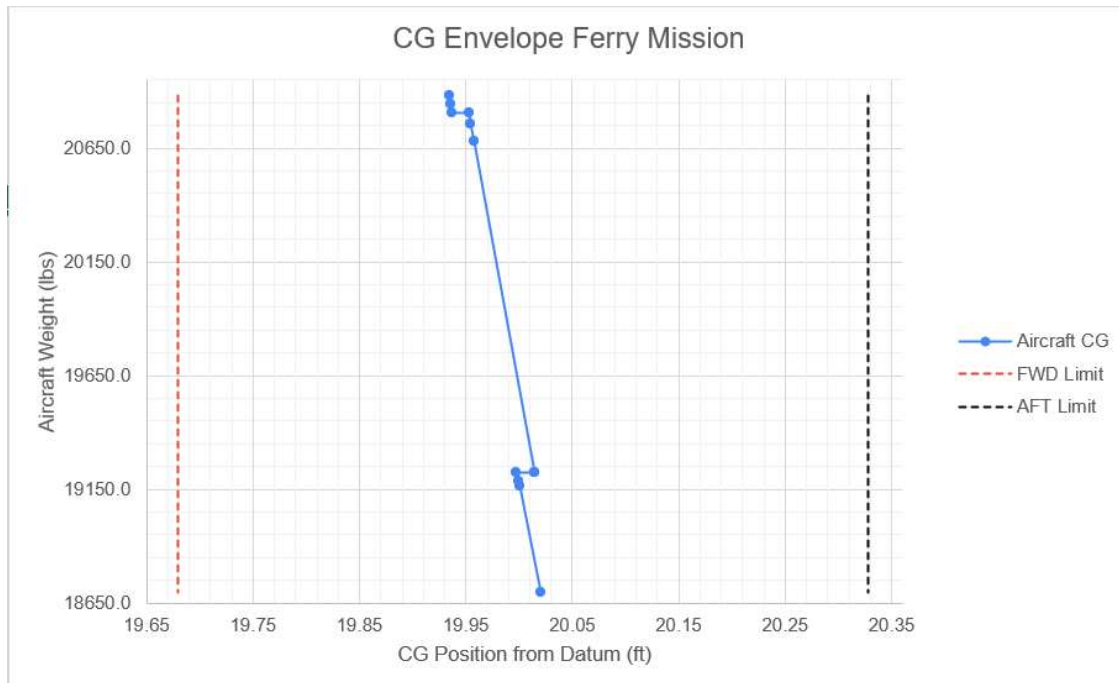
Figure 58: CG Envelope Ferry Mission

While stores drops are not necessary for the design mission, it is interesting to see that in the plot, the aircraft still stays well within its CG limits. Based off these plots, it is valid to say that the aircraft will have no issues staying within the CG limits imposed by the 8% rule of thumb given by Raymer [25]. The ferry mission is the ideal CG mission with a shift of only 0.05 feet AFT as the mission continues. Even with more dynamic arms loading and alternative payloads, the Shrike is expected to remain well within CG limits.

XIII. Auxiliary Systems

A. Flight Controls

Control surfaces on the Shrike are actuated using an entirely electric system. Electronic actuators are situated along the hinge points of each control surface. These electronic actuators are then controlled by the centrally located flight control computer. The aircraft has an elevator on each horizontal stabilizer as well as a rudder on each vertical tail. Additionally, the main wings each have one aileron and a leading and trailing edge flap assembly. The ZA-21 has 3 redundant flight control computers. Two located in the forward avionics bay, and one located behind the rear seat, in front of the firewall. The three flight control computers are split apart to ensure the aircraft can maintain control in the event of damage to one or more computers.

The flight control computers employ a fly-by-wire system where the computer receives input from the cockpit controls, determines the optimal deflection of control surfaces, and then outputs the proper instructions to the control surface actuators. Fly-by-wire was chosen due to its low weight, high survivability, and responsive control in comparison to hydraulic or mechanical systems. This is offset by a greater cost in terms of repair but considering the greater survivability of a wholly electronic system, the cost savings in aircraft combat loss/damages are likely greater.

Due to the complex, aircraft-specific nature of fly-by-wire control systems, existing actuators and control units can be used from other aircraft, however the development of a programmatic control scheme specific to the Shrike will be required. The ZA-21 is a naturally stable aircraft, so it is not an immediate danger if temporary power loss to the control systems is sustained.

B. Engine Controls

The engine controls of the aircraft are what gives the pilot authority over the engine. The engine controls mainly deal with the throttle control, but also provide information on fuel connections, health/monitoring of the engine, safety measures, and air data. The ZA-21 twin PW-306b engines are controlled using a Full Authority Digital Electronic Control (FADEC) system provided by Pratt and Whitney. Pratt and Whitney has developed their own FADEC system for use on their engines and will require slight modification to conform to the high-performance operation expected in the ZA-21. Like most modern aircraft, using FADEC will provide a direct data stream from the engine to the control systems. This will allow the pilots to have instant access to valuable engine data as well as allow automated engine monitoring and efficiency tuning to take place.

For engine starting, the Shrike employs a jet fuel starter to spin a single engine using a small turbine powered by compressed air. The onboard air tanks contain enough air for two starting attempts, but the system can also be operated using external compressed air. Once one engine is started, bleed air can be used to start the second engine and the onboard air tanks are refilled from a pneumatic pump operating from the engine's constant-speed accessory drive. The jet fuel starter can also be used for engine starts in air in the event of flameout. At high enough speeds, the compressed air tanks may not even be required as bleed air is at high enough pressure. The starting assembly and air storage is situated above and between the two engines in the engine service bay.

C. Fuel Systems

Fuel on the ZA-21 is split between two tanks: A primary fuel tank located behind the cockpit, just behind the firewall leading to the engines, and a smaller secondary fuel tank below the rear crew seat in the cockpit fuselage section. The primary fuel tank holds a volume of 520 gallons and the secondary tank holds a volume of 101 gallons. This allows the Shrike to carry 621 gallons of onboard fuel which equates to 4200 lbs of fuel (approximate with density of JP-8). In the event more fuel is needed, either for longer ferry missions or extended loiter times, the Shrike is also capable of carrying a 150-gallon external fuel tank on the fuselage weapon station. Because both fuel tanks are in close proximity to the aircraft center of gravity, they can be drained either sequentially or in parallel with the transfer tubing that connects to them. Additionally, both engines have separate fuel lines to the main fuel tank as well as a joint fuel line to the secondary tank. This ensures that the engines can continue receiving fuel in the event one tank or one of the fuel lines is damaged.

The ZA-21 engine and fueling system is designed for use with JP-8 to achieve the best performance and efficiency possible from both engines. However, if circumstances require - such as in the case of operating from austere or unprepared runways - the Shrike is capable of using commercial Jet A and Jet A-1 fuels.
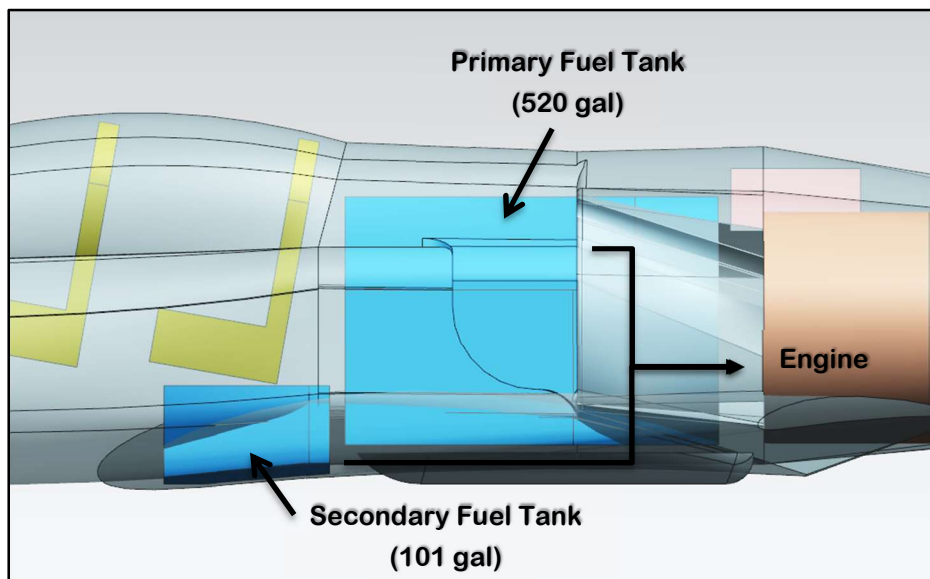
Figure 59: ZA-21 Fuel Storage

D. Electrical Systems

The ZA-21 is equipped with two separate generator units, one on the accessory drive of each engine. There are two 30 kVA generators each supplying 200 Volts of 400 Hz, 3-phase alternating current power. This power is used to power electronic actuators and any major electrical functions of the aircraft. Transformer units are used to convert the 200 V, 400 Hz AC power into 24V DC power that can also be used throughout the aircraft in other necessary equipment. Additionally, the aircraft is equipped with a low-capacity battery used to power the aircraft temporarily in the event of main generator loss before the auxiliary power unit engages. All primary electrical equipment is mounted in the gap space between and above the two engine mount frames, as well as above the primary fuel tank.

Figure 60: Electrical System Layout

E. Emergency Systems

In a dynamic combat environment, emergencies can arise from a variety of sources, be it mechanical/electrical failures of the aircraft itself, or damage done to combat circumstances. In these cases, the priority of safety and salvage is always the crew first, plane second.

As such, the Shrike is equipped with two Martin Baker Mk16 ejection seats. Capable of zero-airspeed, zero-altitude safe ejection, as well as a maximum ejection sp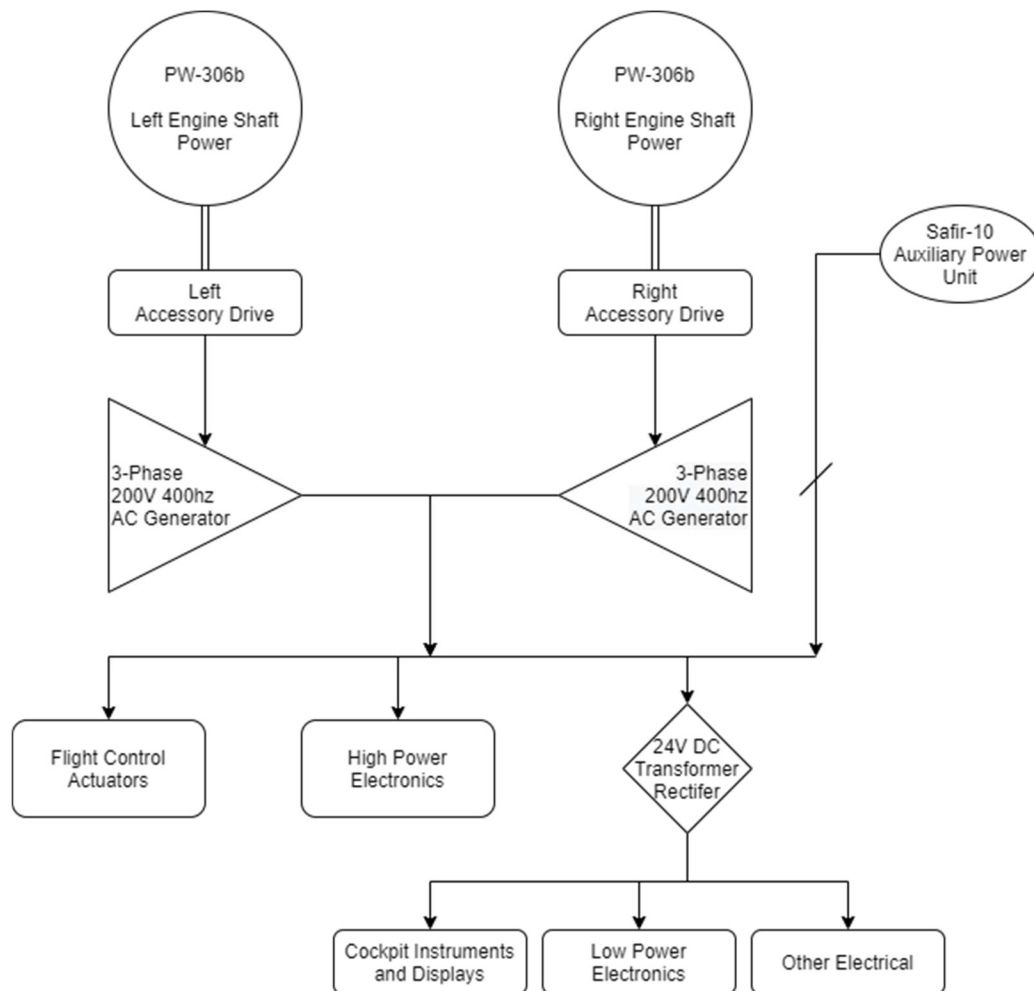eed and altitude of 625 KEAS and 65,000 ft, these seats are operational across the entire operating envelope of the Shrike. Additionally, with an automatically inflating life raft as well as a personal survival pack installed, the Mk16 seats ensure pilot safety in emergency bailouts.

In the event of emergency power loss or engine failure, the Shrike is equipped with two independent engines with full accessory drive assemblies ensuring limited operation can continue on only one engine. Should both engines fail, the Shrike also has a Saphir 10 auxiliary power unit developed by Safran. This APU provides 12 kVA of sustained electrical power as long as bleed airflow is maintained. This is enough to operate primary control systems in the event of dual engine-out emergencies. Additionally, the Saphir 10 also acts as an air turbine engine starter. At 81 pounds, it provides valuable emergency operational ability at a low weight cost.

F. Avionics

The avionics suite of the Shrike is taken up largely by existing military systems with proven effectiveness in combat environments. For large components, existing off-the-shelf systems were chosen, whereas instruments, sensors, and other low-scale devices will be drawn from other aircraft of similar performant ability. This was done to allow more time to be spent on the functional aspects for the aircraft design during this phase of development.

The off the shelf systems chosen come from other military aircraft implementations to reduce cost and maintain effectiveness. The first classification of this is navigation. The Shrike is equipped with the AN/ARN-151 GPS navigation set developed by Collins Aerospace, as well the AN/ARN-118 tactical air navigation system (TACAN) also developed by Rockwell Collins. For navigation in poor conditions, the Shrike also has the AN/ARN-108 instrument landing system onboard. Other positional and navigational equipment include the AN/APN-194 altimeter and the AN/APX-113 IFF interrogator/transponder. For communications, the Shrike is equipped with the AN/ARC-210 as a UHF, VHF, AM, and FM receiver-transmitter system. The ARC-210 was initially developed for the F-16 by Collins Aerospace, but will provide viable communications ability for the Shrike. For onboard

communications between crew as well as audio recording and pickup, the Orion system from Orbit Communications was chosen. The last major avionics component is the Armament Datalink System. The AN/AXQ-14 was chosen as it is already operationally capable with all of our expected arms to be carried.

If additional navigation or ground-following performance is required for low flight, the ZA-21 is also able to carry a variety of external navigation pods. Compatibility is guaranteed with the LANTIRN Navigation Pod system on wing stations 2, 3, 5, and 6.

G. Integrated Gun

A required component of the aircraft was an integrated gun suitable for engaging ground targets. To maintain a cheaper and lighter aircraft that still had a capable weapons suite, a 20 mm caliber gatling type cannon was chosen. The 20 mm caliber is a good balance between size/weight and the damage the weapon is capable of inflicting. The three cannons considered were the M-61, the M-197, and the XM-301. A trade study was performed analyzing the benefits and drawbacks of each cannon. The results of this comparison can be found in Table 49 below.

Quality	Weight of Importance	Score		
		M-61	**M-197**	**XM-301**
Weight	4	1	2	3
Fire rate	2	3	1	1
Accuracy	3	1	1	3
Recoil	3	1	2	3
Total Score:		**16**	**19**	**32**

Table 61: 20 mm Cannon Trade Study

As a result of the above trade study, it was determined that the onboard integrated cannon for the Shrike would be the General Dynamics XM-301. The XM-301 is an experimental gatling gun that was originally designed for the RAH-66 stealth attack helicopter program. While the program was unsuccessful, the gun itself has many desirable characteristics and multiple working models were built. It is a 3-barrel rotating gatling cannon chambered in 20mm ammunition standard to NATO 3585 ammunition. It was initially conceived as a modified M61. The gun itself weighs only 80.5 lbs with a recoil force of only 800 lbs yet is capable of firing 1,500 rounds per minute at the same muzzle velocity as its parent M61. Additionally, it is significantly more accurate than any other cannon considered with a spread of only 2.2 milliradians. The small size, weight, and low recoil allows the cannon to be

placed along the left side of the fuselage, below and to the side of the cockpit. There is a notch in the fuselage cut out along the left side to allow the firing barrel of the gun to be exposed. This is similar to how the F-16 employs its integrated gun.

For ammunition feed and storage, a modified form of the F-16's rotary storage drum assembly will be used. The system will be expanded slightly to hold a total of 566 rounds with a loaded ammunition weight of approximately 300 lbs. The weight of the feed and storage system after modification by General Dynamics is 258 lbs, as less support fixturing will be required for the lighter gun. The ammunition feed and storage system will be mounted to the center of the aircraft, underneath the rear crew seat. Ammunition loading ports will be positioned to the right side of the fuselage while the gun and breech assembly itself will be on the left side of the aircraft. The overall, completely loaded gun assembly weight would come to approximately 640 lbs, well below the weight of comparably armed systems.

H. Targeting Systems

The primary targeting component for the Shrike is the radar system. For the radar, a modern AESA type system was selected. An AESA radar provides high resolution scanning and tracking of adversarial air and ground targets and can also act as a radar warning receiver to determine when the Shrike is being targeted by non-friendly forces. For this system, the AN/APG-83 SABR was chosen. It is a modern full-performance fire control radar system based off of the APG-77 and APG-81 currently in use in the F-22 and F-35. As a scalable array, it can be sized to fit the 26-inch diameter limit imposed by the nose cone radome of the Shrike. The advantages of using the AN/APG-83 SABR is that it is a newer, proven system type, and is similar enough to that of the F-22 and F-35 that some of the filtering and scanning software used on them can be ported over to this model. Specifications of the radar are limited with only an estimated range of 230 miles and a field-of-view of 120 degrees available. The system was chosen due to the proven combat effectiveness of its sister systems in the F-22 and F-35, and high-performance ability at a reasonable price. The price estimate used for the scaling and installation for the SABR into the Shrike was US $2.5 million.

For additional targeting ability, the ZA-21 is capable of carrying a variety of additional external targeting pods. Compatibility is guaranteed with the AN/AAQ Sniper Advanced Targeting Pod as well as the LANTIRN

Targeting Pod. Both pods can be mounted on wing stations 2, 3, 5, and 6 as outlined in the Payload and Armament section.

I. Survivability Systems

For survivability, the ZA-21 is equipped with multiple emergency and auxiliary systems to ensure that operation can continue long enough for a safe landing or bail out in the event of significant damage to the aircraft. To prevent damage in the first place, the ZA-21, like other military aircraft, will be equipped with a radar detection warning system and countermeasures dispenser. The system chosen for this is the AN/ALE-47 chaff and flares countermeasures dispenser manufactured by BAE Systems. This system was chosen for its low cost and weight, as well as tried-and-true performance. It has been used on over 38 different aircraft including many attack aircraft. For the Shrike, it is the best and most reliable performance that can be achieved from a countermeasures system for its low cost and small size.

In the event damage is sustained, the Shrike is designed to ensure it can remain aloft long enough for the aircraft to divert to a safe airport, conduct an emergency landing, or for the crew to safely bail out. Likely damage to the Shrike will be to the rear exhaust and engine area of the aircraft due as a result of heat-seeking missiles which are extremely common in combat environments. In the event of a missile near-miss or strike on the tail of the craft, the ZA-21 has twin vertical tails and can be flown with limited control when only one tail is operable. Additionally, the aircraft can sustain a single engine loss and fly with limited ability. While not enough for complex combat maneuvers or high speed, single-engine operation is viable for emergency endurance cruising to nearby friendly airfields. Initial engine-out cruise range estimates.

XIV. Cost Analysis

A. Production Cost

Typically, an aircraft's cost can be estimated using the empty weight of the aircraft and using a multiplier to determine the weight per pound. Using this strategy, the entire cost of the aircraft can be estimated. The factors used for the initial estimation is empty weight times 2,000-3,500 lbs. Raymer gives that estimation based on military aircraft. This process is backed by other aircraft's empty weights and applying that range, the cost of those aircraft will be within that range. For example, using the similar aircraft A-29, the cost is between 20,000,000 to 30,000,000

dollars. The empty weight of the A-29 is approximately 7,055 lbs. So, using the estimate given the A-29 should cost

between 14,000,000 to 25,000,000 dollars. This estimate number is between the official estimates of the A-29 aircraft.

LAB-7's aircraft empty weight is 14,492 lbs, thus the cost of the aircraft should be between $28,985,080-$50,723,890.

While this is not a perfect estimate, it gives a good idea of what the cost of the aircraft will be and a rage the cost

should be in. Moving forward, the cost per aircraft shall be within the estimated range.

Raymer lays out a list of variables that are used to evaluate each aircraft. These variables are listed in Table

61. There is also a list of equations that calculate either the cost of a component, or the hours of work required to

design, manufacture, and maintain the aircraft. Adding both of these, along with the corresponding coefficients to put

hours worked to cost, the cost of the entire project can be calculated.

Variables	Value
We (Empty Weight)	13,653
V (Max Velocity Knots)	510
Q (Quantity 5 Years)	50
FTA (Flight Test Aircraft)	3
Neng (Number of Engines per Aircraft)	2
Tmax (Max Thrust)	12666
Mmax (Engine Max Mach Number)	0.85
Tturb (Turbine Inlet Temp)	1445
Cavi (Avionics Cost)	$3,750,000
Ca (Aircraft Cost Minus Engine)	$31,125,937
Ce (Cost per Engine)	$2,500,000
Vc (Cruise Velocity)	450
Wo (Design TOGW)	21,985

Table 62: Variables Used in Cost Calculations

The equations provided by Raymer calculate the work hours for Engineering, Tooling, Manufacturing, and

Quality Control. The cost per engineering hour is estimated to be approximately $115 per hour. The equation estimates

that there are approximately 1.1 million hours. Combining these, the estimated engineering cost is approximately $132

million. The cost per Tooling hour is estimated to be approximately $118 per hour for 2 million hours. The

approximate cost of tooling is $247 million. The cost for manufacturing is $108 per hour for 4.5 million hours. The

approximate cost of manufacturing is $491 million. Finally, the cost for quality control is $98 per hour for 604 thousand hours. The approximate cost of quality control is $59 million.

After calculating the hourly cost of labor, the cost of development support, flight test, and manufacturing materials are considered. Like the hourly equations, Raymer [25] lays out calculations for each one. Development support is approximately $121 million. Using 3 flight test vehicles, the cost of flight testing becomes $35 million. Manufacturing materials become $155 million. The cost of each engine is $2.5 million, which leaves a cost of $5 million worth of engine per aircraft. There is also the added cost of upscaling the engine. The methodology with this is to take the percentage upscale and multiply by the cost to make an entire new engine. The cost comes out to $401 thousand. To calculate the cost of avionics, similar aircraft and other considerations from Raymer [25] were used, thus the cost of avionics is assumed to be $3.75 million.

After all considerations, the cost of the entire project becomes approximately $1.6 billion. While these is an extremely large project, it is due to the initial estimation of a 5-year projection of 50 aircraft delivered. That means that the valuation of each aircraft is $33 million dollars. This estimation fits well into the lower end of the empty weight estimations made at the start of this section

Production Hours	Hours
Engineering	1,151,090.44
Tooling	2,097,959.03
Manufacturing	4,548,395.90
Quality Control	604,936.66

Table 63: Hours of Production

Production Cost	Cost
Development Support	$121,760,298
Flight Test	$35,033,293
Manufacturing Materials	$155,530,460
Avionics	$3,750,000
Engine	$2,500,000
Propulsion Upscaling	$401,748

Table 64: Production Cost

B. Operating Cost

The operating cost of the aircraft is calculated differently. Raymer gives a ratio of fuel, salary, and maintenance costs of a military operation. Fuel accounts for 15%, salary 35%, and maintenance 50% of the operation and maintenance cost. The salary and maintenance differ per mission but at an hourly rate, the fuel was calculated. The aircraft uses JP8 aircraft fuel. Using a conservative estimate of 135 gallons per hour, the fuel accounts for $400 per hour. This fuel value will give the aircraft a salary cost of $933.33 and a maintenance cost of $1,333.33 per hour. The overall cost to fly per hour is $2,666.67. This is outlined in Table 65.

Aspect	Cost Per Hour
Fuel	$400.00
Salary	$933.33
Maintenance	$1,333.33

Table 65: Hourly Cost of the Aircraft

C. Cost of Armament

The cost of armament for each mission will vary depending on each mission. But considering that the Shrike can hold a plethora of different armaments, each unit will have a corresponding cost that can be made into a full cost of each mission set. In Table 66 the cost per armament is shown.

Armament	Price ($)
Aim-9	$381,069.74
LAU-68	$2,799.00
AGM-65H	$100,000.00
GBU-16	$21,896.00
566 rds 20x102mm	$3,328.08

Table 66: Cost per Armament

D. Overall Cost

Overall Cost	Cost
RDT&E and Flyaway	$1,621,920,916
Valuation of Each Aircraft	$32,438,418
Total Cost per Hour	$6,333.37

Table 67: Total Cost of Aircraft

XV.   Conclusion

Modern combat is an every-changing theater of operations, and technology on both ally and opposition sides has been advancing at an alarming rate. While advanced technology holds its place, affordable and reliable performance is also a desired characteristic. In modern ground attack aircraft, the advanced technology exists, however low-cost alternatives have yet to be proven. Thus, the RFP [26] outlined by AIAA has asked for the design of a new light-attack aircraft to operate effectively at low cost. The ZA-21 was designed to fill this gap in operational cost effectiveness. As demonstrated throughout the contents of this document, the ZA-21 "Shrike" is a highly capable aircraft across its operating environment. It meets all mandatory requirements as specified by the RFP [26] and meets additional objectives including survivability considerations and various armament capabilities.

With the ability to takeoff and land in under 3,200 ft on unprepared, austere fields, the ZA-21 is a perfect aircraft for forward support of ground units. Its 6,600 lb maximum payload can be configured to effectively complete a variety of missions including key target destruction, ground support, anti-helicopter, and anti-tank operations. Additionally, the twin PW-306b engines and large fuel storage onboard allow the Shrike to remain on-station far longer than current ground support aircraft. The program cost for an expected 50 aircraft is estimated at $1.6 billion, resulting in an approximate flyaway cost of $32 million per aircraft. The hourly operational cost is estimated to be $6,333 per hour, well below the cost of other aircraft considered for this role.

Figure 61: ZA-21 Shrike Side Angle

References

[1] "2024 Aluminium Alloy," Wikipedia Available: https://en.wikipedia.org/wiki/2024_aluminium_alloy.

[2] Air Armament Center, Weapons File, 2009.

[3] "AN/APG-83 SABR," Deagel.com Available: https://www.deagel.com/Sensor%20Systems/ANAPG-83%20SABR/a002089.

[4] "AN/APG-83," Wikipedia Available: https://en.wikipedia.org/wiki/AN/APG-83.

[5] AZoM, "Titanium Alloys - Ti4Al4Mo2Sn Properties and Applications," AZo Materials Available: https://www.azom.com/article.aspx?ArticleID=2115.

[6] "Battlespace-Proven SDR Performance," Collins Aerospace, 2020.

[7] Carmichael, R., "Digital Datcom," USAF Digital Datcom Available: https://www.pdas.com/datcom.html.

[8] "Center of Gravity (CG) and Mean Aerodynamic Chord (MAC)," Flight Literacy Available: https://www.flightliteracy.com/center-of-gravity-cg-and-mean-aerodynamic-chord-mac/

[9] "F-16 20MM Gatling Gun System", General Dynamics

[10] "Global Aviation Tires," The Goodyear Tire & Rubber Company, 2018.

[11] "HexPly M65", HEXCEL.

[12] Jackson, P., Munson, K., Peacock, L., and Bushell, S., "AERO L-159," Jane's All the World's Aircraft 2010-11, 1st ed., IHS Jane's, 2010, pp. 154.

[13] Jackson, P., Munson, K., Peacock, L., and Bushell, S., "YAKOVLEV Yak-130," Jane's All the World's Aircraft 2010-11, 1st ed., IHS Jane's, 2010, pp. 558-561.

[14] "Lockheed Martin wins $308.3 million contract modification to upgrade radars on Taiwan F-16 jet fighters," Military&Aerospace Electronics Available: https://www.militaryaerospace.com/computers/article/16719020/lockheed-martin-wins-3083-million-contract-modification-to-upgrade-radars-on-taiwan-f16-jet-fighters.

[15] "Mechanical Properties of Carbon Fibre Composite Materials, Fibre," Performance Composites Ltd, 2009.

[16] "MK16 Ejection Seat for F-35 - Martin-Baker," Martin-Baker Available: https://martin-baker.com/products/mk16-ejection-seat-f-35/.

[17] "Navy Training System Plan for the AN/ALE-47 Countermeasures Dispensing System," 2002.

[18] "OpenVSP 3.23.0 Released," OpenVSP Available: http://openvsp.org/.

[19] "Orion Airborne 3D Audio Management System," Orbit USA Available: http://orbit-cs-usa.com/?product=orion-3d-audio.

[20] Parsch, A., AN/ARD to AN/ARN - Equipment Listing Available: http://www.designation-systems.net/usmilav/jetds/an-ard2arn.html.

[21] Pike, J., and Sherman, R., "Aircraft Systems List," Military Analysis Network Available: https://fas.org/man/dod-101/sys/ac/equip/systems.htm.

[22] "Properties: S-Glass Fibre," AZo Materials Available: https://www.azom.com/properties.aspx?ArticleID=769.

[23] "PW300," MTU Aero Engines Available: https://www.mtu.de/engines/commercial-aircraft-engines/business-jets/pw300/.

[24] "PW300," PW300 - Pratt & Whitney Available: https://www.pwc.ca/en/products-and-services/products/business-aviation-engines/pw300.

[25] Raymer, D. P., Aircraft Design: A Conceptual Approach, 6th ed., AIAA Education Series, 2018

[26] "Request for Proposal - Austere Field Light Attack Aircraft," AIAA, 2021.

[27] "Saphir 10 Auxiliary Power Unit", Safran.

[28] Snodgrass, R. R., A Method for Predicting the Effect of Installed Stores and Missiles on Aircraft Drag, 1986.

[29] "Specialty Metal Supplier," Industrial Metal Suppliers | TW Metals Available: https://www.twmetals.com/.

[30] "Steel 300M," Tech Steel & Materials Available: https://www.techsteel.net/alloy/steel/300m.

[31] Taylor, J. W. R., "CESSNA A-37," Jane's All the World's Aircraft 1973-74, 1st ed., IHS Jane's, 1973, pp. 303-304.

[32] Taylor, J. W. R., "MCDONNELL DOUGLAS SKYHAWK," Jane's All the World's Aircraft 1973-74, 1st ed., IHS Jane's, 1973, pp. 379-380.

[33] "TCN-500 An ARN-153V Advanced Digital TACAN Receiver-Transmitter," Collins Aerospace Available: https://www.collinsaerospace.com/what-we-do/Military-And-Defense/Navigation/Airborne-Products/Radio-Navigation/Tcn-500-An-Arn-153V-Advanced-Digital-Tacan-Receiver-Transmitter.

[34] "The Market for U.S. Military Airborne Communication Systems," Forecast International, 2010.

[35] "Turbofan Engine," National Aeronautics and Space Administration Available: https://www.grc.nasa.gov/www/k-12/airplane/aturbf.html.

[36] "Type-Certificate Data Sheet", Pratt and Whitney Canada Corporation, Nov. 2015.

[37] XFLR5 Available: http://www.xflr5.tech/xflr5.htm.

[38] "XM301 20MM Lightweight Gatling Gun", General Dynamics, 2005.